

THESIS

PRESSURE FLOW EFFECTS ON SCOUR AT BRIDGES

Submitted by

Michael D. Robeson

Department of Civil Engineering

In partial fulfillment of the requirements

for the Degree of Master of Science

Colorado State University

Fort Collins, Colorado

Fall, 2000

TG
320
.R624
2000
THESIS

COLORADO STATE UNIVERSITY

OCTOBER 23, 2000

WE HEREBY RECOMMEND THAT THE THESIS PREPARED UNDER OUR SUPERVISION BY MICHAEL D. ROBESON ENTITLED "PRESSURE FLOW EFFECTS ON SCOUR AT BRIDGES" BE ACCEPTED AS FULFILLING IN PART REQUIREMENTS FOR THE DEGREE OF MASTER OF SCIENCE.

Committee on Graduate Work



Advisor



Department Head

ABSTRACT OF THESIS

PRESSURE FLOW EFFECTS ON SCOUR AT BRIDGES

Scour caused by the occurrence of pressure flow requires a comprehensive understanding. Pressure flow can be defined as flow in which the low chord of a bridge becomes inundated and the flow through the bridge opening transitions from free surface flow to a pressurized condition, leading to a submerged or partially submerged bridge deck condition. A pressure flow condition often occurs at a bridge during a flood, potentially leading to bridge failure.

Scour of bridge foundations (piers and abutments) represents the largest single cause of bridge failure in the United States (ASCE, 1999). Methodical scour research began in 1949 with the research of E.M. Laursen. Unfortunately, the application of scour research to the design of bridges did not occur until several bridges failed due to local scour. Over the years, bridge scour research has focused on the study of free surface flow. During the past decade, research related to pressure flow scour has become increasingly important.

A testing program was developed and performed at the Hydraulics Laboratory of Colorado State University to examine pressure flow effects on scour at and around

bridges. Flume experiments were conducted incorporating a physical model of a generic bridge with supporting abutments constructed at an approximate scale of 8:1. In an effort to simulate varying magnitudes of a pressure flow condition, the model was constructed in a manner that permitted the bridge deck to be lowered into the flow. By lowering the bridge deck and holding the level of the approach flow constant, multiple levels of deck submergence could be examined. Six vertical bridge positions, three discharges, two abutment widths and two sediment sizes were incorporated into a matrix comprising 69 tests. Data collected included hydraulic parameters and topographic surveys.

Analysis of data collected during the study resulted in the formulation of a set of multivariate linear regression equations enabling the user to estimate abutment, local and deck scour depths during a pressure flow condition. Results of a dimensional analysis indicate that the dominant variables in predicting scour depths for a pressure flow condition include; the critical velocity of a given sediment size, the average velocity under the bridge deck, the height of the bridge deck above the initial and final bed surface, the depth of flow upstream of the bridge and the Froude number of the approach flow. Coefficients of determination for the developed equations ranged from 0.82 to 0.95.

Michael D. Robeson
Civil Engineering Department
Colorado State University
Fort Collins, CO 80523
Fall, 2000

ACKNOWLEDGEMENTS

I would like to take the opportunity to express my appreciation for the people that made this thesis possible. A very meaningful thanks to Dr. Christopher I. Thornton, my advisor, for his support and guidance throughout this study. Dr Thornton spent many hours thoroughly reviewing this thesis. It has been both a pleasure and an honor to serve and study under the supervision of Dr. Christopher I. Thornton. Additionally, I would like to thank my other committee members, Dr. Steven R. Abt, Dr. Larry A. Arneson and Dr. William W. Doe for their guidance, support and suggestions. A special thanks to Chad M. Lipscomb for his assistance with questions and examination of the raw laboratory data.

Completion of a thesis requires patience, sacrifice and dedication of the student's family. Over the years of schooling and throughout this thesis, my parents and relatives have been instrumental in providing the necessary love and support for my continued motivation. A big thanks to my fiancée Darcee, who has provided me with the love and understanding needed to make this goal possible and worthwhile.

TABLE OF CONTENTS

1	INTRODUCTION.....	1
1.1	GENERAL BACKGROUND.....	1
1.2	DEFINITION OF PRESSURE FLOW	2
1.3	RESEARCH OBJECTIVES AND SCOPE.....	4
2	LITERATURE REVIEW.....	6
2.1	INTRODUCTION.....	6
2.2	BACKGROUND INFORMATION.....	6
2.3	BRIDGE SCOUR REVIEW.....	7
2.3.1	<i>Contraction Scour</i>	10
2.3.1.1	Free Surface Contraction Scour	10
2.3.1.2	Pressure Flow Contraction Scour	14
2.3.2	<i>Local Scour</i>	14
2.3.2.1	Local Scour at Bridge Piers	14
2.3.2.2	Local Scour at Bridge Abutments.....	20
2.3.2.3	Local Scour Under Pressure Flow	25
2.3.2.3.1	<i>Abed (1991)</i>	27
2.3.2.3.2	<i>Jones (1993, 1995-1996)</i>	28
2.3.2.3.3	<i>Chang (1995)</i>	29
2.3.2.3.4	<i>Arneson (1997)</i>	30
2.3.3	<i>Degradational Scour</i>	32
2.4	SUMMARY	34
3	DATA COLLECTION.....	36
3.1	INTRODUCTION.....	36
3.2	FLUME DESCRIPTION.....	36
3.3	MODEL DESCRIPTION.....	38
3.4	DATA ACQUISITION EQUIPMENT.....	41
3.5	TEST PARAMETERS	43
3.5.1	<i>Test Matrix</i>	43
3.5.2	<i>Nomenclature</i>	49
3.6	TESTING PREPARATION AND PROCEDURE	51
3.6.1	<i>Test Preparation</i>	51
3.6.2	<i>Test Procedure</i>	52
4	DATA ANALYSIS.....	59
4.1	INTRODUCTION.....	59
4.2	DIMENSIONAL ANALYSIS	59
4.3	STATISTICAL ANALYSIS	62
4.3.1	<i>Statistical Theory</i>	63
4.3.2	<i>Statistical Assumptions</i>	68
5	DISCUSSION OF RESULTS.....	71
5.1	INTRODUCTION.....	71
5.2	PRESSURE FLOW DECK SCOUR EQUATIONS	75
5.3	PRESSURE FLOW ABUTMENT SCOUR EQUATIONS	98
5.4	LIMITATIONS.....	116
6	CONCLUSIONS AND RECOMMENDATIONS.....	117
6.1	INTRODUCTION.....	117
6.2	CONCLUSIONS	117
6.3	RECOMMENDATIONS FOR FURTHER RESEARCH.....	120
7	REFERENCES	122
	APPENDIX – SUMMARY DATA TABLES	127

LIST OF FIGURES

• Figure 1.1 – Example of bridge failure due to local scour and flooding.....	2
• Figure 1.2 – Profile view of typical bridge deck flowing under a partially submerged pressure flow condition.....	3
• Figure 2.1 – Profile view displaying types of scour at a bridge opening.....	8
• Figure 2.2 – Flow field and scour patterns at a circular pier (Melville & Coleman, 2000).....	16
• Figure 2.3 – Flow field and scour patterns at a short abutment (Melville & Coleman, 2000).....	21
• Figure 2.4 – Flow field and scour patterns at a long abutment (Melville & Coleman, 2000).....	22
• Figure 2.5 – Pressure flow scour variables at a partially submerged bridge.....	26
• Figure 3.1 – Plan view of flume and test section.....	37
• Figure 3.2 – Cross section of data platform and point gage assembly.....	38
• Figure 3.3 – Cross section of model bridge deck.....	39
• Figure 3.4 – Plan view showing placement of smaller abutments in model bridge deck.....	40
• Figure 3.5 – Profile view of ADV probe head.....	41
• Figure 3.6 – Profile view of ADV probe positioning.....	42
• Figure 3.7 – Grain size distribution for 1.5 mm sand.....	47
• Figure 3.8 – Grain size distribution for 3.3 mm sand.....	48
• Figure 3.9 – Data acquisition map for test numbers 1 through 6.....	54
• Figure 3.10 – Data acquisition map for test numbers 7 through 36.....	55
• Figure 3.11 – Data acquisition map for test numbers 37 through 72.....	56
• Figure 3.12 – Photographs of testing from initial to final conditions.....	58
• Figure 5.1 – Plot of raw data for pressure flow deck scour data.....	76
• Figure 5.2 – Graphical definition of variables used in Equation 5.2.....	77
• Figure 5.3 – Observed versus predicted values for pressure flow deck scour data.....	80
• Figure 5.4 – Predicted values versus residual scores for y_{pds}/y	81
• Figure 5.5 – Residuals versus deleted residuals for y_{pds}/y	82
• Figure 5.6 – Normal probability plot of residuals for pressure flow deck scour data.....	83
• Figure 5.7 - Observed versus predicted values for the pressure flow deck scour prediction equation (Equation 5.2) against the pressure flow deck scour equation (Equation 2.11) developed by Arneson (1997).....	84
• Figure 5.8 – Plot of raw data for combined pressure flow deck scour data.....	90
• Figure 5.9 – Observed versus predicted values for combined pressure flow deck scour data.....	94
• Figure 5.10 – Predicted values versus residual scores for combined y_{pds}/y	95
• Figure 5.11 – Residuals versus deleted residuals for combined pressure flow deck scour data.....	96
• Figure 5.12 – Normal probability plot of residuals for combined pressure flow scour data.....	97
• Figure 5.13 – Plot of raw data for pressure flow deck scour data.....	99
• Figure 5.14 – Observed versus predicted values for pressure flow abutment scour.....	102
• Figure 5.15 – Predicted values versus residual scores for y_{pas}/a	103
• Figure 5.16 – Residuals versus deleted residuals for y_{pas}/a	104
• Figure 5.17 – Normal probability plot of residuals for pressure flow abutment scour data.....	105
• Figure 5.18 - Observed versus predicted values for the pressure flow abutment scour prediction equation (Equation 5.7) against the pressure flow pier scour equation (Equation 2.12) developed by Arneson (1997).....	106
• Figure 5.19 – Plot of raw data for combined pressure flow local scour data.....	108
• Figure 5.20 – Observed versus predicted values for pressure flow local scour.....	112
• Figure 5.21 – Predicted values versus residual scores for y_{pls}/B	113
• Figure 5.22 – Residuals versus deleted residuals for y_{pls}/B	114
• Figure 5.23 – Normal probability plot of residuals for pressure flow local scour data.....	115

LIST OF TABLES

• Table 2.1 – Correction factors for mode of sediment transport	12
• Table 2.2 – Commonly used free surface pier scour equations	17
• Table 2.2 (continued) – Commonly used free surface pier scour equations	18
• Table 2.3 – Correction factor, K_s , for pier nose shape	19
• Table 2.4 – Correction factor, K_3 , for bed condition	20
• Table 2.5 – A selection of free surface abutment scour equations.....	23
• Table 2.6 – Correction factor, K_s , for abutment shape.....	24
• Table 2.7 – Main causes of degradational scour.....	33
• Table 3.1 – Variation in test parameters	45
• Table 3.1 (continued) – Variation in test parameters.....	46
• Table 3.2 – Summary statistics of utilized sediment	48
• Table 3.3 – Initial bridge opening corresponding to bridge position.....	49
• Table 3.4 – List of variables used for data analysis	50
• Table 3.5 – Summary of test matrix with data acquisition map correspondence.....	52
• Table 3.6 – Depth in feet of velocity data acquisition points below low chord bridge elevation	53
• Table 4.1 – Potential variables for describing pressure flow scour	60
• Table 4.2 – Example of quantities often shown in an ANOVA table.....	67
• Table 5.1 – Summary of dimensionless parameters used during analysis	73
• Table 5.1 (continued) – Summary of dimensionless parameters used during analysis.....	74
• Table 5.2 – Multivariate linear regression summary statistics corresponding to Equation 5.2.....	78
• Table 5.3 - ANOVA table associated with Equation 5.2.....	79
• Table 5.4 – Summary of calculated pressure flow deck scour data from Arneson (1997)	86
• Table 5.4 (continued) – Summary of calculated pressure flow deck scour data from Arneson (1997).....	87
• Table 5.4 (continued) – Summary of calculated pressure flow deck scour data from Arneson (1997).....	88
• Table 5.4 (continued) – Summary of calculated pressure flow deck scour data from Arneson (1997).....	89
• Table 5.5 – Multivariate linear regression summary statistics corresponding to Equation 5.4.....	92
• Table 5.6 - ANOVA table associated with Equation 5.4.....	92
• Table 5.7 – Multivariate linear regression summary statistics corresponding to Equation 5.7.....	100
• Table 5.8 – ANOVA table associated with Equation 5.7	101
• Table 5.9 – Summary of calculated pressure flow local scour data from Arneson (1997)	107
• Table 5.10 – Multivariate linear regression summary statistics corresponding to Equation 5.8.....	110
• Table 5.11 – ANOVA table associated with Equation 5.8	110
• Table A1 – Summary data table for 1.5 mm sediment size – Test numbers 1 to 36.....	128
• Table A2 – Summary data table for 3.3 mm sediment size – Test numbers 37 to 72.....	129
• Table A3 – Summary data table for 0.6 mm sediment size – Data used from Arneson (1997).....	130
• Table A4 – Summary data table for 0.9 mm sediment size – Data used from Arneson (1997).....	131
• Table A5 – Summary data table for 1.5 mm sediment size – Data used from Arneson (1997).....	132
• Table A6 – Summary data table for 3.3 mm sediment size – Data used from Arneson (1997).....	133

LIST OF SYMBOLS

a	=	abutment protrusion length, L;
b	=	pier width, L;
C_c	=	vertical contraction correction;
C_f	=	Froude number reduction;
C_q	=	discharge reduction;
d_s	=	maximum free surface scour depth, L;
D_{50}	=	grain size for which 50 percent of the bed material is finer, L;
D_m	=	diameter of the bed material ($1.25 D_{50}$) in the contracted section, L;
F	=	value for test statistic;
Fr	=	Froude number of the approach flow;
Fr_1	=	Froude number directly upstream of the pier = $V_1/(gy_1)^{1/2}$;
Fr_c	=	Critical Froude number = $V_c/(gy)^{1/2}$;
g	=	acceleration due to gravity, L/T^2 ;
H_0	=	null hypothesis;
H_b	=	distance from the low chord of the bridge to the average elevation of the bed material, L;
k	=	number of independent variables;
k_1	=	correction factor for mode of sediment transport;
k_2	=	correction factor for mode of sediment transport;
K_s	=	correction factor for pier nose shape;
K_θ	=	correction factor for angle of attack of flow;
K_3	=	correction factor for bed condition;
K_4	=	correction factor for armoring by bed material size;
K_I	=	flow intensity factor;
K_{yb}	=	depth-pier width factor;
K_d	=	sediment size factor;
K_σ	=	geometric standard deviation for sediment size factor;
K_ζ	=	shape and alignment factor;
K_{ya}	=	depth-abutment protrusion length factor;
K_G	=	geometry factor;

L	=	length of pier or abutment (along flow direction), L;
MSR	=	mean square of residuals;
MSE	=	mean square of errors;
n	=	number of data points used for statistical analysis;
n_1	=	Manning's n for the upstream main channel;
n_2	=	Manning's n for the contracted section;
P	=	value for test statistic;
q_{br}	=	unit discharge that passes under the bridge deck, L^2/T ;
Q	=	volumetric flow rate of water in flume, L^3/T ;
Q_1	=	flow in the upstream channel transporting sediment, L^3/T ;
Q_2	=	flow in the contracted channel, L^3/T ;
Q_s	=	total sediment transport of approach flow, M/T ;
R^2	=	coefficient of determination;
S_1	=	slope of energy grade line of main channel, L/L ;
SSE	=	sum of the squares of the errors;
SSR	=	sum of the squares of the residuals;
SSY	=	total sum of squares;
t	=	time of scour, T;
V_a	=	velocity of the approach flow upstream of the bridge deck, L/T ;
V_b	=	average velocity of flow under the bridge deck, L/T ;
V_c	=	critical velocity of the flow for incipient motion of the bed material, L/T ;
V_c'	=	critical velocity at the pier, L/T ;
V_1	=	mean velocity of flow directly upstream of the pier, L/T ;
V_{ac}	=	average velocity in the contracted section, L/T ;
V_*	=	$(gy_1S_1)^{1/2}$; shear velocity in the upstream section, L/T ;
w	=	depth of flow overtopping the bridge, L;
W_1	=	bottom width of the approach (unconstricted) section, L;
W_2	=	bottom width of the bridge (constricted) section, L.
X_k	=	k th independent variable;
y	=	depth of approach flow, L;
y_1	=	average depth in the upstream main channel, L;
y_2	=	average depth in the contracted section, L;
y_0	=	existing depth in the contracted section before scour, L;

y_r	=	regime flow depth, L;
y_{pds}	=	equilibrium depth of pressure flow deck scour measured from the mean bed elevation, L;
y_{pps}	=	equilibrium depth of pressure flow pier scour measured from the mean bed elevation, L;
y_{pas}	=	equilibrium depth of pressure flow abutment scour measured from the mean bed elevation, L;
y_{pls}	=	equilibrium depth of pressure flow local scour measured from the mean elevation, L;
Y	=	dependent variable;
Y_i	=	the value of a measured data point;
Y_s	=	maximum local scour depth. This depth includes both pier and pressure scour caused by the submerged bridge deck, L;
Y_1	=	depth of flow immediately upstream of the bridge pier, L;
Y_0	=	depth of flow in the bridge opening, L.
β	=	contraction ratio;
β_0	=	y-intercept of the linear relationship;
β_k	=	slope of the regression line for the kth independent variable;
Δh	=	change in WSE from upstream bridge face to downstream, L;
ε	=	random deviation or random error;
γ_s	=	sediment submerged specific weight, M/L^2T^2 ;
μ	=	dynamic viscosity, M/LT ;
ν	=	kinematic viscosity, L^2/T ;
θ	=	angle of attack of flow, degrees;
ρ	=	fluid density, M/L^3 ;
σ_g	=	geometric standard deviation of the bed material;
σ	=	standard deviation;
σ^2	=	statistical variance;
τ_1	=	grain shear stress, M/LT^2 ;
τ_c	=	critical shear stress, M/LT^2 ;
ω	=	median fall velocity of the bed material based on D_{50} , L/T ;

1 INTRODUCTION

1.1 GENERAL BACKGROUND

As the population of the world continues to grow, so does the requirement of transportation across waterways. Many factors influence the design and construction of bridges. From a civil engineering standpoint, hydraulic analysis for a bridge over a waterway can be considered essential for the design and operation of safe and reliable bridges. Scour can be considered one of the key components in the design of bridges through hydraulic analysis. Scour can be classified as the removal of sediment by a swift current of water. A scour hole remains as the depression when sediment washes away from the bottom of a channel. Specifically related to bridges, there are three types of scour: local scour, the removal of sediment from around bridge piers or abutments; contraction scour, the removal of sediment from the bottom and sides of the channel; and degradational scour, the general removal of sediment from the channel bottom by the flow of the channel. Before 1985, design and construction of highway bridges did not incorporate the effects of scour. After several bridge failures attributed to local scour and flood conditions, bridge design procedures were required to incorporate an analysis of the effects of scour. Consequently, bridge scour estimation procedures have undergone scrutiny in an attempt to improve the techniques available for use by the hydraulic

engineering community. Figure 1.1 presents a photograph showing an example of bridge failure due to local scour and flooding.

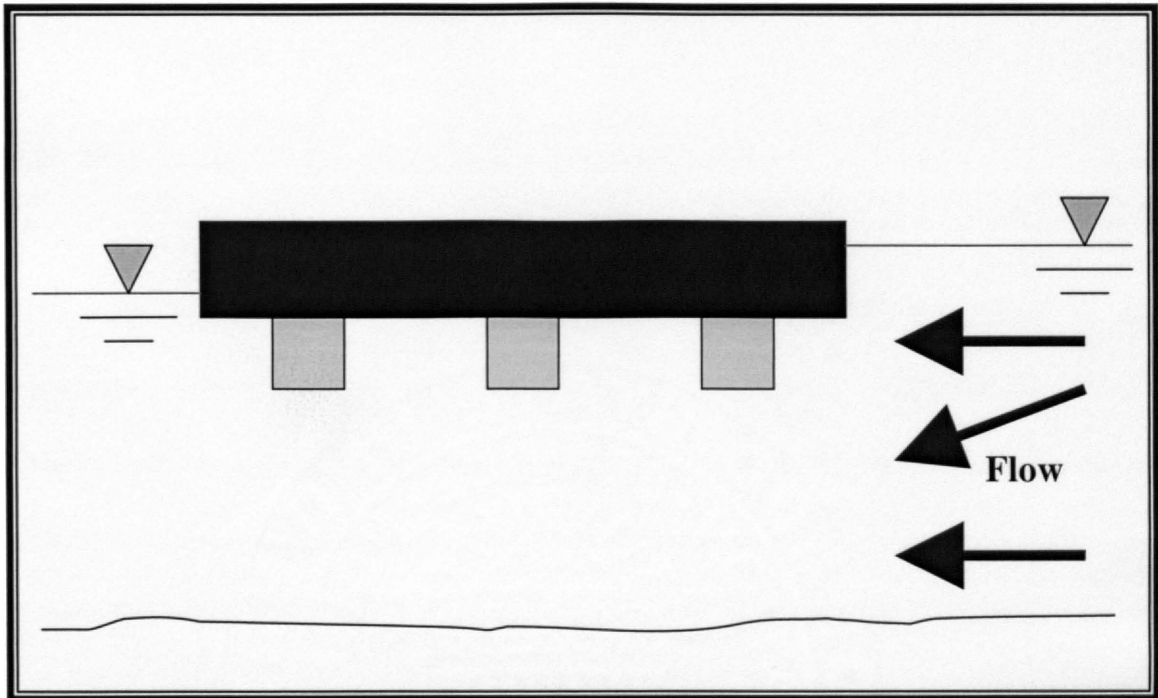


• **Figure 1.1 – Example of bridge failure due to local scour and flooding**

1.2 DEFINITION OF PRESSURE FLOW

Scour caused by the occurrence of pressure flow requires a comprehensive understanding. Pressure flow can be defined as flow in which the low chord of a bridge becomes inundated and the flow through the bridge opening transitions from a free surface flow to a pressurized condition, leading to a submerged or partially submerged

bridge deck condition. Figure 1.2 presents a schematic of a typical bridge deck flowing under a partially submerged pressure flow condition.



• **Figure 1.2 – Profile view of typical bridge deck flowing under a partially submerged pressure flow condition**

Most scour estimation techniques have been developed for free surface flow conditions. Free surface flow conditions can be modeled assuming a hydrostatic pressure distribution, yielding known relationships between depth, velocity, and shear stress of the flow. Pressure flow conditions should not be modeled assuming a hydrostatic pressure distribution, as pressure flow violates the known relationships defining a hydrostatic pressure distribution. A non-hydrostatic pressure distribution leads to distorted velocity profiles, resulting in larger magnitudes of scour at bridges than for free surface flow. With the intent of determining the magnitude of scour at bridges under a pressure flow

condition, Colorado State University (CSU) and the Federal Highway Administration (FHWA) developed a testing program to examine pressure flow effects on scour at bridges.

1.3 RESEARCH OBJECTIVES AND SCOPE

The testing program was performed in the Hydraulics Laboratory at the Engineering Research Center (ERC), Colorado State University. Two sets of pressure flow scour data were acquired during the study. Arneson (1997) analyzed the first set of data and developed two scour prediction equations for a pressure flow condition. One equation was for pressure flow deck scour and the other equation was for pressure flow pier scour. Data from the second set were collected for further development of a pressure flow deck scour predictive equation and a pressure flow abutment scour prediction equation. This thesis will utilize the second set of data for development while examining and referencing data reported by Arneson (1997). The objectives of this research are:

1. Define the processes by which pressure flow scour occurs at bridges;
2. Develop relationships which can be utilized to predict bridge scour under a pressure flow condition; and
3. Compare the findings of this study with Arneson (1997).

In order to meet the previous three objectives, a scope of research was defined as:

1. Conduct a literature review including the necessary background information to fully understand and develop the foundation for defining pressure flow scour for both free surface and pressure flow conditions at bridges.
2. Compile and verify the second set of data produced from the testing program to provide the foundation for development of a series of relationships to predict pressurized bridge scour.
3. Develop pressure flow bridge scour predictive relationships for comparison with Arneson (1997).

2 LITERATURE REVIEW

2.1 INTRODUCTION

Scour of bridge foundations (piers and abutments) has been studied for many years. To fully understand pressure flow scour research efforts, an understanding of the background information and a literature review were performed. Subsequent sections provide the necessary background information, a bridge scour review and a summary of the literature review.

2.2 BACKGROUND INFORMATION

During the 1920's, bridge specifications were developed by the American Association of State Highway and Transportation Officials (AASHTO) in conjunction with the U.S. Bureau of Public Roads (BPR), now the FHWA. When developing bridge specifications, only minor consideration was given to hydraulic analysis and little consideration to the effect of local scour during bridge design. Most of the actual design, even into the late 1970's, was based on the experience of the state bridge engineer. In the 1940's, Carl Izzard established the Hydraulics Research Division within the BPR to

develop research programs. In 1950, Lester Herr continued to develop the bridge hydraulics research programs. Over the years, the scientific base for bridge hydraulics continued to grow, and in 1986, the FHWA authored a manual providing the best tools for safe design to include stream dynamics and scour (ASCE, 1999). Following the Schoharie Creek Bridge failure in April 1987, the FHWA established a national scour evaluation program as an integral part of the National Bridge Inspection Program. The FHWA published Hydraulic Engineering Circular 18 (HEC-18), "Evaluating Scour at Bridges," (Richardson & Davis, 1995) and Hydraulic Engineering Circular 20 (HEC-20), "Stream Stability at Highway Structures," (Lagasse et al., 1995) and Hydraulic Engineering Circular 23 (HEC-23), "Bridge Scour and Stream Instability Countermeasures," (Lagasse et al., 1997) to provide appropriate design manuals for bridge scour.

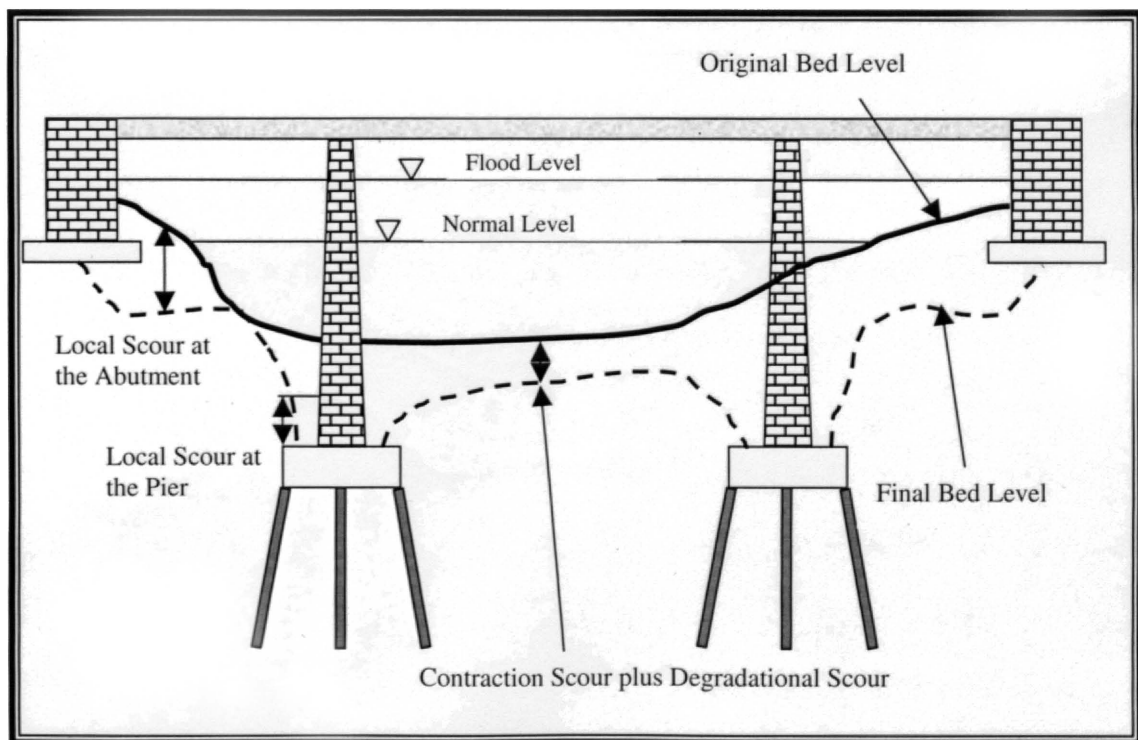
In 1998, the FHWA reported that 80 percent of the 485,000 bridges over water in the U.S. have been screened or evaluated for scour vulnerability. Results indicate that 66,000 bridges are scour susceptible and another 97,000 have unknown foundations. About 17,000 of the 66,000 scour susceptible bridges have been classified as scour critical (Richardson, 1999). The FHWA directed that scour critical bridges be monitored, repaired or scour protected.

2.3 BRIDGE SCOUR REVIEW

Scour of bridge foundations (piers and abutments) represents the largest single cause of bridge failure in the United States (ASCE, 1999). Methodical scour research

began in 1949 with the research of E.M. Laursen (ASCE, 1999). Unfortunately, the application of scour research to the design of bridges did not occur until several bridges failed due to local scour. Over the years, bridge scour research has focused on the study of free surface flow. During the past decade, research related to pressure flow scour has become increasingly important.

Bridge scour can be segmented into three components: contraction scour, the removal of sediment from the bottom and sides of the channel; local scour, the removal of sediment from around bridge piers or abutments; and degradational scour, the general removal of sediment from the channel bottom by the flow of the channel. Figure 2.1 presents a diagram of the three different types of scour that can occur at a bridge opening.



• Figure 2.1 – Profile view displaying types of scour at a bridge opening

Scour at a bridge can further be classified as clear water or live-bed conditions. Clear water conditions refer to conditions in which the bed material upstream of the scour area does not move, implying that the bed shear stresses in the areas upstream of the bridge are at or below the critical shear stress value for incipient motion of the bed material. Wash load, however could be present. Live-bed conditions occur when the hydraulics acting on the bed material upstream of the bridge have exceeded the critical shear stress value for incipient motion and thereby cause sediment input into the scour zone from upstream. Calculating the critical velocity assists in determining whether the section upstream of a bridge can be classified as a live-bed or clear water condition. According to Richardson & Davis (1995), to determine if the flow upstream of a bridge will be transporting bed material, calculate the critical velocity for incipient motion, V_c , of the median grain size of the bed material and compare it with the mean flow velocity, V , in the main channel. When the critical velocity of the bed material exceeds the mean flow velocity ($V_c > V$), clear water conditions exist. However, if the critical velocity falls below the mean flow velocity ($V_c < V$), then live-bed conditions exist. Critical velocity, as presented in HEC-18 (Richardson & Davis, 1995), can be computed with

$$V_c = 6.19y^{1/6}D_{50}^{1/3}$$

• **Equation 2.1**

Where,

V_c = critical velocity above which bed material will be transported, m/s;
 y = depth of approach flow, m; and
 D_{50} = grain size for which 50 percent of the bed material is finer, m.

In the following discussion of many of the pertinent studies on scour at bridges, the variables in the equations are dimensionless unless they are explicitly defined with units. Additionally, some of the variables in the equations have been modified from the author's original format as to be consistent throughout this thesis. Succeeding sections discuss the three types of bridge scour with their respective bridge scour predictive equations for free surface and pressure flow conditions.

2.3.1 CONTRACTION SCOUR

Contraction scour can occur where a foundation and/or road approach embankments of a bridge constrict the waterway. Alternatively, contraction scour can occur if a bridge is placed in a natural constriction in the width of a channel. Ensuing sections discuss free surface contraction scour and pressure flow contraction scour.

2.3.1.1 FREE SURFACE CONTRACTION SCOUR

Richardson & Davis (1995), presented two forms of contraction scour relating to the competence of the uncontracted approach flow to transport bed material into the contraction. Live-bed and clear water contraction scour equations presented in HEC-18 (Richardson & Davis, 1995), were developed with the application of the principle of conservation of sediment transport.

For bridge piers, abutments, or any width contraction, the degree of contraction can be calculated using the contraction ratio, β , given by Melville & Coleman (2000) as

$$\beta = \frac{W_1}{W_2}$$

• Equation 2.2

Where,

- β = contraction ratio;
- W_1 = bottom width of the approach (unconstricted) section, L; and
- W_2 = bottom width of the bridge (constricted) section, L.

As an example, a ten percent reduction in channel width due to the presence of piers, abutments and/or approach embankments results in a contraction ratio of 1.11. From continuity, a decrease in flow area results in an increase in average velocity and bed shear stress through the contraction. Hence, an increase in erosive forces through the contraction would be expected.

During live-bed conditions, fully developed scour in a bridge opening reaches a state of equilibrium when the rate of sediment transported into the contracted section equals the rate of sediment transported out of the contracted section (Richardson & Davis, 1995). Laursen (1960) derived a live-bed contraction scour equation based on a simplified transport function, transport of sediment in a long contraction, and other simplifying assumptions. Laursen's contraction scour predictive equation for live-bed conditions follows as

$$\frac{y_2}{y_1} = \left(\frac{Q_2}{Q_1} \right)^{6/7} \beta^{k_1} \left(\frac{n_2}{n_1} \right)^{k_2} \text{ and } d_s = y_2 - y_0$$

• Equation 2.3

Where,

- d_s = average depth of scour, m;
- y_1 = average depth in the upstream main channel, m;
- y_2 = average depth in the contracted section, m;
- y_0 = existing depth in the contracted section before scour, m;
- Q_1 = flow in the upstream channel transporting sediment, m³/s;
- Q_2 = flow in the contracted channel, m³/s;
- β = contraction ratio;
- n_1 = Manning's n for the upstream main channel;
- n_2 = Manning's n for the contracted section;
- k_1 = correction factor for mode of sediment transport, Table 2.1; and
- k_2 = correction factor for mode of sediment transport, Table 2.1.

• Table 2.1 – Correction factors for mode of sediment transport

V_*/ω	k_1	k_2	Mode of Bed Material Transport
<0.50	0.59	0.066	Mostly contact bed material discharge
0.50 to 2.0	0.64	0.21	Some suspended bed material discharge
>2.0	0.69	0.37	Mostly suspended bed material discharge

Where,

- V_* = $(gy_1S_1)^{1/2}$; shear velocity in the upstream section, m/s;
- ω = median fall velocity of the bed material based on D_{50} , m/s;
- g = acceleration due to gravity, m/s²;
- S_1 = slope of energy grade line of main channel, m/m
- D_{50} = grain size for which 50 percent of the bed material is finer, m.

Under clear water conditions, sediment transport into a contracted section equals zero and maximum scour occurs when the shear stress reaches the critical shear stress of the bed material in the contracted section. Richardson & Davis (1995), with initial work developed by Laursen (1963), the equation for clear water contraction scour can be presented as

$$y_2 = \left[\frac{V_{ac}^2}{40D_m^{2/3}} \right]^3 \text{ and } d_s = y_2 - y_0$$

• Equation 2.4

Where,

- d_s = average depth of scour, m;
- y_2 = average depth in the contracted section, m;
- y_0 = existing depth in the contracted section before scour, m;
- V_{ac} = average velocity in the contracted section, m/s; and
- D_m = diameter of the bed material ($1.25D_{50}$) in the contracted section, m.

Equation 2.4 assumes a homogeneous bed material. However, with clear water conditions in non-homogeneous materials, using the sediment layer with the finest D_{50} to compute contraction scour would result in the most conservative estimate of contraction scour (Richardson & Davis, 1995).

2.3.1.2 PRESSURE FLOW CONTRACTION SCOUR

Currently there is no known research related to a predictive equation or documentation on mechanics of contraction scour under pressure flow. Although, one could theorize that contraction scour under pressure flow conditions would be greater than for free surface conditions given that the velocities under that bridge deck would be increased due to the pressurized condition.

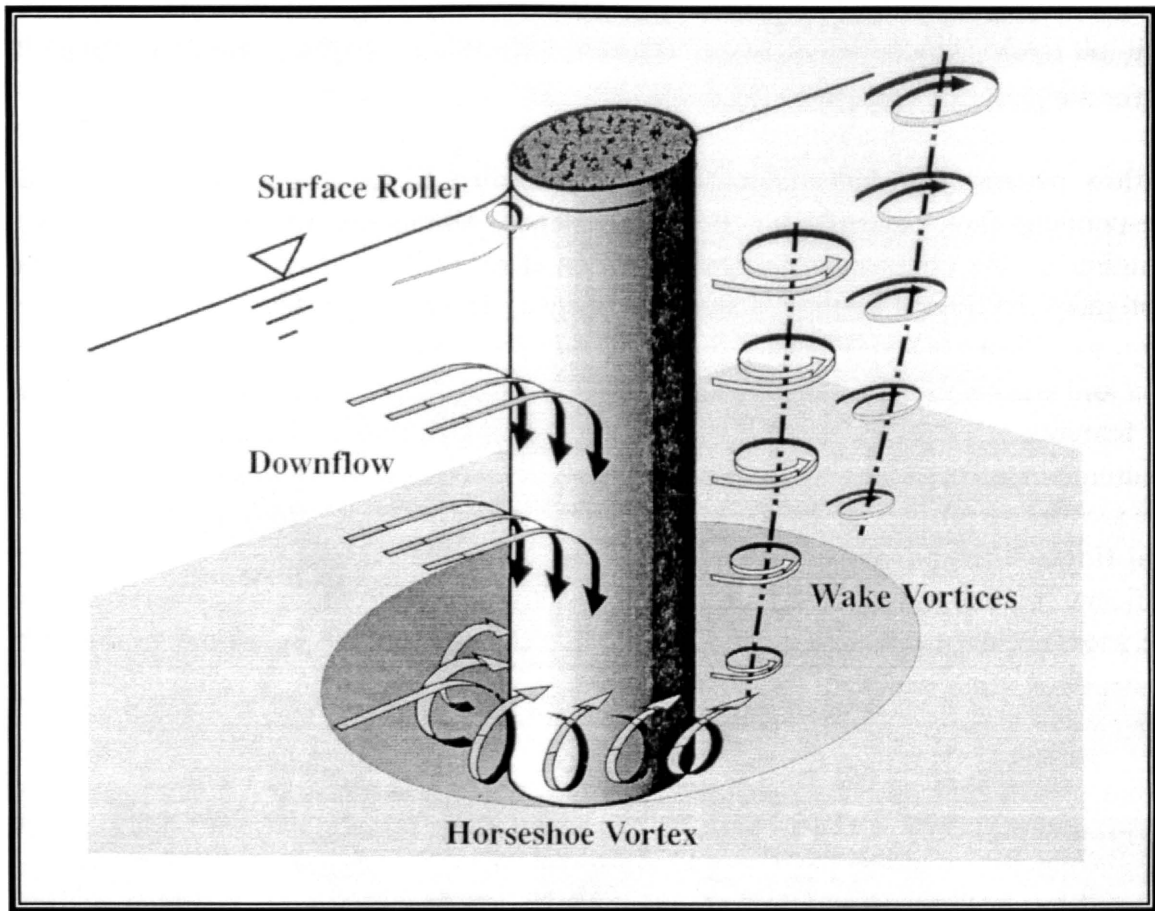
2.3.2 LOCAL SCOUR

Local scour occurs at a bridge opening when the local flow field near the bridge piers and/or abutments generates erosive forces greater than the resistance force of the bed material. Dominant features of the flow field near a pier or abutment are large-scale eddy structures, or a system of vortices, which develop around the structure. Vortex systems constitute the basic mechanism of local scour and strongly affect the vertical component of velocity near the structure. Succeeding sections discuss local scour at bridge piers, at bridge abutments and under pressure flow conditions.

2.3.2.1 LOCAL SCOUR AT BRIDGE PIERS

Flow field and scour hole patterns at and around a circular pier are presented schematically in Figure 2.2 (Melville & Coleman, 2000). Upstream of the pier, the section of the scour hole resembles a frustum of an inverted cone. Principle features of the flow, discretised in Figure 2.2 for simplicity, include downflow ahead of the pier, the

horseshoe vortex at the base of the pier, the surface roller upstream of the pier and wake vortices downstream of the pier. Downflow results as a consequence of flow deceleration ahead of the pier and the associated stagnation pressure on the face of the pier. A resulting downward pressure gradient at the pier face generates downflow. Downflow impinging on the bed acts like a vertical jet in eroding a groove immediately adjacent to the front of the pier. Formation of the groove undermines the scour hole slope. Bed material slope collapses in local avalanches of sediment into the erosion zone, thus maintaining the slope at the local angle of repose of the sediment. Development of the scour hole around the pier also creates a lee eddy, also known as the horseshoe vortex. Dislodged particles are transported past the pier via the horseshoe vortex. Resultant forces of downflow and the horseshoe vortex provide the primary mechanisms responsible for producing scour. Wake vortices arise from flow separation at the sides of a pier. Wake vortices translate downstream and collect sediment from the bed while transporting sediment entrained by downflow and the horseshoe vortex. Flow field and scour hole patterns shown in Figure 2.2 are analogous for piers of varying geometry.



• **Figure 2.2 – Flow field and scour patterns at a circular pier (Melville & Coleman, 2000)**

A selection of some of the most commonly used and referenced equations for free surface pier scour are given in Table 2.2 from Melville & Coleman (2000). In addition to the equations presented in Table 2.2, Richardson & Davis (1995), recommend Equation 2.5 as the standard from HEC-18 for both live-bed and clear water free surface pier scour.

• Table 2.2 – Commonly used free surface pier scour equations

Reference	Equation	Comments
Laursen (1958)	$\frac{b}{y} = 5.5 \frac{d_s}{y} \left[\left(\frac{d_s}{11.5y} + 1 \right)^{1.7} - 1 \right]$	applies to live-bed scour d_s = depth of pier scour, L b = pier width, L; y = flow depth, L
Laursen (1963)	$\frac{b}{y} = 5.5 \frac{d_s}{y} \left[\frac{\left(\frac{d_s}{11.5y} + 1 \right)^{7/6}}{\left(\frac{\tau_1}{\tau_c} \right)^{0.5}} - 1 \right]$	applies to clear water scour τ_1 = grain roughness component of shear, M/LT^2 τ_c = critical shear stress at incipient motion, M/LT^2
Larras (1963)	$d_s = 1.05 K_s K_\theta b^{0.75}$	K_s = shape factor; K_θ = angle of attack factor
Breusers (1965)	$d_s = 1.4b$	derived from data for tidal flows
Blench (1969)	$\frac{d_s + y}{y_r} = 1.8 \left(\frac{b}{y_r} \right)^{0.25}$	y_r = regime depth = $1.48(q^2/F_B)^{1/3}$ where $F_B = 1.9d^{0.5}$, d in mm and q in m^2/s
Shen et al. (1969)	$d_s = 0.000223 \left(\frac{vb}{v} \right)^{0.619}$	V = average flow velocity, L/T ; v = kinematic viscosity, L^2/T
Coleman (1971)	$\frac{V}{\sqrt{2gd_s}} = 0.6 \left(\frac{V}{b} \right)^{0.9}$	g = acceleration due to gravity, L/T^2
Hancu (1971)	$\frac{d_s}{b} = 2.42 \left(\frac{2V}{V_c} - 1 \right) \left(\frac{V^2}{gb} \right)^{1/3}$	$(2V/V_c - 1) = 1$ for live-bed scour; V_c = critical velocity
Neill (1973)	$d_s = K_s b$	$K_s = 1.5$ for round-nosed and circular piers; $K_s = 2.0$ for rectangular piers
Breusers et al. (1977)	$\frac{d_s}{b} = f \left(\frac{V}{V_c} \right) \left[2.0 \tanh \left(\frac{y}{b} \right) \right] K_s K_\theta$	$f(V/V_c) = 0$ for $V/V_c \leq 0.5$ $= (2V/V_c - 1)$ for $0.5 < V/V_c < 1$ $= 1$ for $V/V_c > 1$

• Table 2.2 (continued) – Commonly used free surface pier scour equations

Reference	Equation	Comments
Jain & Fischer (1980)	$\frac{d_s}{b} = 1.86 \left(\frac{y}{b}\right)^{0.5} (Fr - Fr_c)^{0.25}$	$Fr = V/(gy)^{0.5}$ $Fr_c = V_c/(gy)^{0.5}$
Jain (1981)	$\frac{d_s}{b} = 1.84 \left(\frac{y}{b}\right)^{0.3} Fr_c^{0.25}$	
Chitale (1988)	$d_s = 2.5b$	
Melville & Sutherland (1988)	$\frac{d_s}{b} = K_I K_{yb} K_d K_s K_\theta$	K_I = flow intensity factor; K_{yb} = depth-size factor; K_d = sediment size factor
Breusers & Raudkivi (1991)	$\frac{d_s}{b} = 2.3 K_{yb} K_s K_d K_\sigma K_\theta$	K_σ = geometric standard deviation for sediment size factor
Gao et al. (1993)	$d_s = 0.46 K_\zeta b^{0.60} y^{0.15} d^{-0.07} \left[\frac{V - V_c'}{V_c - V_c'} \right]^{0.7\eta}$ $V_c = \left(\frac{y}{d}\right)^{0.14} \left[17.6 \left(\frac{\rho_s - \rho}{\rho}\right) d + 6.05 \times 10^{-7} \left(\frac{10 + y}{d^{0.72}}\right) \right]^{0.5}$ $V_c' = 0.645 \left(\frac{d}{b}\right)^{0.053} V_c$	V_c' = incipient velocity at pier; K_ζ = shape and alignment factor; d = grain size; $\eta = 1$ for clear water scour and < 1 for live bed scour; i.e., $\eta = (V_c/V)^{9.35+2.23 \log d}$; where all units are S.I.
Melville (1997)	$d_s = K_{yb} K_I K_d K_s K_\theta$	

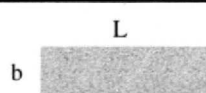
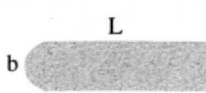
$$\frac{d_s}{b} = 2.0 K_s K_\theta K_3 K_4 \left(\frac{y_1}{b} \right)^{0.35} Fr_1^{0.43}$$

• Equation 2.5

Where,

- d_s = maximum pier scour depth, m;
- b = pier width, m;
- K_s = correction factor for pier nose shape, Table 2.3;
- K_θ = correction factor for angle of attack of flow, Equation 2.6;
- K_3 = correction factor for bed condition, Table 2.4;
- K_4 = correction factor for armoring by bed material size;
- y_1 = flow depth directly upstream of pier, m;
- Fr_1 = Froude number directly upstream of the pier = $V_1/(gy_1)^{1/2}$;
- V_1 = mean velocity of flow directly upstream of the pier, m/s; and
- g = acceleration due to gravity, m/s^2 .

• Table 2.3 – Correction factor, K_s , for pier nose shape

Shape of pier nose	Shape Diagram	K_s
Square nose		1.1
Round nose		1.0
Circular cylinder		1.0
Group of cylinders		1.0
Sharp nose		0.9

$$K_{\theta} = \left(\cos\theta + \frac{L}{b} \sin\theta \right)^{0.65}$$

• Equation 2.6

Where,

- b = pier width, m;
- L = length of pier, m; and
- θ = angle of attack of flow, degrees;

• Table 2.4 – Correction factor, K_3 , for bed condition

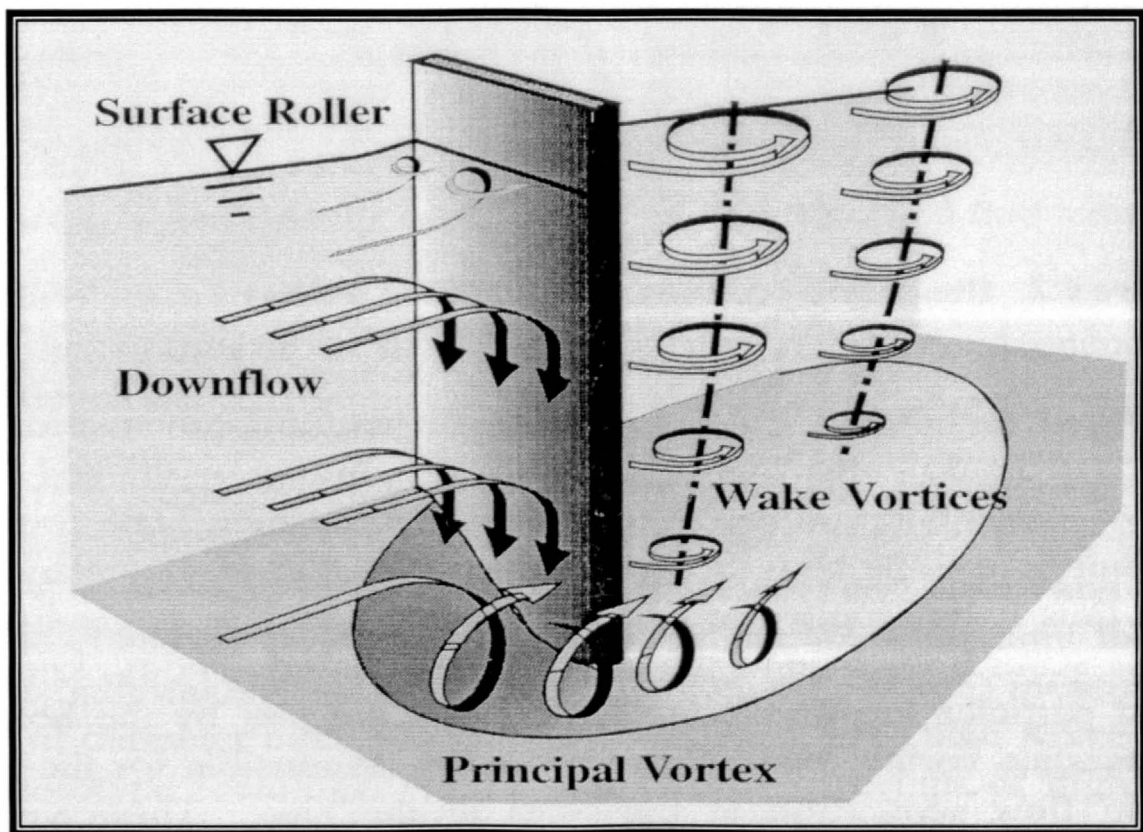
Bed Condition	Dune Height (H), m	K_3
Clear water scour	n/a	1.1
Plane bed and antidune flow	n/a	1.1
Small dunes	$3 > H \geq 0.6$	1.1
Medium dunes	$9 > H \geq 3$	1.2 to 1.1
Large dunes	$H \geq 9$	1.3

Correction factor, K_4 , decreases scour depths for armoring of the scour hole for bed materials that have a D_{50} equal to or larger than 0.06 m. The maximum value for K_4 should not exceed 1.0 and the minimum value for K_4 should not be less than 0.7. Further explanation of the correction factor, K_4 , can be found in HEC-18 (Richardson & Davis, 1995).

2.3.2.2 LOCAL SCOUR AT BRIDGE ABUTMENTS

Shen et al. (1966) recognized that scour at an abutment should be a similar process to scour at a pier of the same dimensions as the abutment. Kwan (1988) indicated that the flow pattern at bridge abutments varies according to the length of the

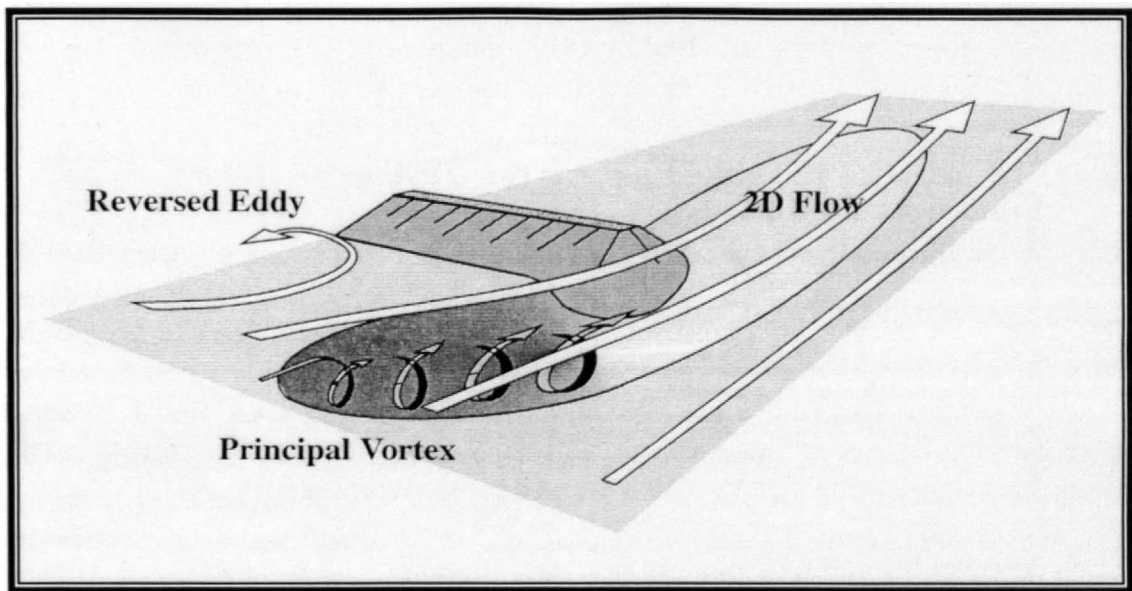
abutment and the corresponding flow obstruction. An illustration of the flow field and scour patterns at a short abutment is shown in Figure 2.3 (Melville & Coleman, 2000). Principle features are discretised for clarity and comprise the surface roller, downflow, principal vortex and wake vortices. The principle vortex can be considered analogous to the horseshoe vortex at piers. Additionally, the flow field at piers and short abutments are similar.



• Figure 2.3 – Flow field and scour patterns at a short abutment (Melville & Coleman, 2000)

A schematic of the flow field and scour patterns at a long abutment are shown in Figure 2.4 (Melville & Coleman, 2000). For a long abutment, the flow field and scour

hole geometry are similar to those at shorter abutments. However, downflow contributes a less significant component, and a large scale circulating reverse eddy occurs ahead of the abutment near the bank. Additionally, due to shallowness of the flow, the velocity has a strong two-dimensional characteristic. Increased scour activity occurs near the end of the abutment, at the principal vortex concentration point.



• **Figure 2.4 – Flow field and scour patterns at a long abutment (Melville & Coleman, 2000)**

Commonly used equations for free surface abutment scour are presented in Table 2.5 from Melville & Coleman (2000). In addition to the equations presented in Table 2.5, Richardson & Davis (1995) recommend Equation 2.7 as the standard from HEC-18, for predicting free surface abutment scour under live-bed conditions. Equation 2.7 was obtained from analysis of 170 live-bed scour measurements in laboratory flumes via regression techniques from Froehlich (1989).

• Table 2.5 – A selection of free surface abutment scour equations

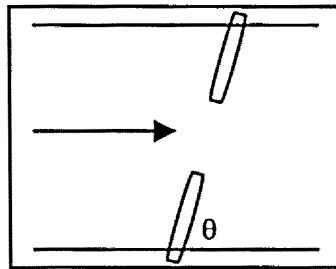
Reference	Equation	Comments
Liu et al. (1961)	$\frac{d_s}{y} = 1.1 \left(\frac{a}{y} \right)^{0.4} Fr^{0.33}$	applies to live-bed scour at spill through abutments; d_s = depth of abutment scour; y = depth of approach flow; a = abutment protrusion length; Fr = Froude number of approach flow
Liu et al. (1961)	$\frac{d_s}{y} = 2.15 \left(\frac{a}{y} \right)^{0.4} Fr^{0.33}$	applies to live-bed scour at wing-wall or vertical wall abutments
Liu et al. (1961)	$\frac{d_s}{y} = 12.5 Fr \beta$	applies to clear water scour at vertical wall abutment; β = contraction ratio
Laursen (1962)	$\frac{a}{y} = 2.75 \frac{d_s}{y} \left[\left(\frac{d_s}{11.5y} + 1 \right)^{1.7} - 1 \right]$	applies to live-bed scour at a protruding abutment
Laursen (1963)	$\frac{a}{y} = 2.75 \frac{d_s}{y} \left[\frac{\left(\frac{d_s}{11.5y} + 1 \right)^{7/6}}{\left(\frac{\tau_1}{\tau_c} \right)^{0.5}} - 1 \right]$	applies to clear water scour; τ_1 = grain roughness component of bed shear; τ_c = critical shear stress
Melville (1992, 1997)	$\frac{d_s}{a} = K_I K_{ya} K_d K_s K_\theta K_G$	K_I = flow intensity factor; K_{ya} = depth-size factor; K_d = sediment size factor; K_s = shape factor; K_θ = angle of attack of flow factor; K_G = geometry factor

$$\frac{d_s}{y} = 2.27 K_s K_\theta \left(\frac{a}{y} \right)^{0.43} Fr^{0.61} + 1$$

• Equation 2.7

Where,

- d_s = maximum abutment scour depth, m;
 a = abutment protrusion length, m;
 K_s = correction factor for abutment shape, Table 2.6;
 K_θ = correction factor for angle of abutment to flow = $(\theta/90)^{0.13}$;
 $\theta < 90$ degrees if abutments point downstream;
 $\theta > 90$ degrees if abutments point upstream;



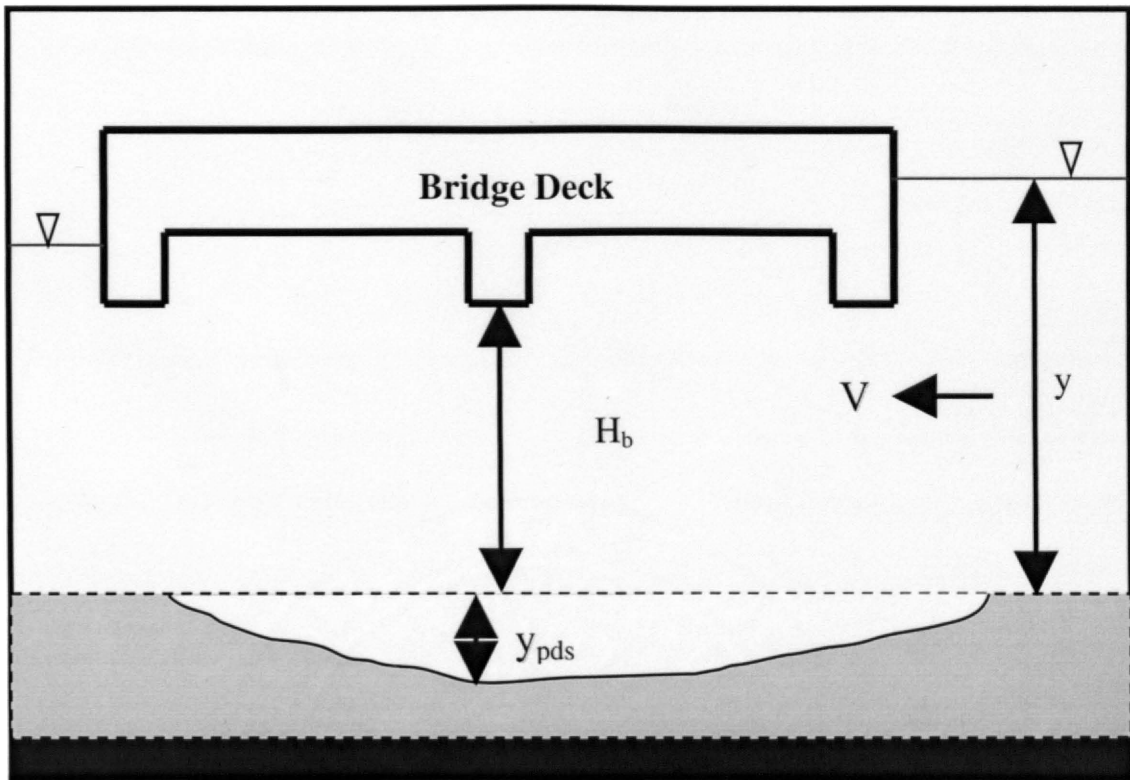
- θ = angle of inclination;
 y = flow depth directly upstream of abutment, m; and
 Fr = Froude number of approach flow upstream of abutment.

• Table 2.6 – Correction factor, K_s , for abutment shape

Description	K_s
Vertical-wall abutment	1.00
Vertical-wall abutment with wing walls	0.82
Spill-through abutment	0.55

2.3.2.3 LOCAL SCOUR UNDER PRESSURE FLOW

Pressure flow can be defined as flow in which the low chord of a bridge becomes inundated and the flow through the bridge opening transitions from a free surface flow to a pressurized flow condition, yielding a submerged or partially submerged bridge deck. Common variables used to perform scour analysis at a partially submerged bridge are displayed in Figure 2.5. Pressure flow conditions should not be modeled assuming of a hydrostatic pressure distribution, as pressure flow violates the known relationships defining a hydrostatic pressure distribution (Arneson, 1997). A non-hydrostatic pressure distribution leads to distorted velocity profiles, resulting in larger magnitudes of scour at bridges than for free surface flow. Hence, submergence of a bridge increases the scour at the bridge compared to a bridge in an unsubmerged condition (Melville & Coleman, 2000). Scour that develops during submerged or partially submerged conditions can be segmented into two components; local pressure scour and scour due to bridge deck submergence, termed pressure flow deck scour. Local pressure scour refers to the scour that occurs under a pressure flow condition at a pier or an abutment. Pressure flow deck scour refers to the scour that occurs under a pressure flow condition due to bridge deck submergence.



• **Figure 2.5 – Pressure flow scour variables at a partially submerged bridge**

In 1991, Abed reported on the development of a large-scale eddy during pressure flow conditions. This large-scale eddy can be considered analogous to the downflow that occurs during free surface local scour, which leads to the principle vortex. As with free surface local scour, vortex systems constitute the basic mechanism of pressure flow scour and strongly affect the vertical component of velocity near the structure. Vortex systems, which develop during pressure flow conditions, are not present during free flow conditions. Hence, scour that occurs due to the submergence of the bridge deck will be greater than for unsubmerged bridge deck conditions. Additionally, the local scour which occurs under pressure flow conditions, will be greater than for free surface conditions

because the downflow component of the vortex system will be increased during pressure flow conditions adding to the system of vortices already present at a pier or abutment.

2.3.2.3.1 ABED (1991)

Research conducted at Colorado State University by Abed in 1991 resulted in a prediction equation for pier scour under pressure flow conditions. Essential parameters in Abed's research were bridge opening, approach flow depth and approach flow velocity. From dimensional analysis, Abed determined for pressure conditions that the bridge opening and the Froude number of the approach flow were the significant variables in describing scour. Testing consisted of free flow conditions and pressure flow conditions. Relationships that were developed employed dimensional and regression analyses in both free and pressure flow conditions. Abed stated that the maximum depth of scour expected at a pier under pressure flow could be as high as 2.3 to 10 times as large as the scour that could be expected under free surface flow conditions. However, Abed's experiments did not separate the pressure flow pier scour component from the scour caused by pressure flow deck scour. Abed presented Equation 2.8 which can be used to predict the maximum local pressure flow scour depth for clear water conditions.

$$\frac{Y_s}{Y_1} = K_s K_\theta (4.92 Fr + 0.46 \frac{Y_0}{Y_1} - 0.74)$$

• Equation 2.8

Where,

- Y_s = maximum local scour depth. This depth includes both pier and pressure scour caused by the submerged bridge deck, L;
- Y_1 = depth of flow immediately upstream of the bridge pier, L;
- K_s = correction factor for pier nose shape;
- K_θ = correction factor for angle of attack of approach flow;
- Fr = Froude number of the approach flow; and
- Y_0 = depth of flow in the bridge opening, L.

2.3.2.3.2 JONES (1993, 1995-1996)

Jones (1993, 1995-1996) developed a relationship based on laboratory experiments that could be used to estimate the amount of scour that would result due to the vertical flow contraction associated with pressure flow conditions. Jones concluded that the magnitude of pier scour under pressure conditions approximately equals the magnitude of pier scour under free surface flow conditions. Additionally, Jones determined that the components of pressure flow deck scour and pressure flow pier scour were additive. Jones' equation tended to underestimate the actual scour measured in a bridge opening. This underestimate could be explained in that the tests were performed under clear water conditions and test durations were not long enough to attain maximum scour depths (Arneson & Abt, 1999). Based on dimensional and regression analysis for clear water conditions, Jones presented Equation 2.9 which can be used to predict pressure flow deck scour.

$$\frac{(H_b + y_{pds})}{y} = 1.1021 \left[\left(1 - \frac{w}{y} \right) \frac{V_a}{V_c} \right]^{0.6031}$$

• Equation 2.9

Where,

- H_b = distance from the low chord of the bridge to the average elevation of the bed material, L;
- y_{pds} = equilibrium depth of pressure flow deck scour measured from the mean bed elevation, L;
- y = depth of flow upstream of the bridge deck, L;
- w = depth of flow overtopping the bridge, L;
- V_a = velocity of flow immediately upstream of the bridge deck, L/T;
and
- V_c = velocity under the bridge deck which corresponds to the incipient motion velocity, L/T.

2.3.2.3.3 CHANG (1995)

Chang (1995) used the data collected by Jones (1993, 1995-1996) in an attempt to produce a more general relationship for the prediction of live-bed pressure flow deck scour. Equation 2.10, developed by Chang, over predicted the measured scour. Chang's equation was intended for use in live-bed conditions, but the data used to develop the equation were from a clear water data set.

$$H_b + y_{pds} = \frac{C_q q_{br}}{V_c}$$

• Equation 2.10

Where,

$$C_q = \frac{1}{C_f C_c};$$

$$C_f = 1.5Fr^{0.43} \leq 1.0;$$

$$C_c = \sqrt{0.1 \left(\frac{H_b}{y-w} - 0.56 \right)} + 0.79 \leq 1.0;$$

- q_{br} = unit discharge that passes under the bridge deck, L^2/T ;
 C_f = Froude number reduction (should not exceed 1.0);
 C_q = discharge reduction (should not exceed 1.0);
 C_c = vertical contraction correction (should not exceed 1.0); and
 all other variables are defined previously.

2.3.2.3.4 ARNESON (1997)

Arneson (1997) developed two scour estimation equations for pressure flow conditions. One equation was developed for predicting pressure flow deck scour and the second for predicting pressure flow pier scour.

Experiments were performed in a flume 8 feet wide and 200 feet long with 4 sediment sizes ranging from 0.6 to 3.3 mm, with and without a pier, discharges ranging from 8 to 24 cubic feet per second, and six bridge submergence positions. In total, 24

live-bed tests were conducted. A total of 116 data points were used for the development of a pressure flow deck scour prediction equation. A total of 45 data points were used for the development of a pressure flow pier scour prediction equation.

A dimensional analysis was performed on the hydraulic and geometric parameters collected during the pressure flow experiments. Arneson applied the concept of similitude and then analyzed the model to derive dimensionless parameters. Additionally, statistical analyses were performed applying the principles of least squares and multiple linear regression. Statistical variables included variance, σ^2 , coefficient of determination, R^2 , F statistic, and P-level. Data were checked to assure that relationships between the independent variables were linear, that the variables and residuals were normally distributed, and that multicollinearity between independent variables was avoided. A residual analysis was used to detect the presence of outliers in the data set that could bias the results of the regression analysis.

Arneson's study concluded that the magnitude of total scour at a bridge flowing under pressure flow conditions results from the sum of pressure flow deck scour and pressure flow pier scour. The coefficient of determination for the pressure flow deck scour equation was 0.89, indicating that 89 percent of the variability in the data were explained by the relationship. The coefficient of determination for the pressure flow pier scour equation was 0.71, which explains 71 percent of the data variability. Arneson derived Equations 2.11 and 2.12 for calculating pressure flow deck scour and pressure flow pier scour, respectively.

$$\frac{y_{pds}}{y} = -0.93 + 0.23 \left(\frac{y}{H_b} \right) + 0.82 \left(\frac{y_{pds} + H_b}{y} \right) + 0.03 \left(\frac{V_a}{V_c} \right)$$

• Equation 2.11

Where,

- y_{pds} = equilibrium depth of pressure flow deck scour measured from the mean bed elevation, L;
- y = depth of flow immediately upstream of the bridge deck, L;
- H_b = distance from the low chord of the bridge to the average elevation of the bed material, L;
- V_a = average velocity of flow through the bridge opening, L/T; and
- V_c = velocity of flow at incipient motion of bed material, L/T.

$$\frac{y_{pps}}{b} = -0.25 + 3.59 \left(\frac{V_a}{\sqrt{gy}} \right) + 0.14 \left(\frac{y}{H_b} \right)$$

• Equation 2.12

Where,

- y_{pps} = equilibrium depth of pressure flow pier scour measured from the mean bed elevation;
- b = pier width; and
- all other variables defined previously.

2.3.3 DEGRADATIONAL SCOUR

Degradational scour occurs irrespective of the existence of a bridge and can occur as either long-term or short-term scour, depending upon the time taken for scour development. Short-term degradational scour develops during a single or several closely

spaced large flow events. Long-term degradational scour has a considerably longer time scale, normally on the order of several years and includes lateral bank erosion (Melville & Coleman, 2000). Melville & Coleman (2000) state that long-term degradational scour can be defined as the semi-permanent general lowering of the riverbed due to hydrometeorological changes. Examples of long-term degradational scour include prolonged high flows, geomorphological changes, or human activities. Lateral bank erosion can lead to a bridge being outflanked by the river or to undermining of the abutments. Bank erosion may result from a change in the river controls, such as a sudden change in the river course, meander migration or channel widening. The main causes of degradational scour according to Melville and Coleman (2000) are listed in Table 2.7.

• **Table 2.7 – Main causes of degradational scour**

Action	Type of Cause
Channel Alternations	Human
dredging	Human
channelization	Human
straightening	Human
cut-off formation	Human
Stream Bed Mining	Human
Dam/Reservoir Construction	Human
Land Use Changes	Human
urbanization	Human
deforestation	Human
agricultural activity	Human
Channel Straightening	Nature
cut-off formation	Nature
Tectonic/Volcanic Activity	Nature
landslides, mud flows	Nature
liquefaction	Nature
Fire	Nature
Climate Change	Nature

An estimation of degradational scour and aggradation generally requires significant knowledge of sediment transport and river mechanics. Richardson and Davis (1995) comment that long-term streambed profile changes will usually be difficult to access. Therefore, a review of the pertinent equations for degradational scour was beyond the scope of this thesis.

2.4 SUMMARY

For free surface flow conditions, HEC-18 (Richardson & Davis, 1995) can be considered the standard in the United States for evaluating scour at bridges (piers, abutments, etc.). HEC-18 presents the best available equations for the prediction of free surface contraction scour, prediction of local scour at piers and abutments, and discussion of procedures for examining degradational scour. HEC-18 presents limited information with regard to pressure flow scour.

Research efforts for pressure flow conditions at bridges, aside from information presented in HEC-18, are also limited. In 1991, Abed presented the first known predictive equation for pressure flow scour at bridges. Abed's equation was limited to clear water conditions and did not separate pressure flow local scour from pressure flow deck scour. Jones (1993, 1995-1996) developed a pressure flow deck scour predictive equation, although Jones' equation was developed for clear water conditions and tended to underestimate the actual pressure flow deck scour measured at a bridge. Chang (1995) developed a predictive equation from Jones' data set intended for use under live bed conditions for prediction of pressure flow deck scour. Chang's live-bed predictive

equation was developed from a clear water data set and tended to overestimate the actual pressure flow deck scour measured at a bridge. Arneson (1997) presented one predictive equation for live-bed pressure flow deck scour and another predictive equation for live-bed pressure flow pier scour. Both of the equations presented by Arneson reasonably predicted the actual pressure flow scour measured at a bridge.

There are a few predictive equations for pressure flow deck scour, one predictive equation for pressure flow pier scour, but no predictive equation for pressure flow abutment scour. Validation of the predictive equations for pressure flow deck scour and pressure flow pier scour along with development of a predictive equation for pressure flow abutment scour would help provide a complete set of predictive equations for pressure flow scour at bridges.

3 DATA COLLECTION

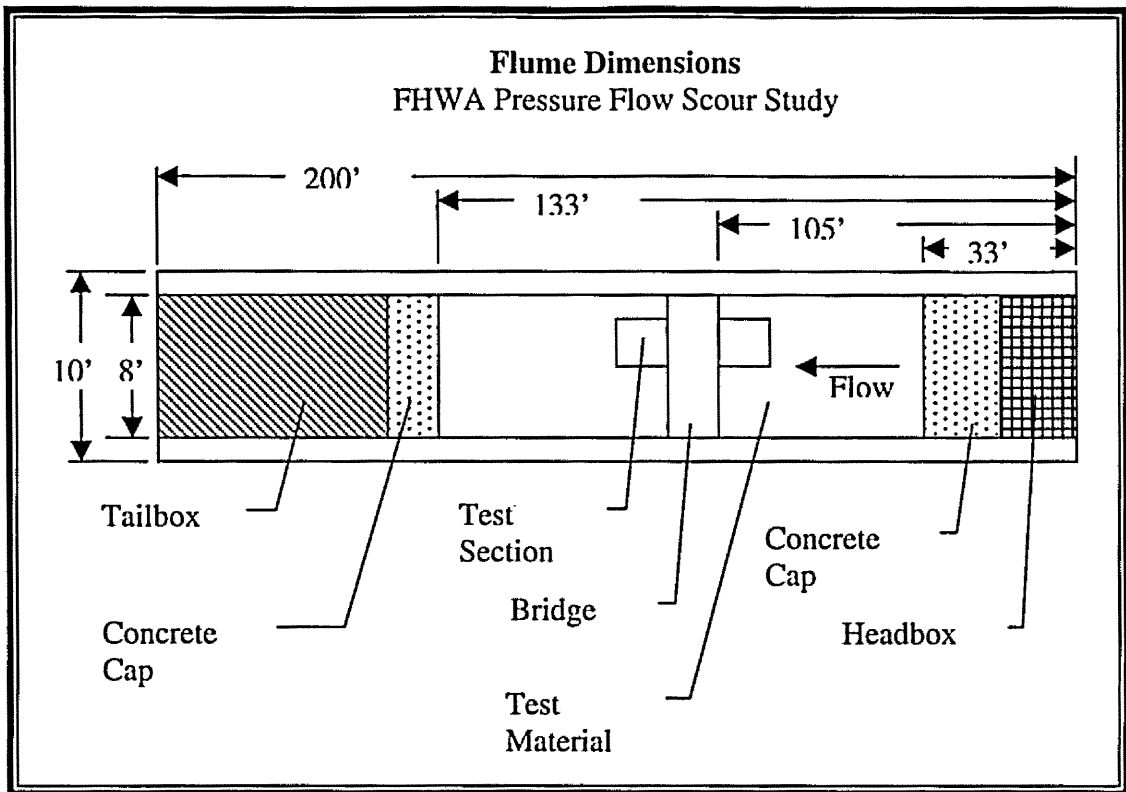
3.1 INTRODUCTION

A series of experiments was conducted to examine the effects of a pressure flow condition on scour at bridges. A model study was conducted at the Hydraulics Laboratory of Colorado State University. A sand bed channel with an abutment supported bridge crossing was simulated in the laboratory. During the testing program, pressure flow effects on scour were examined under varying flow conditions with two sediment sizes. A description of the flume, the model and the data acquisition equipment will be presented.

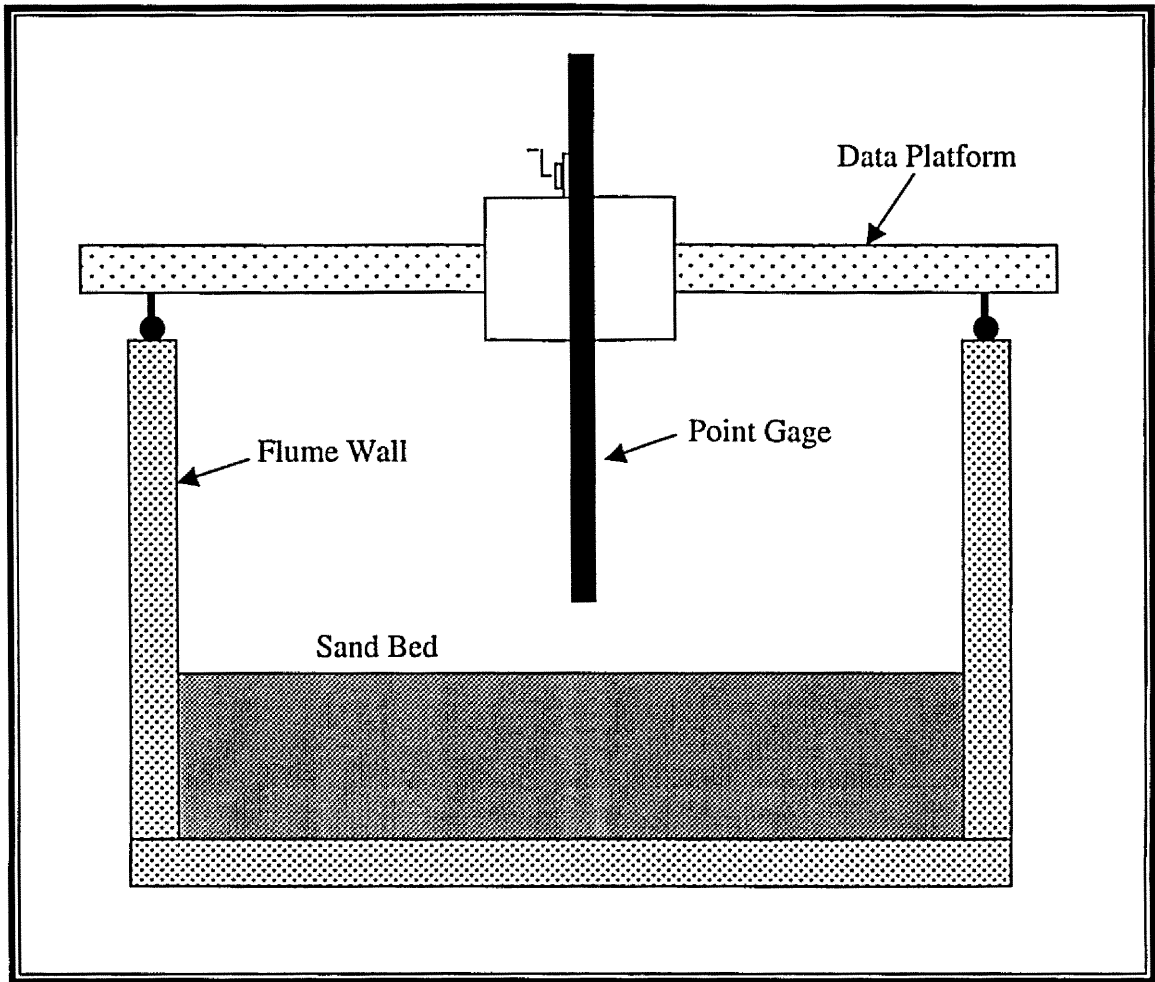
3.2 FLUME DESCRIPTION

A recirculating flume 200 ft long by 8 ft wide was used for the testing program. Figure 3.1 presents a plan view of the flume and test section. Water was supplied to the flume by one 125 horsepower electric pump and two 175 horsepower electric pumps, which could be run separately or in parallel, to achieve a desired discharge. Maximum flume capacity was 100 cubic feet per second (cfs) and the bed slope could be

horizontally adjusted to approximately two percent. A bed slope of 0.09 percent was utilized for all experiments. A motorized cart traversed the flume along a track attached to the top of the flume and served as a platform to mount data acquisition equipment. Data acquisition instrumentation was mounted to a point gauge assembly that attached to the front of the platform, as shown in Figure 3.2.



• Figure 3.1 – Plan view of flume and test section

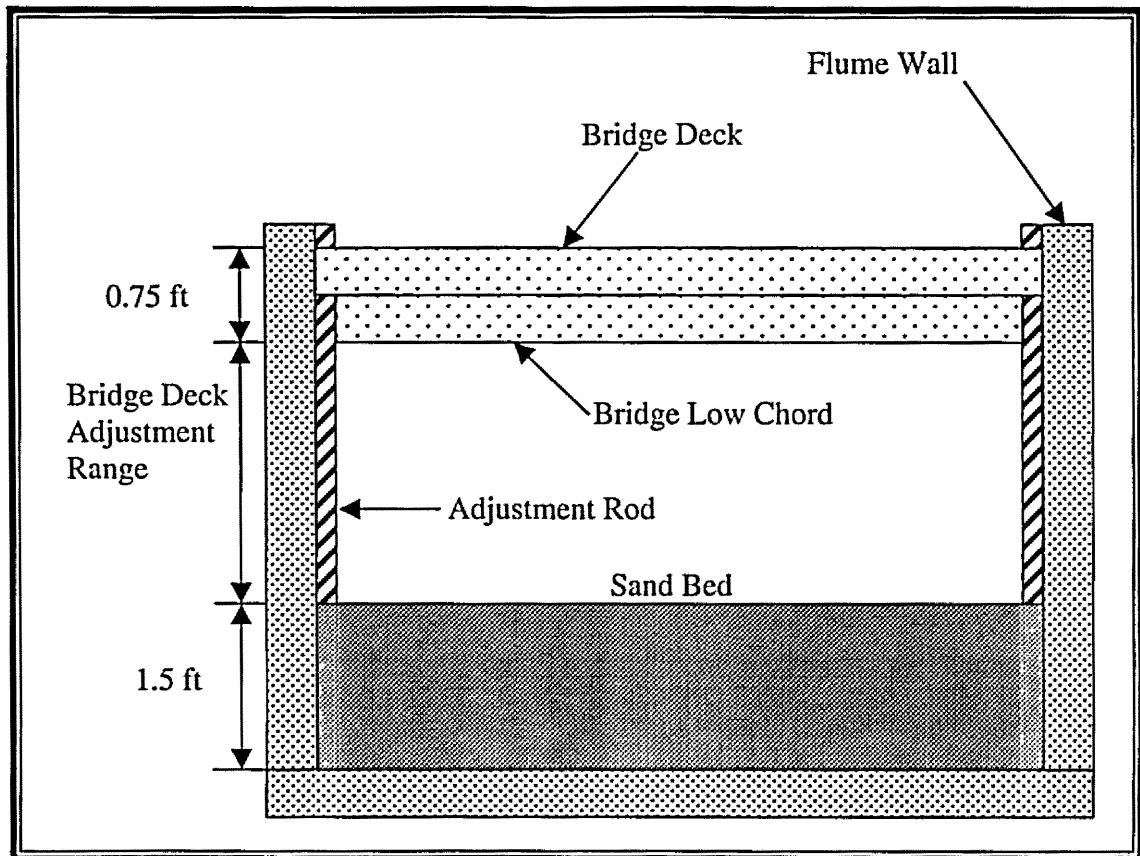


• Figure 3.2 – Cross section of data platform and point gage assembly

3.3 MODEL DESCRIPTION

A model bridge, constructed at an approximate 8:1 scale, was installed in the flume and positioned perpendicular to the direction of flow. Spanning the width of the flume, the model bridge was three feet wide in the direction of flow and 0.75 feet thick from bridge deck to bridge low chord as shown in Figure 3.3. Elevation of the bridge

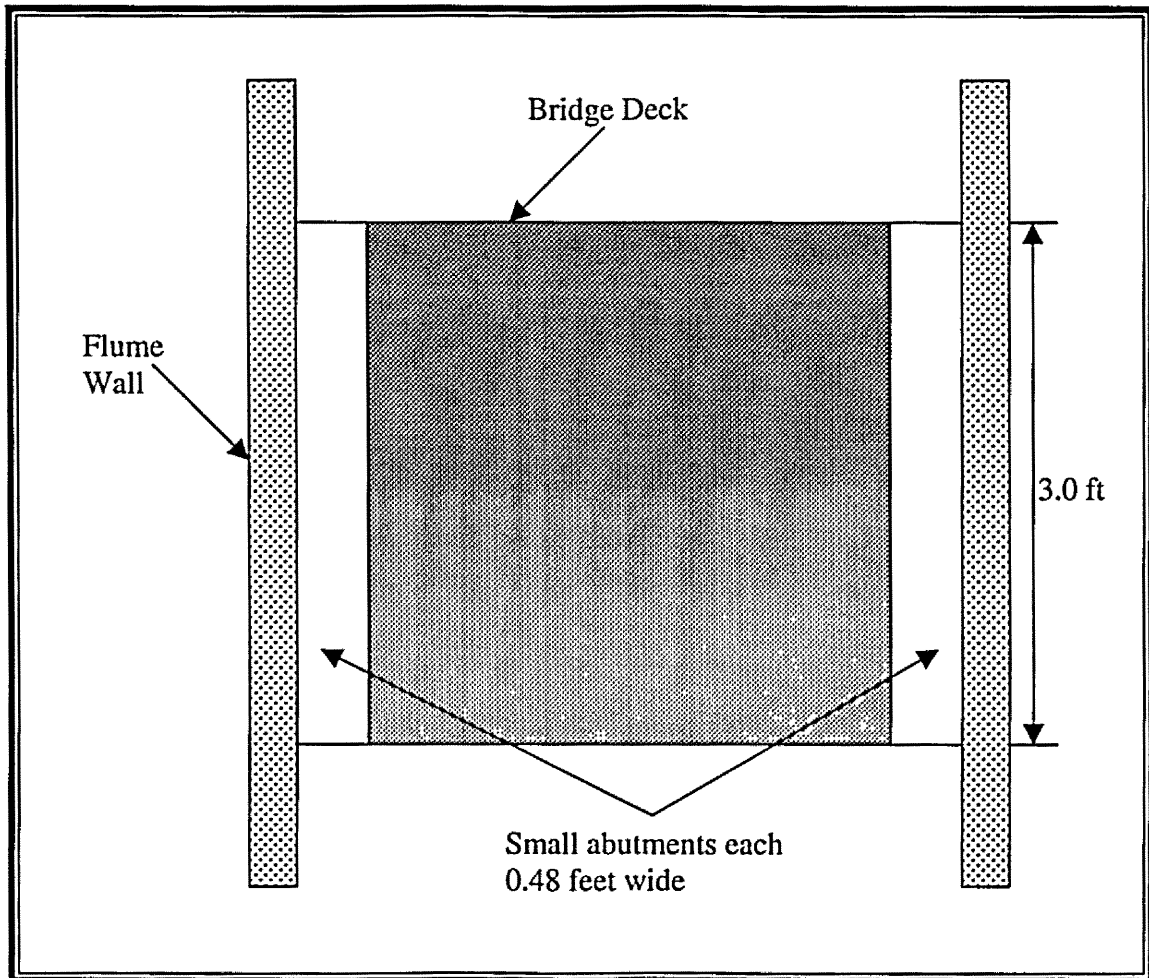
deck was adjustable, permitting the bridge to be raised and lowered in the flume. Six bridge deck elevations were selected to simulate conditions of various stages along the rising limb of a storm flow hydrograph. Figure 3.3 presents a sectional view of the model bridge.



• Figure 3.3 – Cross section of model bridge deck

Two sets of abutments were constructed of wood and mounted along the left and right sides of the flume under the bridge deck opening. A 12 percent horizontal constriction of flow resulting from inserting abutments measuring 3.0 ft by 0.48 ft (small). A 36 percent horizontal constriction of flow resulted from inserting abutments

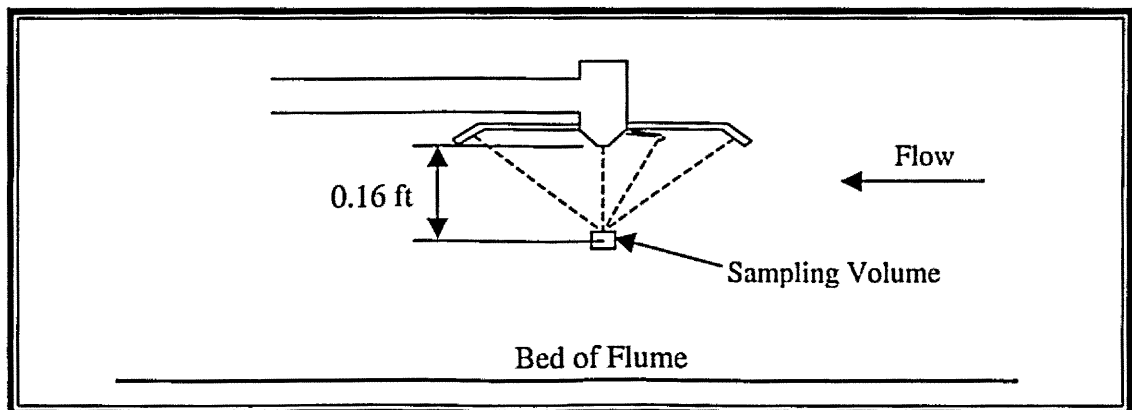
measuring 3.0 ft by 1.44 ft (large). Both sets of abutments were constructed in such a fashion that 0.17-foot sections could be removed to accommodate the lowering of the bridge deck. Figure 3.4 presents a plan view of the bridge deck with the small abutments inserted.



• Figure 3.4 – Plan view showing placement of smaller abutments in model bridge deck

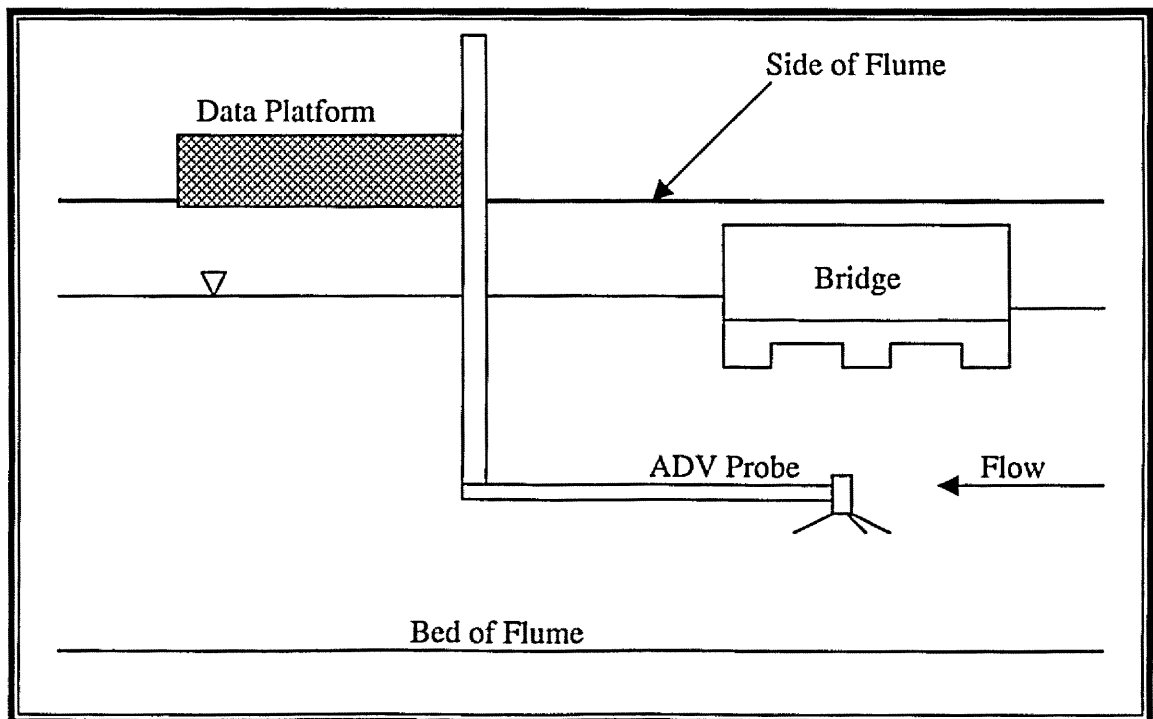
3.4 DATA ACQUISITION EQUIPMENT

Data were collected and recorded with a SonTek® Acoustic Doppler Velocimeter (ADV). Velocities were collected in a three-space coordinate system utilizing the ADV. Three components comprised the ADV: probe head, conditioning module and data recorder. While attached to the point gauge assembly, the probe head, which was a three-pronged apparatus, was submerged into the flow. Velocities, in a three-space coordinate system, were measured at a sampling volume located approximately 0.16 feet below the probe head. Figure 3.5 presents a diagram of the probe head. The conditioning module consisted of a cylindrical unit, which provided the link between the probe head and data recorder and performed the digital processing necessary to interpret the Doppler signal. A personal computer was used as a data recorder. While the data acquisition system was capable of operating at sampling rates between 0.1 and 25 Hz, a sampling frequency of 5 Hz for a 30 second duration was used throughout the experiment. Sampling frequency and duration were determined based on a sensitivity analysis of frequency and duration.



• Figure 3.5 – Profile view of ADV probe head

Bed elevations and water surface elevations were measured utilizing the ADV's ability to determine the distance from the probe head to a fixed boundary, or an air-water interface. Distances were determined by the probe emitting a sonar pulse and the conditioning module analyzing the return signal. The maximum boundary distance the conditioning module was capable of detecting was approximately 1.1 ft. Figure 3.6 illustrates the relative positioning of the ADV probe, point gauge assembly and data collection platform. By changing the location of the data platform along the flume and by varying the location and elevation of the point gauge, the probe could be positioned at any location within the test section. While velocity data were recorded directly to the computer, boundary locations were displayed and recorded manually.



• Figure 3.6 – Profile view of ADV probe positioning

3.5 TEST PARAMETERS

A clear and comprehensive testing matrix and detailed nomenclature was developed to assist in obtaining the desired results. Subsequent sections discuss the test matrix and nomenclature.

3.5.1 TEST MATRIX

A test matrix was developed to quantify the effects of variation in the following parameters: discharge, sediment size, initial bridge opening, and abutment size. Initial bridge opening was defined as the distance from the low chord bridge elevation to the mean initial bed elevation (prior to testing). Table 3.1 displays an overview of the variation in testing parameters for the 1.5 mm sand and the 3.3 mm sand.

Discharge was targeted at 8 cfs, 18 cfs, and 24 cfs to while the upstream flow depth was held at approximately 1.25 ft to achieve an increase in flow velocity. Sediment used during testing included median grain sizes of 1.5 mm and 3.3 mm. Gradation curves for the sediments utilized during testing are presented in Figures 3.7 and 3.8, respectively. Table 3.2 outlines the summary statistics for each of the two sediments. For each sediment size examined, two series of tests were conducted, one series of 18 tests with small abutments (12% constriction) and one series of 18 tests with large abutments (36% constriction). Both series of tests included 6 tests at 8 cfs, 6 tests at 18 cfs and 6 test at 24 cfs, unless the bed material scoured to the floor of the flume, in which case, testing was terminated. In total, 62 of the proposed 72 tests were conducted.

Data for test numbers 32 through 36, 66 and 69 through 72 were not obtained due to the bed material scouring to the floor on the previous test.

• Table 3.1 – Variation in test parameters

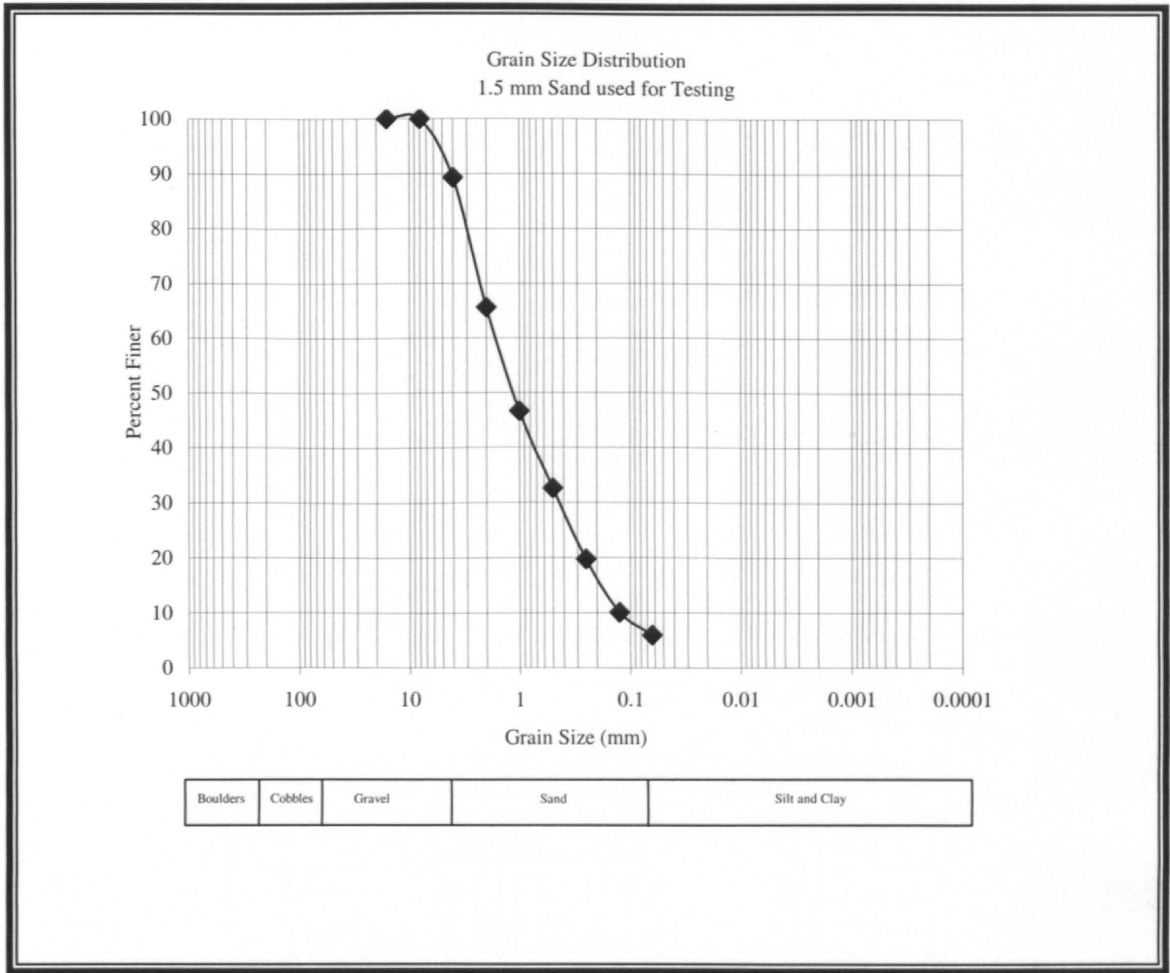
Test Number	Discharge (ft ³ /s)	Sediment Size (D ₅₀ , in mm)	Initial Bridge Opening (ft)	Abutment Constriction Percentage (%)
1	8	1.5	1.37	12
2	8	1.5	1.20	12
3	8	1.5	1.03	12
4	8	1.5	0.86	12
5	8	1.5	0.69	12
6	8	1.5	0.52	12
7	18	1.5	1.37	12
8	18	1.5	1.20	12
9	18	1.5	1.03	12
10	18	1.5	0.86	12
11	18	1.5	0.69	12
12	18	1.5	0.52	12
13	24	1.5	1.37	12
14	24	1.5	1.20	12
15	24	1.5	1.03	12
16	24	1.5	0.86	12
17	24	1.5	0.69	12
18	24	1.5	0.52	12
19	8	1.5	1.37	36
20	8	1.5	1.20	36
21	8	1.5	1.03	36
22	8	1.5	0.86	36
23	8	1.5	0.69	36
24	8	1.5	0.52	36
25	18	1.5	1.37	36
26	18	1.5	1.20	36
27	18	1.5	1.03	36
28	18	1.5	0.86	36
29	18	1.5	0.69	36
30	18	1.5	0.52	36
31	24	1.5	1.37	36
32*	24	1.5	1.20	36
33*	24	1.5	1.03	36
34*	24	1.5	0.86	36
35*	24	1.5	0.69	36
36*	24	1.5	0.52	36

* Data not collected due to scour depths beyond limits of the facility.

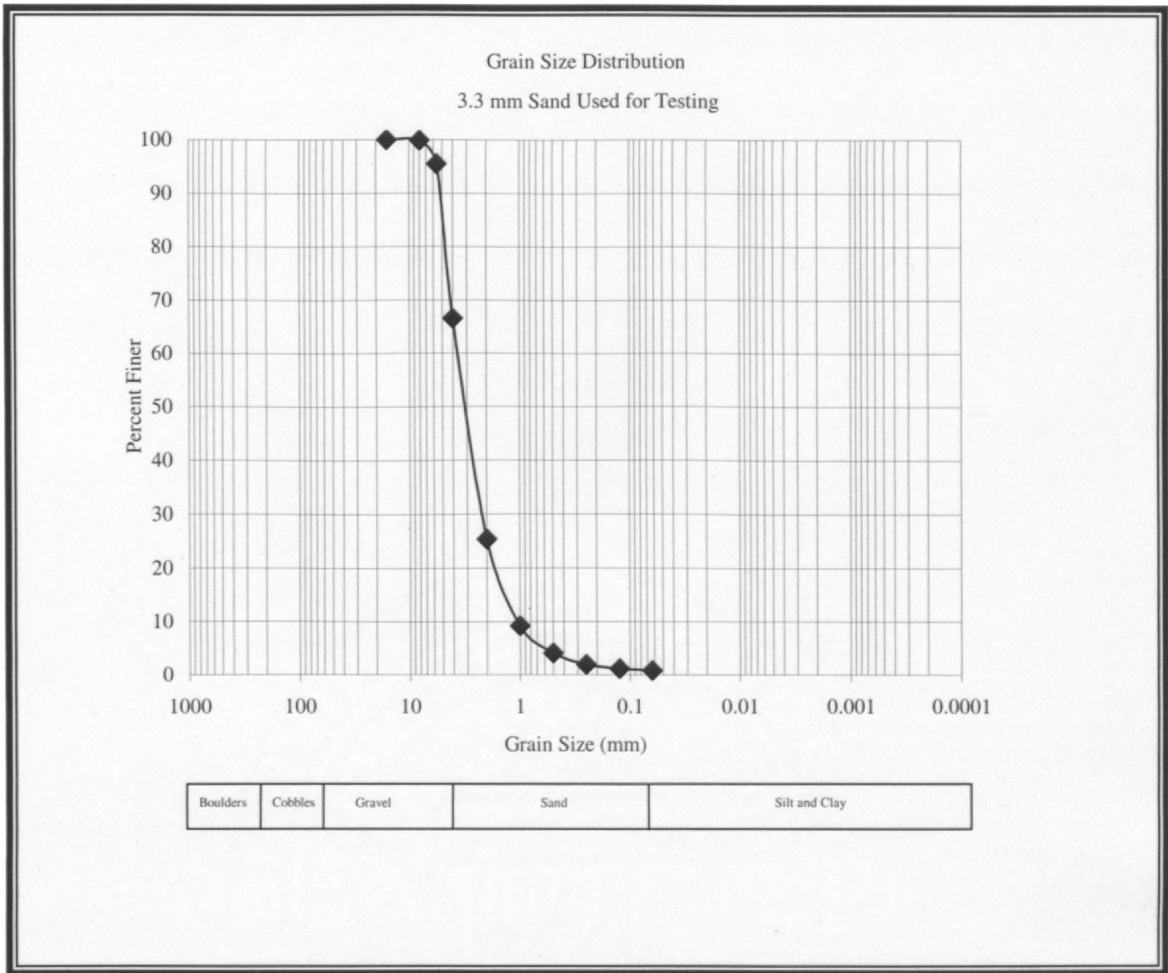
• Table 3.1 (continued) – Variation in test parameters

Test Number	Discharge (ft ³ /s)	Sediment Size (D ₅₀ , in mm)	Initial Bridge Opening (ft)	Abutment Constriction Percentage (%)
37	8	3.3	1.37	12
38	8	3.3	1.20	12
39	8	3.3	1.03	12
40	8	3.3	0.86	12
41	8	3.3	0.69	12
42	8	3.3	0.52	12
43	18	3.3	1.37	12
44	18	3.3	1.20	12
45	18	3.3	1.03	12
46	18	3.3	0.86	12
47	18	3.3	0.69	12
48	18	3.3	0.52	12
49	24	3.3	1.37	12
50	24	3.3	1.20	12
51	24	3.3	1.03	12
52	24	3.3	0.86	12
53	24	3.3	0.69	12
54	24	3.3	0.52	12
55	8	3.3	1.37	36
56	8	3.3	1.20	36
57	8	3.3	1.03	36
58	8	3.3	0.86	36
59	8	3.3	0.69	36
60	8	3.3	0.52	36
61	18	3.3	1.37	36
62	18	3.3	1.20	36
63	18	3.3	1.03	36
64	18	3.3	0.86	36
65	18	3.3	0.69	36
66*	18	3.3	0.52	36
67	24	3.3	1.37	36
68	24	3.3	1.20	36
69*	24	3.3	1.03	36
70*	24	3.3	0.86	36
71*	24	3.3	0.69	36
72*	24	3.3	0.52	36

* Data not collected due to scour depths beyond limits of the facility.



• **Figure 3.7 – Grain size distribution for 1.5 mm sand**



• Figure 3.8 – Grain size distribution for 3.3 mm sand

• Table 3.2 – Summary statistics of utilized sediment

Sediment	Median Grain Size (D_{50} , mm)	Geometric Standard Deviation (σ_g)
1	1.5	4.23
2	3.3	1.41

Initial bridge opening was defined as the distance from the low chord bridge elevation to the mean initial bed elevation (prior to testing). Initial bridge opening was varied to simulate the rising limb of a hydrograph. Table 3.3 displays the initial bridge

opening corresponding to each of the six bridge positions. Each test began with the low chord positioned just above the water surface, labeled position one. Velocity, bed elevation and water surface elevation were then measured and documented. Once all data had been collected, the bridge was lowered 0.17 feet to position two. This process was repeated until all six bridge positions were completed. Position six was the final position of the bridge, located 0.85 feet below the original deck elevation.

• **Table 3.3 – Initial bridge opening corresponding to bridge position**

Bridge Position (#)	Initial Bridge Opening (ft)
1	1.37
2	1.20
3	1.03
4	0.86
5	0.69
6	0.52

3.5.2 NOMENCLATURE

Data were collected in a test section 16 feet long for each test in the test matrix. Sampling sections were located upstream, downstream and directly under the bridge deck. Although data acquisition locations remained similar, labeling and locations changed during evolution of the testing matrix. A system of nomenclature was developed to describe the location of points of interest in the test section. Each sampling point used for data collection was identified by one of four letters, D, U, A or B, and a number (i.e. B1, D5, A1 or U3). Letters, D, U, A or B signify downstream, upstream, abutment or bridge point, respectively. These letters apply to all tests performed, although the numerical component for each label varied in some tests.

To describe the dimensions and other quantities of the testing procedure, many terms were used. A list of terms, definitions and corresponding units used for the data analysis are presented in Table 3.4.

• Table 3.4 – List of variables used for data analysis

Variable	Description	Units
Test Number	Number corresponding to an individual data point obtained during testing	n/a
Q	Volumetric flow rate of water in the flume	ft ³ /s
q _{br}	Unit discharge through bridge opening	ft ² /s
D ₅₀	Grain size for which 50 percent of the bed material is finer	mm
Bridge Position	Position of bridge corresponding to an initial bridge opening, H _b	n/a
Vertical Constriction %	Percentage of vertical constriction caused by the bridge elevation	%
Horizontal Constriction %	Percentage of horizontal constriction caused by the presence of abutments	%
y _{pds}	Equilibrium depth of pressure flow deck scour measured from the mean bed elevation	ft
y _{pas}	Equilibrium depth of pressure flow abutment scour measured from the mean bed elevation	ft
H _b	Distance from the low chord of the bridge to the initial mean bed elevation (initial bridge opening)	ft
y	Depth of approach flow upstream of the bridge deck	ft
Fr	Froude number of the approach flow = $V_a/(gy)^{0.5}$	n/a
V _a	Velocity of the approach flow	ft/s
V _b	Average velocity of the flow under the bridge	ft/s
V _c	Velocity of the flow for incipient motion of the bed material, Critical velocity	ft/s
g	Acceleration due to gravity	ft/s ²
a	Abutment protrusion length	ft

3.6 TESTING PREPARATION AND PROCEDURE

To ensure that the data collected and results desired were accurate and complete, a rigorous testing preparation and procedure format was developed. Succeeding sections discuss test preparation and test procedure.

3.6.1 TEST PREPARATION

The initial bed elevation for each test was prepared by leveling the bed material prior to each test. To ensure repeatability of the initial bed setting, a board, suspended from the moveable cart with chains, was used as a reference. These chains were adjusted an appropriate elevation and the cart was pulled along the length of the flume. Necessary adjustments to the bed material were made to match the elevation of the bed material with the elevation of the reference board.

Once the bed material was leveled, the flume was filled with water. One 125 horsepower pump, operating at a low discharge, was used to fill the flume. A calibrated orifice plate and a water-filled manometer were used to set and monitor the discharge during each test. To preserve the initial elevation and condition of the bed material, the flume was filled slowly. Water filled the flume until approximately 1.25 ft of depth covered the bed. The discharge was then slowly increased to the desired flow and the water surface was adjusted. An initial water surface elevation was set to provide 1.36 feet of water depth immediately upstream of the bridge opening to obtain a condition just below partial bridge deck submergence.

3.6.2 TEST PROCEDURE

After the flow was set to the appropriate discharge, the actual test procedure would commence. The test procedure consisted of three parts; collecting velocity, bed elevation, and water surface elevation. All three sets of measurements were conducted in a regular pattern. Locations of data acquisition points for each type of test are cataloged in Table 3.5 and presented in Figures 3.9 through 3.11.

• **Table 3.5 – Summary of test matrix with data acquisition map correspondence**

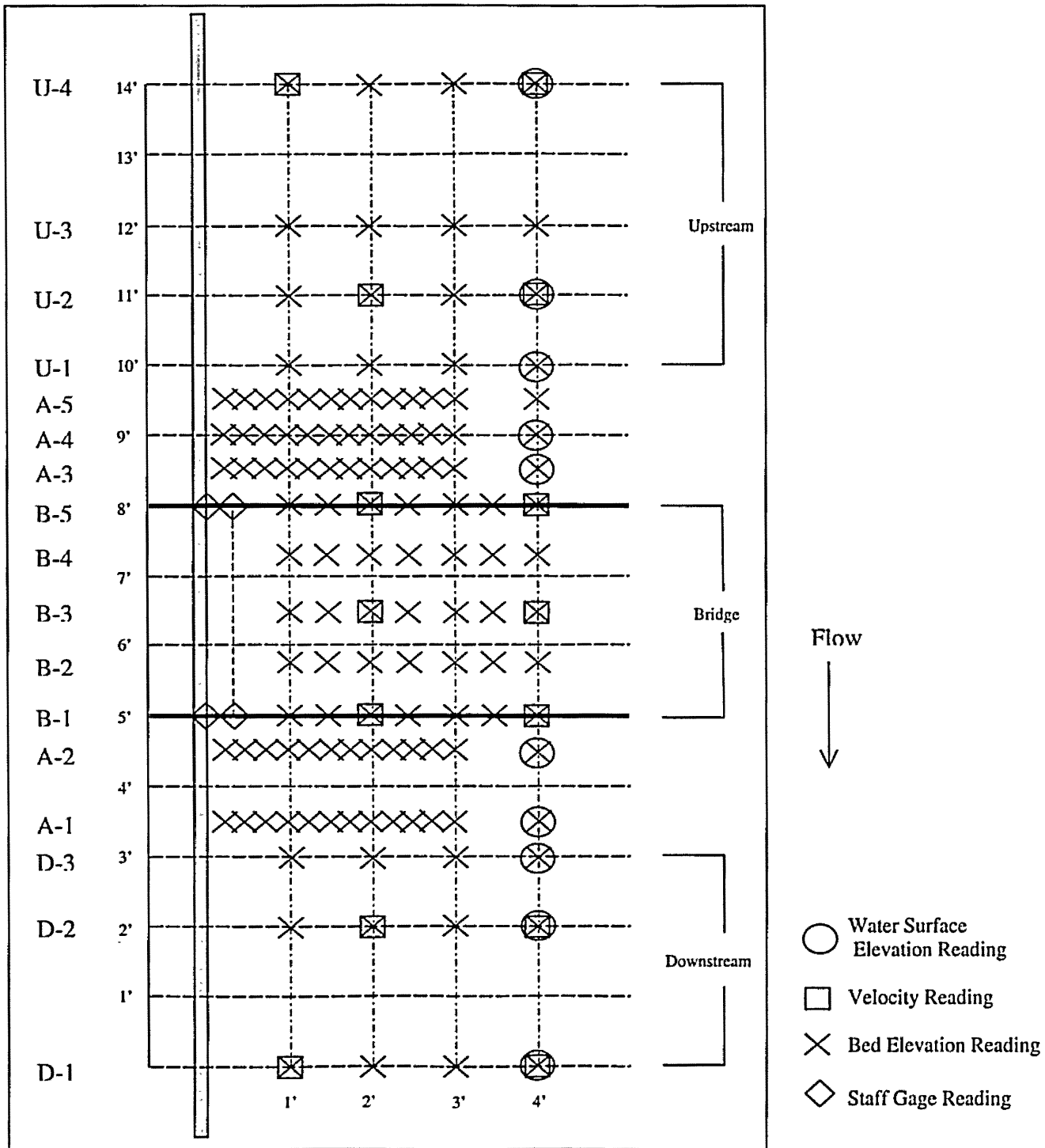
Test Numbers	Discharge (cfs)	Sediment Size (D_{50} , in mm)	Abutment Size	Figure Number for Data Acquisition Map
1 to 6	8	1.5	Small	Figure 3.9
7 to 12	18	1.5	Small	Figure 3.10
13 to 18	24	1.5	Small	Figure 3.10
19 to 24	8	3.3	Small	Figure 3.10
25 to 30	18	3.3	Small	Figure 3.10
31 to 36	24	3.3	Small	Figure 3.10
37 to 42	8	1.5	Large	Figure 3.11
43 to 48	18	1.5	Large	Figure 3.11
49 to 54	24	1.5	Large	Figure 3.11
55 to 60	8	3.3	Large	Figure 3.11
61 to 66	18	3.3	Large	Figure 3.11
67 to 72	24	3.3	Large	Figure 3.11

Due to the change in absolute elevation of the bridge deck with each of the six bridge positions, a unique set of velocity sampling elevations directly under the bridge were required for each position. Table 3.6 presents a summary of the depths in feet below the low chord elevation at which velocity samples were obtained for each bridge position. As observed from Table 3.6, lowering of the bridge deck into the flume resulted in the number of velocity sampling positions to be reduced. At each of the bridge

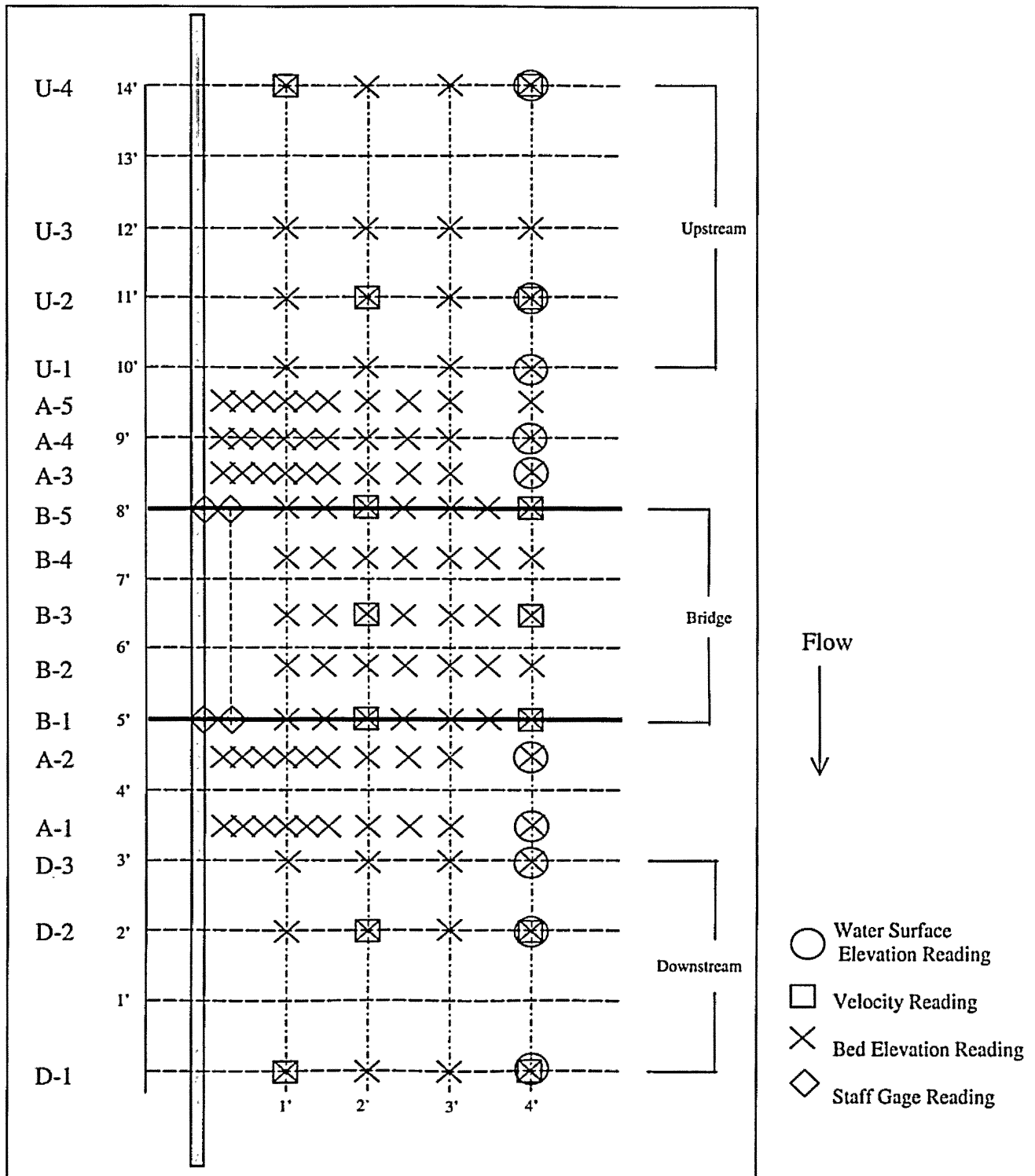
positions, velocity sampling depths were chosen to uniformly divide the opening in the vertical section directly under the bridge. At sampling sections located upstream and downstream of the bridge deck, velocities were collected at elevations consistent with bridge position one, regardless of the actual bridge deck elevation.

• **Table 3.6 – Depth in feet of velocity data acquisition points below low chord bridge elevation**

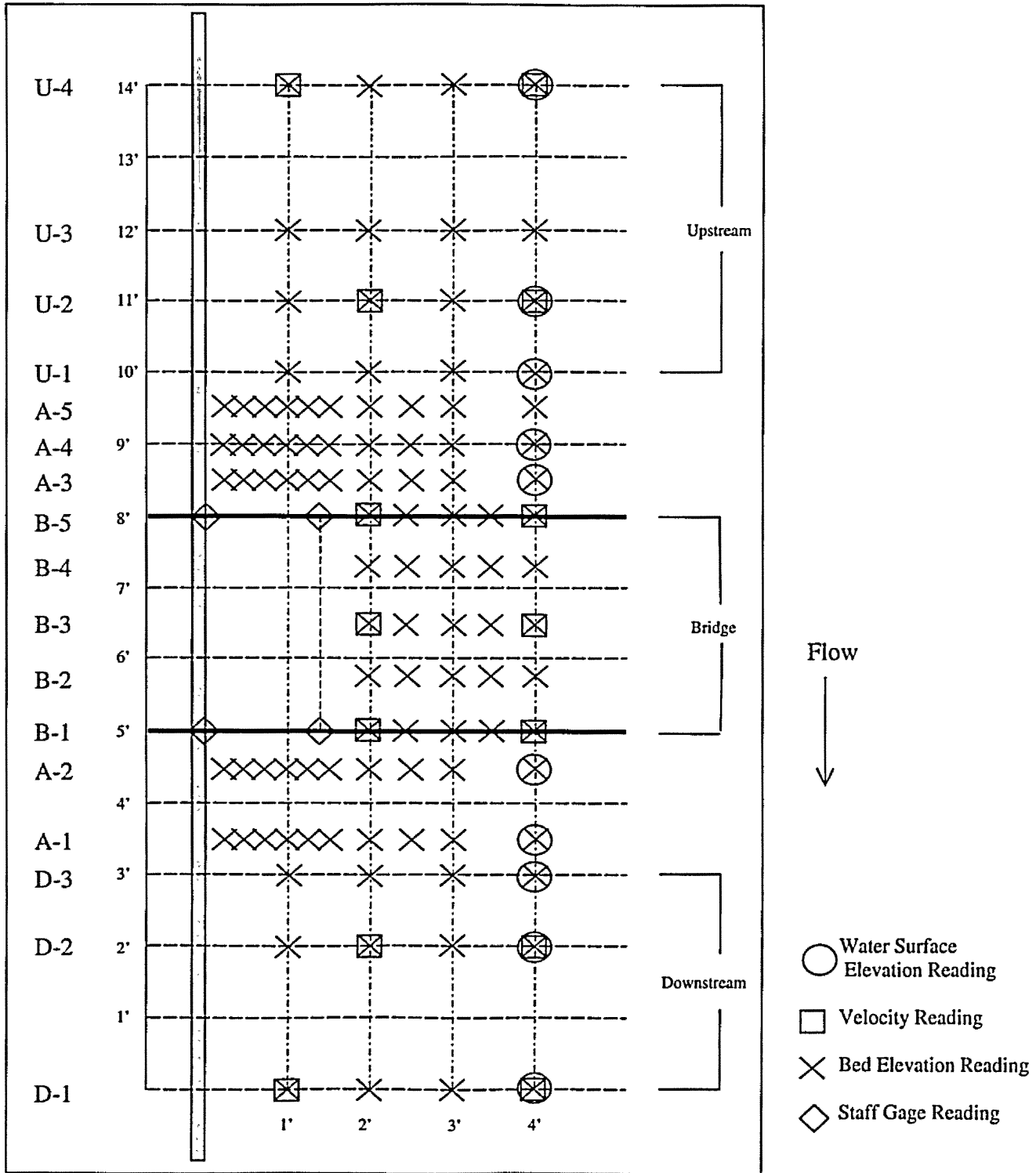
Sample Location	Bridge Position 1	Bridge Position 2	Bridge Position 3	Bridge Position 4	Bridge Position 5	Bridge Position 6
1	0.3	0.3	0.3	0.3	0.3	0.3
2	0.63	0.63	0.63	0.63	0.63	n/a
3	0.96	0.96	0.96	n/a	n/a	n/a
4	1.29	n/a	n/a	n/a	n/a	n/a



• Figure 3.9 – Data acquisition map for test numbers 1 through 6



• Figure 3.10 – Data acquisition map for test numbers 7 through 36



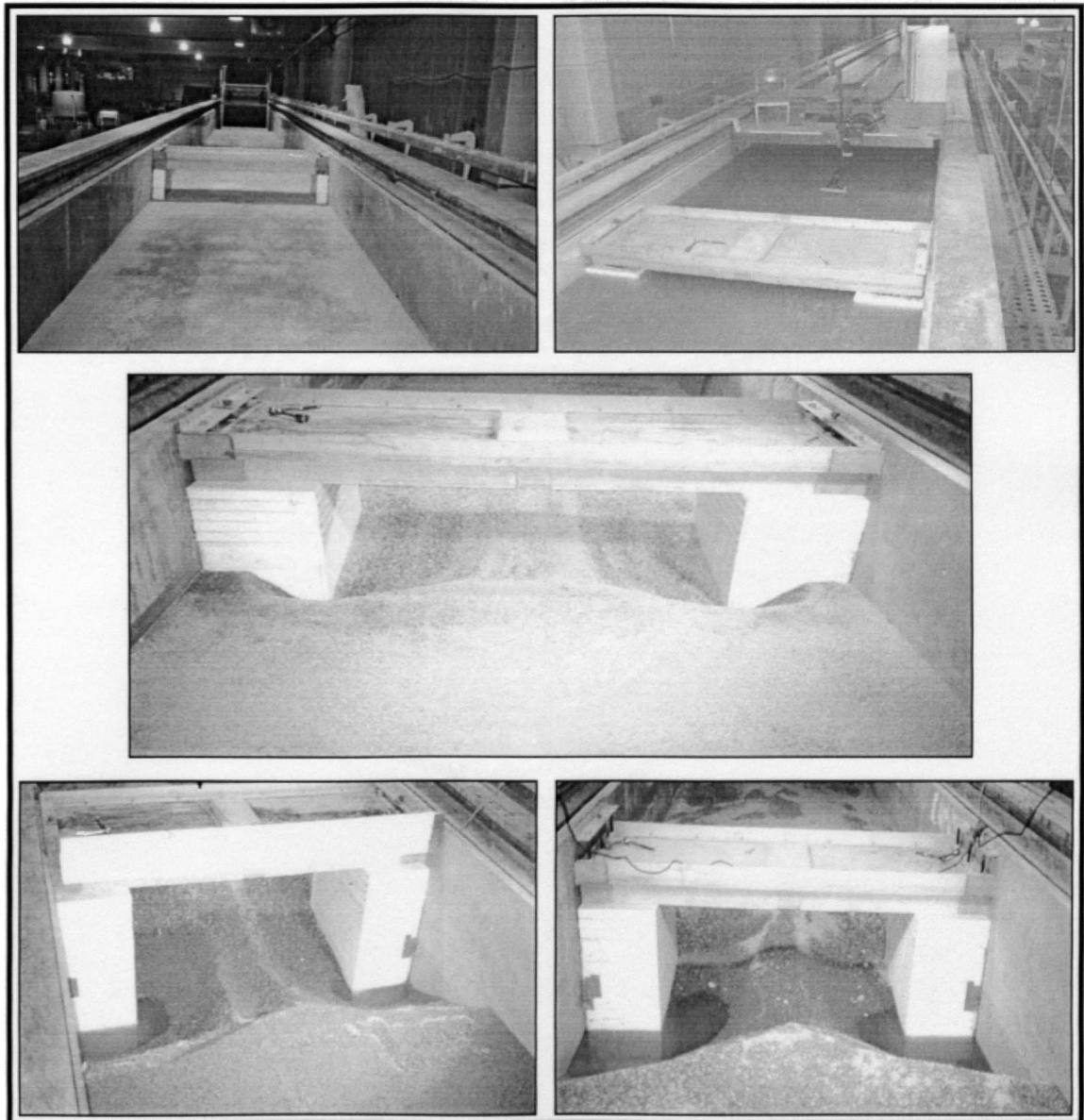
• Figure 3.11 – Data acquisition map for test numbers 37 through 72

Velocity measurements were taken upstream, downstream and beneath the bridge. Upstream and downstream measurements were taken at the same four depths and consistent locations in the flume. Symmetry was assumed because the flume was rectangular, allowing for the formation of a grid of data collection points in one half of the flume. Measurements under the bridge were also taken in a consistent pattern in the horizontal plane, however, measurements varied in depth with the submergence condition of the bridge. For all velocity readings, the probe would be brought to the desired position and data collected for thirty seconds. Then, the probe was moved to the next location and the process repeated until data had been collected at all locations.

To record bed elevations, the probe was set at a known elevation on the point gauge and positioned at the data location point. A computer then displayed the reading emitted from the probe, representing the distance from the probe head to the flume bed. Both the probe reading and point gauge elevation were recorded for each location. In addition to the bed elevation readings, water surface elevation readings were taken for each bridge position. After being raised out of the flow, the probe was turned upside down then lowered back into the flow. Distance to the water surface was displayed from the probe and recorded in the same manner as the bed elevation readings. Other water surface readings were obtained from staff gauges mounted on the left and right side of the bridge. Water surface elevation was noted before changing bridge position. Once the velocities, bed elevations and water surface elevations had been taken, the bridge position was changed.

For each discharge, the bridge deck was lowered 0.17-feet six times. After the bridge was lowered from the previous position to the next position, data collection for the

new position did not commence until an equilibrium depth of scour over time was formed under the bridge. Once equilibrium was established, the process of collecting velocity, depth and water surface readings was repeated. Figure 3.12 displays a collage of photographs showing the initial condition through post testing bridge positions, clearly depicting pressure flow abutment scour and pressure flow deck scour.



• Figure 3.12 –Photographs of testing from initial to final conditions

4 DATA ANALYSIS

4.1 INTRODUCTION

A comprehensive understanding of the processes at work during pressure flow conditions at bridges has not been fully developed. Consequently, data analysis for pressure flow conditions at bridges can be best understood by performing a dimensional analysis to determine the variables necessary to accurately develop a predictive relationship. Once a dimensional analysis has been performed, statistical analysis with applied regression techniques can be implemented to develop relationships between the chosen dimensionless variables. Subsequent sections discuss the dimensional and statistical analyses performed under the scope of this study.

4.2 DIMENSIONAL ANALYSIS

Although many practical engineering problems involving fluid mechanics can be solved using analytical procedures and fundamental equations of fluid mechanics, there remains a large number of problems that rely on experimentally obtained data for their solution. A goal of any experiment should be to make the results as widely applicable as

possible. To achieve this goal, the concept of similitude can be used so that measurements obtained on one system (for example, in the laboratory) may be used to describe the behavior of similar systems (outside the laboratory). One of the most important and difficult steps in applying dimensional analysis includes the selection of variables that are involved (Munson, et al, 1998). A reliance on a good understanding of the governing physical laws is necessary, but in the case of pressure flow, experience and previous research are critical for identifying the relevant variables. As determined by previous researchers (Abed, Jones, Chang, Arneson), the magnitude of any type of pressure flow scour at a submerged bridge, may be a function of the variables displayed in Table 4.1.

• **Table 4.1 – Potential variables for describing pressure flow scour**

Symbol	Definition	Units
ρ	fluid (water) density	M/L^3
g	acceleration due to gravity	L/T^2
μ	dynamic viscosity of water-sediment mixture	M/LT
ν	kinematic viscosity	L^2/T
Q	volumetric flowrate	L^3/T
V	flow velocity	L/T
y	flow depth	L
θ	angle of attach of approach flow	Degrees
a	abutment protusion length	L
b	pier width	L
K_s	correction factor for shape	Dimensionless
K_θ	correction factor for angle of attack of flow	Dimensionless
D_{50}	grain size for which 50 percent of bed material is finer	L
σ_g	geometric standard deviation of bed material	Dimensionless
Q_s	total sediment transport of approach flow	M/T
γ_s	sediment submerged specific weight	M/L^2T^2
ω	fall velocity of bed material	L/T
t	time of scour	T

After removing the dependent variables, variables not altered in these experiments, and incorporating the variables obtained during testing, the magnitude of pressure flow deck scour, y_{pds} , or pressure flow abutment scour, y_{pas} , at a submerged bridge can be expressed as follows

$$y_{pds}, y_{pas} = f\left(y, V_a, V_b, V_c, g, \sigma_g, D_{50}, H_b, \Delta h, q_{br}, a\right)$$

• Equation 4.1

Where,

- y_{pds} = depth of pressure flow deck scour relative to mean bed elevation, L;
- y_{pas} = depth of pressure flow abutment scour relative to m.b.e., L;
- y = depth of flow immediately upstream of the bridge deck, L;
- V_a = velocity of approach flow upstream of the bridge deck, L/T;
- V_b = average velocity of flow under the bridge, L/T;
- V_c = velocity of flow for incipient motion of bed material, L/T;
- g = acceleration due to gravity, L/T²;
- σ_g = geometric standard deviation of the bed material;
- D_{50} = grain size for which 50 percent of the bed material is finer, L;
- H_b = distance from bridge low chord to the initial mean bed elevation, L;
- Δh = change in WSE from upstream bridge face to downstream, L;
- q_{br} = unit discharge through the bridge opening, L²/T; and
- a = abutment protrusion length, L.

Through a dimensional analysis discussed by Melville and Coleman (2000) and statistical significance based on Arneson (1997), the following relationship for pressure scour was obtained

$$\frac{y_{pds}}{y}, \frac{y_{pas}}{a} = f \left(\frac{V_b}{V_c}, \frac{V_a}{\sqrt{gy}}, \frac{y}{H_b}, \frac{y_{pds} + H_b}{y} \right)$$

• Equation 4.2

V_b/V_c , termed flow intensity, represents the stage of sediment transport under the bridge and accounts for the effects of velocity. Flow intensity, V_b/V_c , also indirectly accounts for the median sediment size when computing the critical velocity. Froude number, $Fr = V_a/(gy)^{0.5}$, represents the second term on the right hand side of Equation 4.2. Inclusion of Froude number should be an essential consideration for all problems related to flow in open channels, as the Froude number equals a ratio of inertia in the flow to a gravity force. Each of the last two terms on the right-hand side of Equation 4.2 are accounting for the potential constriction effects in conjunction with bridge submergence and are based on statistical significance as determined by Arneson (1997).

4.3 STATISTICAL ANALYSIS

Statistical analysis employed in the analysis of the data incorporated the principle of least squares and multivariate linear regression. The principle of least squares can be applied to one dependent variable and one independent variable or to one dependent and several independent variables. When more than one independent variable has been introduced, then a multivariate linear regression analysis becomes necessary. Subsequent sections discuss the statistical theory and assumptions used for analysis in this study.

4.3.1 STATISTICAL THEORY

Regression analysis involves an area of statistics that provides methods to investigate the existence of associations and, if present, the nature of the associations, among various observable quantities (Graybill & Iyer, 1994). A commonly used method for obtaining a prediction function for predicting the values of a response variable Y using predictor variables X_1, \dots, X_k , utilizes the principle of least squares.

A definition of the principle of least squares was first introduced by the German mathematician Gauss (1777 – 1855) who stated that a line provides a good fit to a series of data if the vertical distances (deviations) from the observed point to the line are small (Devore, 1995). Devore (1995) further stated that a measure of the goodness of fit can be expressed as the sum of the squares of individual deviations. Therefore, the line having the smallest possible sum of squared deviations would be the best-fit line. Equation 4.3 mathematically expresses the principle of least squares.

$$f(\beta_0, \dots, \beta_k) = \sum_{i=1}^n [Y_i - (\beta_0 + \beta_1 X_{1i} + \dots + \beta_k X_{ki})]^2$$

• Equation 4.3

Where,

Y_i = the value of a measured data point;
 $\beta_0 + \beta_1 X_i + \dots + \beta_k X_{ki}$ = equation of the regression line; and
all other variables are defined previously.

Least squares estimates for the y-intercept and slope of the regression lines are found by minimizing $f(\beta_0, \beta_1, \dots, \beta_k)$. Values β_0 through β_k are minimized by taking partial derivatives of $f(\beta_0, \beta_1, \dots, \beta_k)$ with respect to all β 's and then setting them equal to zero. All equations can then be solved for the least-squares estimates of the coefficients $(\beta_0, \beta_1, \dots, \beta_k)$ for the estimated regression line.

Statistical analysis of the data in these experiments incorporated techniques of multivariate linear regression. A general additive multivariate regression model equation can be expressed as

$$Y = \beta_0 + \beta_1 X_1 + \beta_2 X_2 + \dots + \beta_k X_k + \varepsilon$$

• **Equation 4.4**

Where,

- Y = dependent variable;
- β_0 = y-intercept of the linear relationship;
- β_k = slope of the regression line for the kth independent variable;
- X_k = kth independent variable; and
- ε = random deviation or random error.

Random deviation or random error, ε , can be assumed to be normally distributed with $E(\varepsilon) = 0$ and $V(\varepsilon) = \sigma^2$. Values of $E(\varepsilon)$ and $V(\varepsilon)$ are the mean and variance of the random deviation or random error, respectively. As $E(\varepsilon)$ and $V(\varepsilon)$ become small, any observations of the dependent variables approach the true regression line. When the value of ε exceeds zero, the actual data point falls above the regression line and will be

higher than the predicted value. Similarly, when ϵ does not reach zero, the actual data point falls below the regression line and will be lower than the predicted value.

Goodness of fit, or quality of the regression analysis, can be measured through the variance, σ^2 , of the regression model or the mean squared error, MSE. Variance, σ^2 , can be computed through the error sum of squares, SSE, with the following relationship

$$\sigma^2 = \frac{\sum_{i=1}^n (y_i - \hat{\beta}_0 - \hat{\beta}_1 X_{1i} - \dots - \hat{\beta}_k X_{ki})^2}{n - k - 1} = \frac{SSE}{n - k - 1} = MSE$$

• Equation 4.5

Values of $(n-k-1)$ in the denominator of Equation 4.5 represent the number of degrees of freedom associated with the error sum of squares, SSE. Another way to think about SSE would be to use it as a measure of how much variation in the dependent variable, Y, cannot be explained by the model.

Coefficient of determination, R^2 , proves to be another measure of goodness of fit, or quality of the regression analysis model. Coefficient of determination can be determined using SSE and the total sum of squares, SSY. Total sum of squares, SSY computes as follows

$$SSY = \sum_{i=1}^n (Y_i - \bar{Y})^2$$

• Equation 4.6

Total sum of squares, SSY, measures the variability of the actual value of Y_i measured about the mean of the dependent variable Y . Coefficient of determination, R^2 calculates as

$$R^2 = 1 - \frac{SSE}{SSY}$$

• Equation 4.7

R^2 measures the variation in the dependent variable, Y , that can be explained by the bivariate or multivariate linear regression model.

After the completion of a multivariate linear regression, a display of the overall summary of a multivariate linear regression analysis should be presented. An overall summary can be presented with the analysis of variance (ANOVA) as depicted in Table 4.2. An important term for ANOVA, the sum of squares due to regression, SSR, can be computed as follows

$$SSR = SSY - SSE$$

• Equation 4.8

Mean square due to regression, MSR, computes as follows

$$MSR = \frac{SSR}{k}$$

• Equation 4.9

• Table 4.2 – Example of quantities often shown in an ANOVA table

	Degrees of	Sum of	Mean Square	F-Statistic	P-Level
Source	Freedom (df)	Squares (SS)	(MS)		
Regression	k	SSR	MSR	MSR/MSE	p < .05
Residual Error	n-k-1	SSE	MSE		
Total	n-1	SSY			

Once a fitted multivariate linear regression model and estimates for the various parameters of interest are obtained, the question about the contribution of the independent variables to the prediction of the dependent variable, Y, must be answered. One basic type of such test to answer this question, according to Kleinbaum et al. (1988) can be written as: An overall significance test. Taken collectively, does the entire set of independent variables (or equivalently, the fitted model itself) contribute significantly to the prediction of the dependent variable Y?

To perform an overall significance test, use of the MSR and MSE from the ANOVA Table are required. Null hypothesis for this test would be stated as H_0 : “all k independent variables considered together do not explain a significant amount of the variation in the dependent variable Y.” Calculate the F-statistic as $F = MSR/MSE$. Then, the computed value of F can be compared with the critical point $F_{k,n-k-1,1-\alpha}$, with α being the preselected significance level of 0.05. For example, the critical F point with $k = 3$ and $n = 183$ equals 2.66. Critical F point with $k = 3$ and $n = 59$ equals 2.76. Critical F point with $k = 2$ and $n = 53$ equals 3.17. Reject H_0 if the computed F-statistic exceeded the

critical point, meaning that the k independent variables do explain a significant amount of the variation in the dependent variable Y .

P-level determines statistical significance of the analysis. P-level represents a decreasing index of the reliability of a result. Higher P-levels, indicate a less likely occurrence that the observed relation between independent variables will be true. Additionally, P-level represents the probability of error involved in accepting the observed result as valid. Specifically, the P-level represents the probability of error associated with accepting an observed result as valid or representative of the population of observed results. For purposes of this analysis, a value of 0.05 (95% confident) or less for the P-level was treated as an acceptable error level.

4.3.2 STATISTICAL ASSUMPTIONS

Ensuing assumptions were obtained from Kleinbaum et al. (1988). The assumptions listed below are the typical assumptions for multivariate linear regression:

Assumption 1: *Existence.* For each specific combination of values of the independent variables, the dependent variable, Y , represents a random variable with a certain probability distribution having finite mean and variance.

Assumption 2: *Independence.* The Y observations are statistically independent of one another.

Assumption 3: *Linearity*. The mean value of the dependent variable, Y, for each specific combination of independent variables equals a linear function of the independent variables.

Assumption 4: *Homoscedasticity*. Constant variance of the dependent variable, Y, for any fixed combination of independent variables. This assumption may seem very restrictive. However, Assumption 4 must be considered only when the data show very obvious and significant departures from homogeneity. In general, mild departures will not have too adverse an effect on the results.

Assumption 5: *Normality*. For any fixed combination of independent variables, the dependent variable, Y, follows a normally (Gaussian) distribution.

In order to assure that these assumptions are addressed, several tests are performed. A listing of the type of test and a brief description are listed below from Kleinbaum et al. (1988):

1. Preliminary statistical significance – Checks to ensure that the number of observations or data points are at least 20 times the number of independent variables included in the analysis. This test assures that another similar experiment would produce similar results.
2. Partial correlation, Beta – Checks to measure the degree of linearity between the dependent variable and an independent variable. This test assures that each of the independent variables contributes toward the prediction of the dependent variable.

3. Plot of predicted values versus observed values – Checks to determine which portions of the data do not fit particularly well with the rest of the data, suggesting another relationship. This test also shows how well the computed relationship matches the actual data.
4. Plot of predicted values versus the residual scores – Check to ensure that the relationship chosen can be considered linear in nature. If the relationship forms a homogeneous distribution of points around the horizontal center line, the relationship can be considered linear. If any patterns are present in the plot, it may indicate the need for data transformation or that a multivariate linear regression may not be valid.
5. Plot of residuals versus deleted residuals – Checks to ensure if there are significant outliers in the data set, which would bias the regression line toward the outlier. An outlier can be defined as a point that lies outside plus or minus two standard deviations of the mean. If an outlier is detected, it can be removed when justified. This test assures that all data points are valid for the regression line.
6. Normal probability plot of residuals – Checks to ensure that all of the variables and their residuals are normally (Gaussian) distributed. When the plotted data closely approximates the straight line, the variables and their residuals are considered normally distributed. This plot assures that the data can be analyzed using multivariate linear regression.

5 DISCUSSION OF RESULTS

5.1 INTRODUCTION

Once an understanding of the background information and a literature review were obtained, a clear and comprehensive testing matrix with detailed nomenclature was developed and data were collected and verified. Results of the dimensional analysis performed in Section 4.2, and presented in Equation 4.2 indicated that the equilibrium depth of pressure flow deck scour (y_{pds}), the equilibrium depth of pressure flow abutment scour (y_{pas}), the upstream flow depth (y), the abutment protrusion length (a), the average upstream flow velocity (V_a), the average velocity under the bridge deck (V_b), a computed critical velocity (V_c) and the initial bridge opening (H_b) were relevant for subsequent analysis. Equilibrium depth of pressure flow deck and pressure flow abutment scour were determined from the deepest point measured under and around the bridge deck corresponding to a bed elevation measurement. Abutment protrusion length was determined based on which set of abutments were being tested. The upstream flow depth was obtained from water surface elevation minus bed elevation readings at a position three feet upstream of the bridge face in the center of the flume. Average upstream flow velocity was obtained at the 60% depth measurement at a position three feet upstream of the bridge face in the center of the flume. Average velocity under the bridge deck was

computed as the average of the velocities collected vertically in the center of the flume under the center of the bridge deck. Equation 2.1 was used to compute the critical velocity utilizing the corresponding upstream flow depth and appropriate sediment size. Initial bridge opening heights were preselected and presented in Table 3.4. Selected variables were then grouped into dimensionless terms as discussed in Section 4.2, analyzed and evaluated. Table 5.1 presents the data corresponding to each of the dimensionless parameters presented in Equation 4.2 and utilized for analysis. Summary tables of the data used to form the dimensionless variables in Table 5.1 are presented in the Appendix Tables A1 and A2. Succeeding sections present and discuss the developed predictive relationships.

• Table 5.1 – Summary of dimensionless parameters used during analysis

Test Number	Bridge Position	y_{pds}/y	y/H_b	$(y_{pds} + H_b)/y$	V_b/V_c	y_{pas}/a	$(V/(gy))^{0.5}$
1	1	0.15	0.83	1.35	0.52	0.58	0.13
2	2	0.20	0.98	1.23	0.51	0.63	0.13
3	3	0.08	1.41	0.79	0.71	0.27	0.10
4	4	0.08	1.84	0.62	0.88	0.42	0.09
5	5	0.11	2.31	0.54	0.94	0.60	0.09
6	6	0.20	3.40	0.49	0.99	0.80	0.09
7	1	0.23	0.98	1.25	0.99	0.71	0.26
8	2	0.30	1.11	1.20	1.22	0.73	0.28
9	3	0.39	1.32	1.14	1.24	0.88	0.26
10	4	0.55	1.59	1.18	1.31	0.98	0.27
11	5	0.67	2.07	1.15	1.33	1.23	0.28
12	6	0.74	3.01	1.07	1.17	1.30	0.25
13	1	0.41	1.04	1.37	1.30	0.91	0.35
14	2	0.56	1.20	1.39	1.31	1.13	0.33
15	3	0.65	1.40	1.36	1.37	1.19	0.32
16	4	0.76	1.62	1.38	1.47	1.17	0.32
17	5	0.89	2.04	1.38	1.45	1.77	0.31
18	6	0.78	2.91	1.13	1.34	1.75	0.30
19	1	0.11	1.06	1.06	0.69	0.22	0.12
20	2	0.05	1.20	0.88	0.95	0.22	0.11
21	3	0.10	1.40	0.81	1.02	0.22	0.12
22	4	0.34	1.73	0.92	1.09	0.23	0.10
23	5	0.42	2.15	0.88	1.14	0.23	0.12
24	6	0.48	2.91	0.83	1.17	0.26	0.12
25	1	0.43	1.05	1.38	1.07	0.34	0.23
26	2	0.65	1.20	1.48	1.28	0.38	0.25
27	3	0.69	1.40	1.40	1.27	0.43	0.23
28	4	0.85	1.70	1.44	1.39	0.47	0.23
29	5	0.85	2.14	1.32	1.39	0.49	0.24
30	6	0.85	2.98	1.18	1.39	0.56	0.21
31	1	1.08	0.89	2.21	1.18	0.57	0.36

• Table 5.1 (continued) – Summary of dimensionless parameters used during analysis

Test Number	Bridge Position	y_{pds}/y	y/H_b	$(y_{pds} + H_b)/y$	V_b/V_c	y_{pas}/a	$(V/(gy))^{0.5}$
37	1	0.04	1.00	1.05	0.34	0.13	0.10
38	2	0.05	1.23	0.86	0.49	0.13	0.09
39	3	0.04	1.42	0.74	0.52	0.14	0.10
40	4	0.03	1.77	0.60	0.65	0.14	0.09
41	5	0.06	2.26	0.50	0.74	0.22	0.09
42	6	0.21	2.98	0.55	0.82	0.32	0.09
43	1	0.14	0.95	1.18	0.87	0.50	0.29
44	2	0.26	1.07	1.19	1.00	0.63	0.29
45	3	0.37	1.26	1.17	1.02	0.81	0.28
46	4	0.49	1.56	1.13	1.09	0.92	0.26
47	5	0.57	1.93	1.08	1.11	1.13	0.26
48	6	0.71	2.66	1.09	1.11	1.30	0.26
49	1	0.35	0.98	1.37	1.00	0.97	0.37
50	2	0.51	1.17	1.36	1.16	1.18	0.33
51	3	0.64	1.40	1.36	1.17	1.22	0.33
52	4	0.78	1.68	1.37	1.09	1.33	0.35
53	5	0.84	2.09	1.32	1.18	1.59	0.33
54	6	1.01	2.84	1.36	1.03	1.77	0.31
55	1	0.00	1.05	0.96	0.43	0.04	0.09
56	2	0.00	1.16	0.86	0.64	0.09	0.10
57	3	0.00	1.36	0.74	0.70	0.13	0.09
58	4	0.13	1.65	0.74	0.85	0.15	0.10
59	5	0.22	2.09	0.70	0.87	0.20	0.09
60	6	0.31	2.79	0.67	0.87	0.25	0.09
61	1	0.40	1.06	1.35	0.83	0.41	0.22
62	2	0.63	1.20	1.47	0.94	0.48	0.23
63	3	0.69	1.43	1.38	0.92	0.52	0.21
64	4	0.81	1.71	1.40	1.02	0.57	0.23
65	5	0.83	2.16	1.29	0.99	0.59	0.22
67	1	0.78	1.01	1.77	0.90	0.55	0.32
68	2	1.02	1.17	1.88	1.00	0.59	0.34

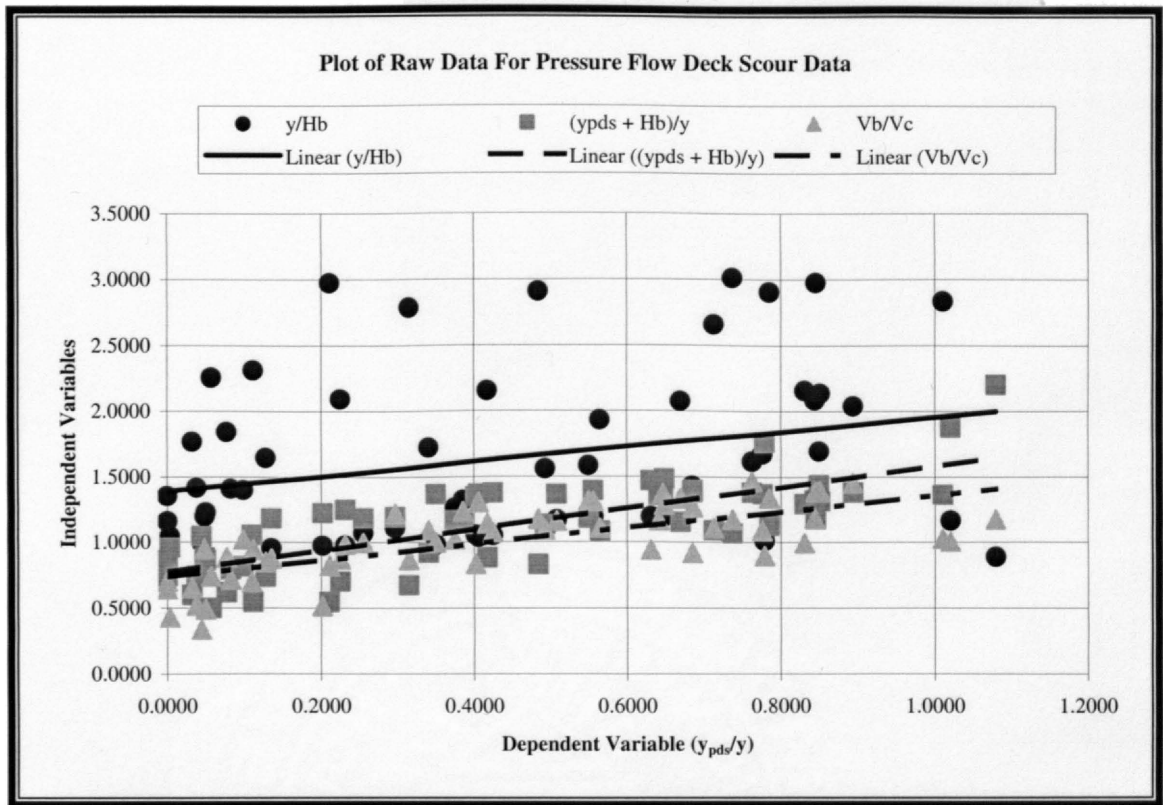
5.2 PRESSURE FLOW DECK SCOUR EQUATIONS

Resulting from the dimensional analysis performed in Section 4.2, it was concluded that a pressure flow deck scour relationship was a function of the independent and dimensionless variables presented in Equation 5.1.

$$\frac{y_{pds}}{y} = f\left(\frac{y}{H_b}, \frac{y_{pds} + H_b}{y}, \frac{V_b}{V_c}\right)$$

• **Equation 5.1**

Based on the plot for each of the independent variables plotted against the dependent variable shown in Figure 5.1, it was determined that a multivariate linear relationship was valid for describing the data. Figure 5.1 shows that each of the independent variables can be considered a linear function of the dependent variable y_{pds}/y and since each of the slopes of the individual regression lines were approximately equal, a multivariate linear relationship was valid.



• Figure 5.1 – Plot of raw data for pressure flow deck scour data

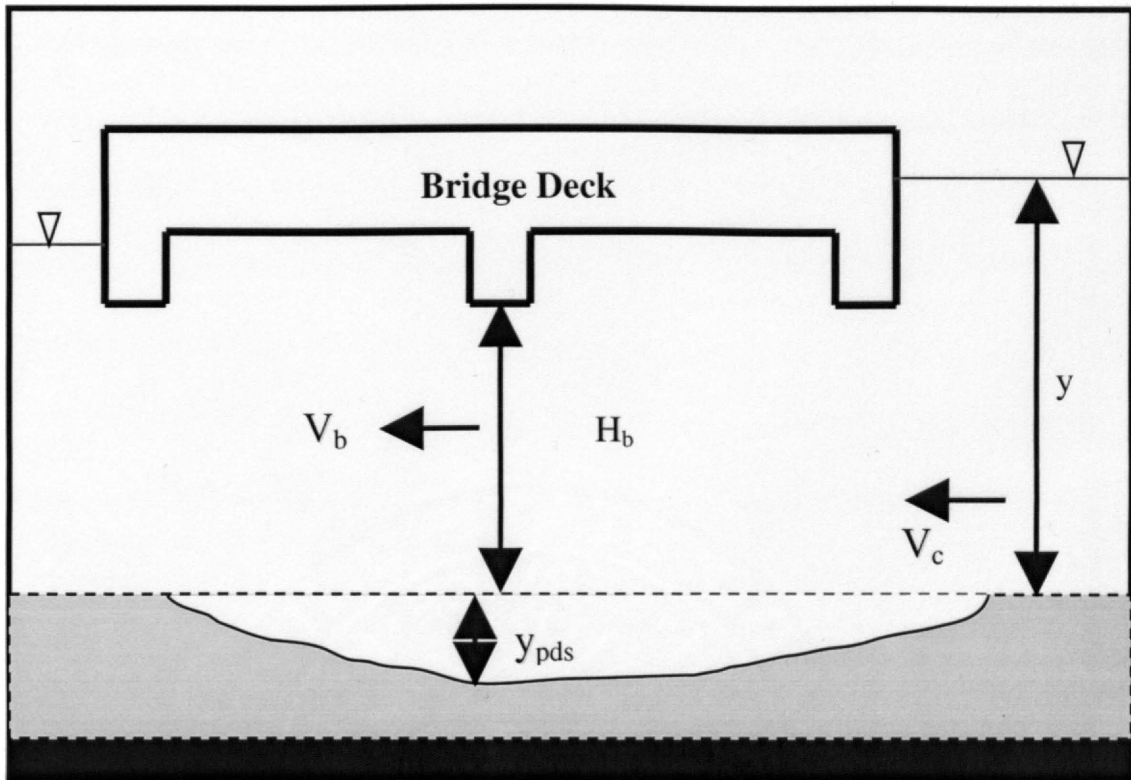
From the statistical analysis presented in Chapter 4 and the regression summary presented in Tables 5.2 and 5.3, the pressure flow deck scour prediction equation follows as

$$\frac{y_{pds}}{y} = -1.173 + 0.298 \left(\frac{y}{H_b} \right) + 0.860 \left(\frac{y_{pds} + H_b}{y} \right) + 0.151 \left(\frac{V_b}{V_c} \right)$$

• Equation 5.2

Figure 5.2 presents a graphical definition of the variables used in Equation 5.2.

Equation 5.2 was rearranged and solved for y_{pds}/y to produce Equation 5.3.



• Figure 5.2 – Graphical definition of variables used in Equation 5.2

$$\frac{y_{pds}}{y} = -8.359 + 2.121 \left(\frac{y}{H_b} \right) + 6.127 \left(\frac{H_b}{y} \right) + 1.079 \left(\frac{V_b}{V_c} \right)$$

• Equation 5.3

Where,

- y_{pds} = depth of pressure flow deck scour relative to mean bed elevation, L;
- y = depth of flow immediately upstream of the bridge deck, L;
- V_b = average velocity of flow under the bridge, L/T;
- V_c = velocity of flow for incipient motion of bed material, L/T; and
- H_b = distance from bridge low chord to the initial mean bed elevation, L.

During the statistical analysis, the 62 data points were reduced to 59 due to the presence of three outliers. All three outliers were removed because each was beyond two standard deviations from the mean. Table 5.2 presents a multivariate linear regression summary associated with Equation 5.2. Table 5.3 displays an ANOVA table corresponding to Equation 5.2.

• **Table 5.2 – Multivariate linear regression summary statistics corresponding to Equation 5.2**

Number of Measurements	59					
Dependent Variable	y_{pds}/y					
Independent Variables	Beta	Standard Error of Beta	B	Standard Error of B	t(50)	P-level
Intercept			-1.173	0.045	-25.782	0.000
y/H_b	0.597	0.034	0.298	0.017	17.532	0.000
$(y_{pds} + H_b)/y$	0.923	0.037	0.860	0.034	24.990	0.000
V_b/V_c	0.131	0.036	0.151	0.041	3.699	0.001
R =	0.981					
R² =	0.962					
Adjusted R² =	0.960					
F(3,55) =	459.405					
p <	0.000					
Standard error of estimate	0.063					

• Table 5.3 - ANOVA table associated with Equation 5.2

	Degrees of	Sum of	Mean Square	F-Statistic	P-Level
Source	Freedom (df)	Squares (SS)	(MS)		
Regression	3	5.467	1.822	459.405	0.000
Error	55	0.218	0.004		
Total	58	5.685			

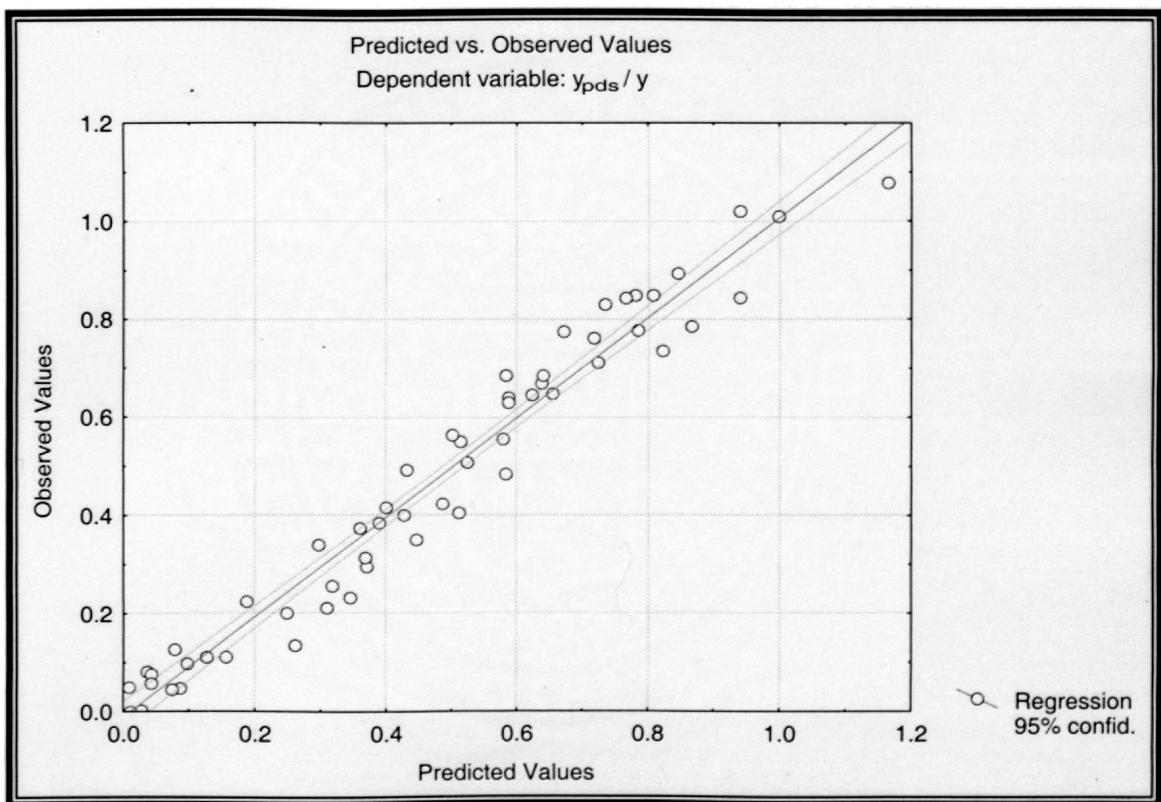
Listed in Table 5.2, the adjusted coefficient of determination, R^2 , from the analysis for Equation 5.2 was 0.96, indicating that 96 percent of the variability in the data was explained by the relationship. An overall significance test indicated that the critical F value for $k = 3$ and $n = 59$ was 2.76. Since the F-Statistic shown in Table 5.3 of 459.40 was greater than 2.76, the three independent variables explained a significant amount of the variation in the dependent variable y_{pds}/y . Additionally, the P-level of all independent variables and the overall P-level were all less than the selected value of 0.05, therefore the analysis was determined to be statistically significant.

Preliminary statistical significance was computed as three independent variables times 20 (Kleinbaum et al., 1988), yielding a number of 60 for the minimum number of data points for statistical analysis to be valid. For the pressure flow deck scour data, there were 59 measurements used for the statistical analysis, therefore the analysis was considered valid.

Partial correlation, Beta, for each of the independent variables indicated that the variable, $(y_{pds} + H_b)/y$, was the most significant with a Beta value of 0.923; the variable, y/H_b , was the next most significant with a Beta value of 0.597; and the variable, V_b/V_c , was the least significant with a Beta value of 0.131. Inclusion of the variable V_b/V_c , while statistically the least significant incorporated the effects of velocity and sediment

size used in the experiments due to the use of the median bed material size in computing the critical velocity, V_c .

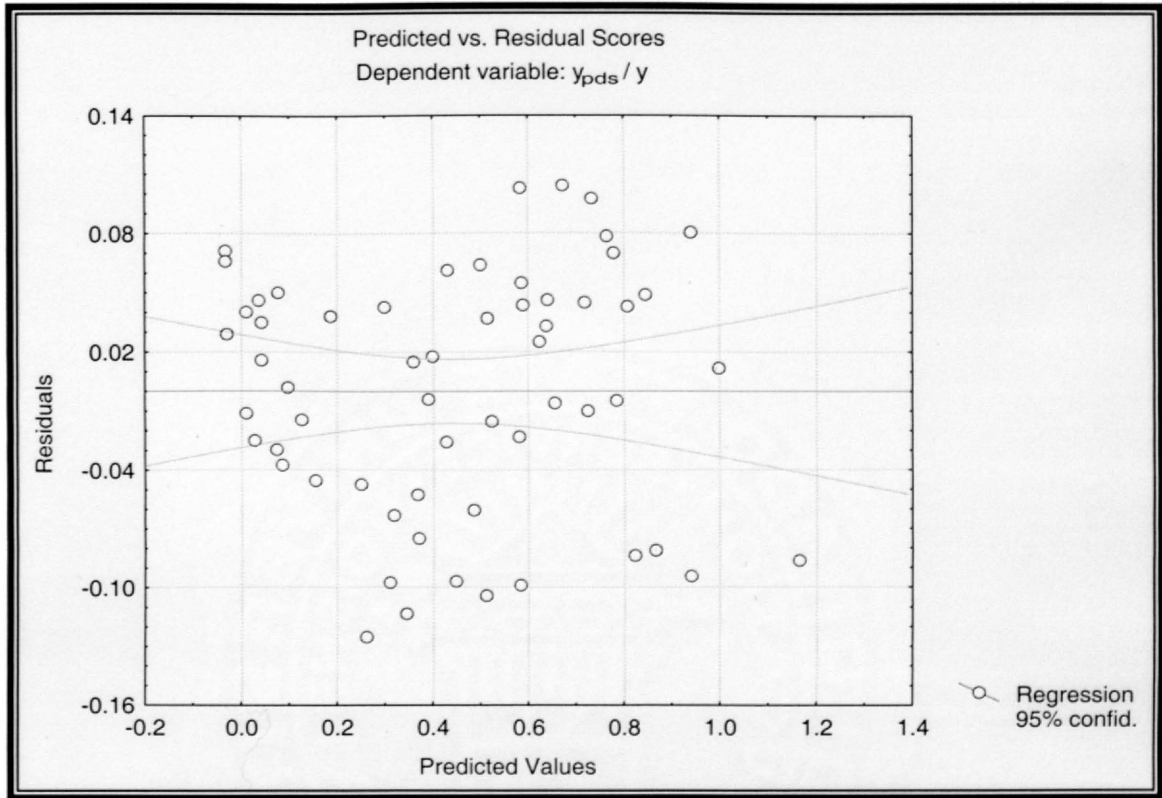
Figure 5.3 presents a plot of observed values versus predicted values for the pressure flow deck scour data. Figure 5.3 indicates that Equation 5.2 can be considered a reliable prediction equation, having points both above and below the line of equal prediction.



• Figure 5.3 – Observed versus predicted values for pressure flow deck scour data

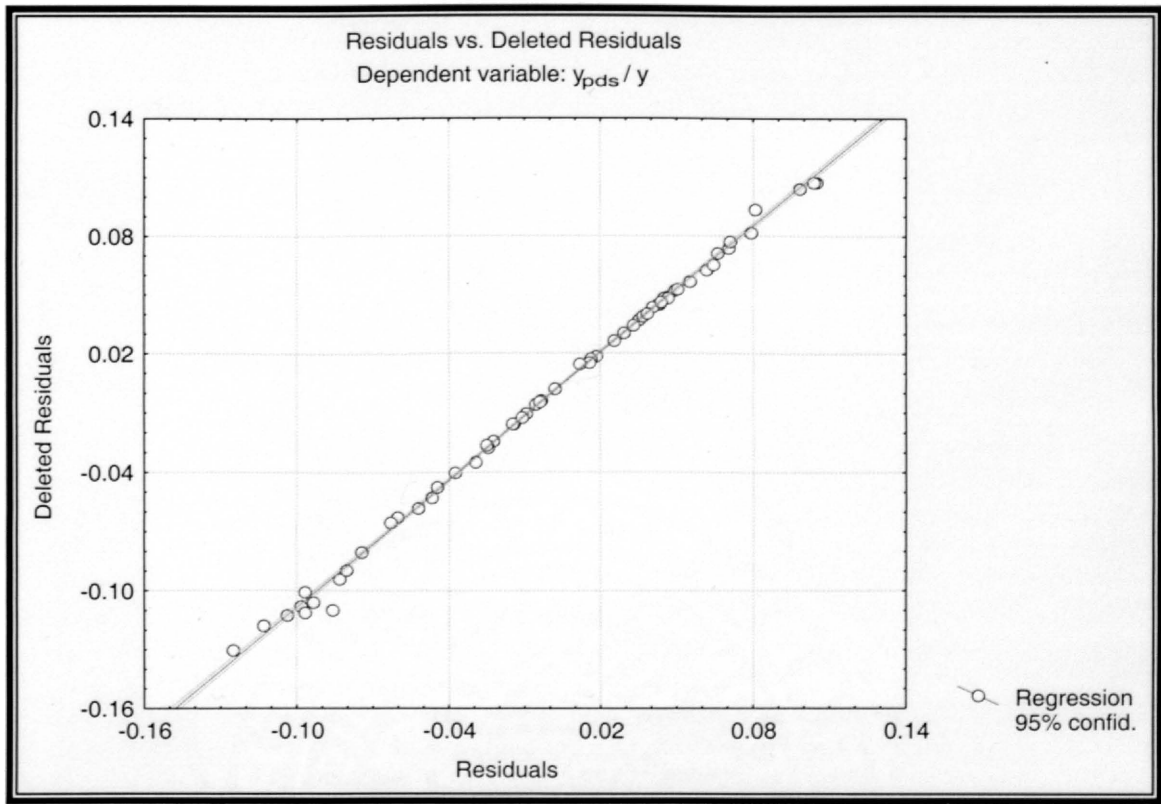
Figure 5.4 displays a plot of predicted values versus the residual scores for the dependent variable y_{pds}/y . Data points plotted in Figure 5.4 form a homogeneous

distribution of points around the horizontal centerline verifying that the relationship was linear.



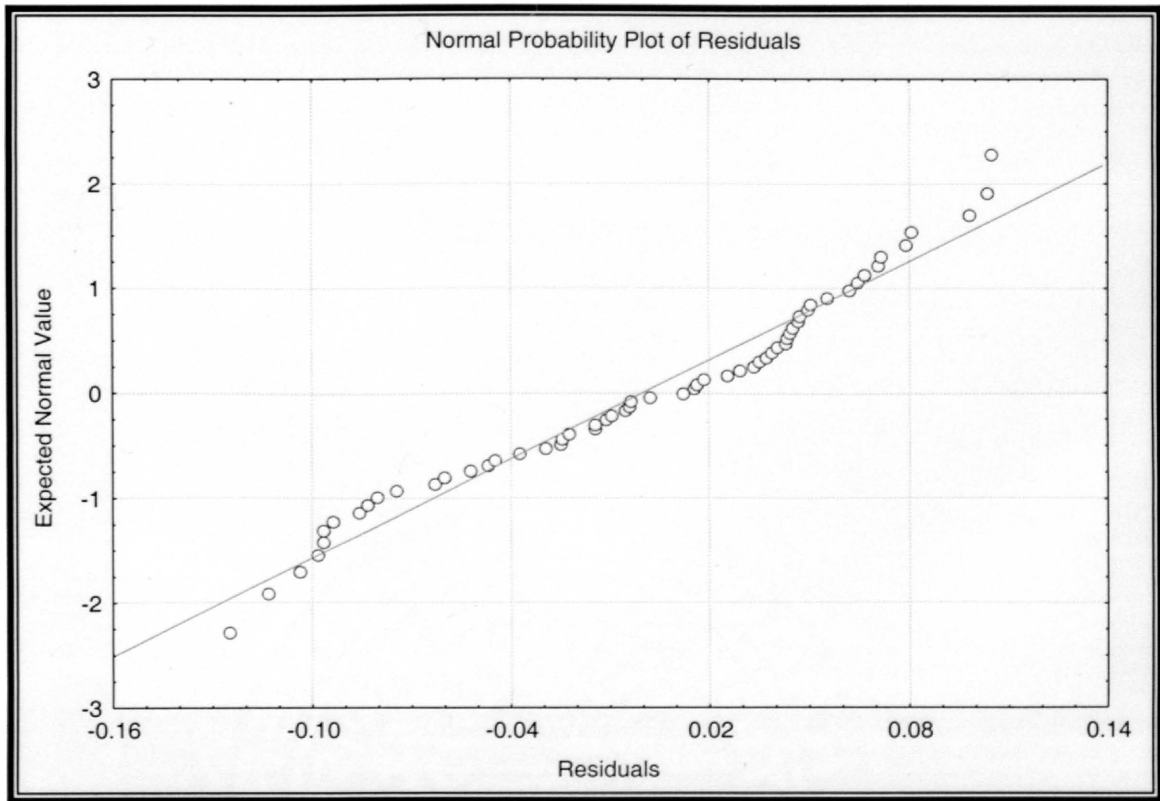
• **Figure 5.4 – Predicted values versus residual scores for y_{pds}/y**

Figure 5.5 displays a plot of residuals versus deleted residuals for the dependent variable y_{pds}/y . Figure 5.5 indicates that no additional outliers exist since all plotted points approximate the straight line, indicating that the data points used were valid for development of Equation 5.2.



• **Figure 5.5 – Residuals versus deleted residuals for y_{pds}/y**

Figure 5.6 presents the normal probability plot of residuals for the pressure flow deck scour data. Figure 5.6 indicates that the residuals very closely approximated a normal distribution since the plotted points follow the straight line, assuring that the data could be analyzed using multivariate linear regression.

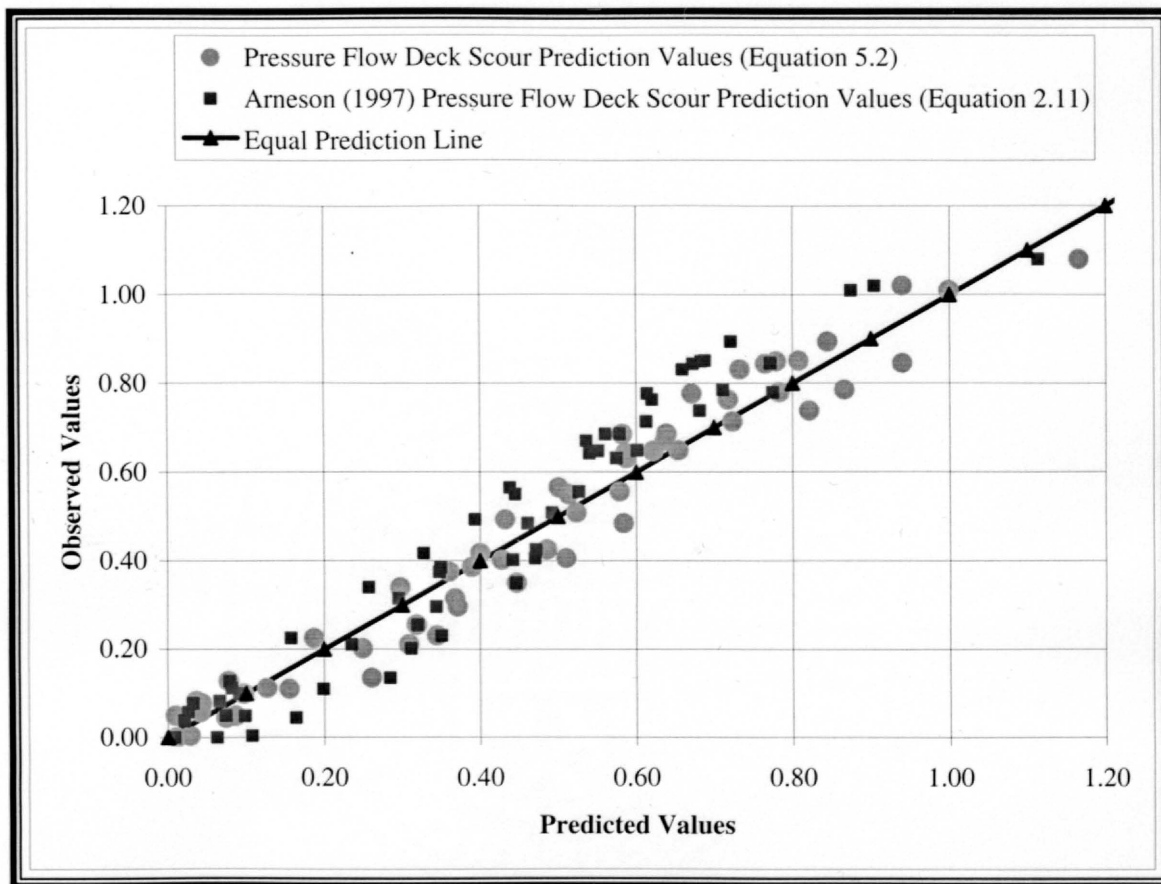


• Figure 5.6 – Normal probability plot of residuals for pressure flow deck scour data

Data collected were developed into dimensionless independent variables that were used in a multivariate linear regression analysis to develop Equation 5.2. Equation 5.2 had a coefficient of determination, R^2 , of 0.96, indicating that 96 percent of the variability in the data was explained by the relationship. Additionally, the data satisfied the overall significance test and the individual tests for checking multivariate linear regression validity.

Since Equation 5.2, for the prediction of pressure flow deck scour, was developed using techniques similar to Arneson (1997), a comparison with Equation 2.11 for the prediction of pressure flow deck scour from Arneson (1997) was warranted.

Figure 5.7 displays a plot of observed versus predicted values for the pressure flow deck scour prediction equation (Equation 5.2) against the pressure flow deck scour equation (Equation 2.11) developed by Arneson (1997).



• **Figure 5.7 - Observed versus predicted values for the pressure flow deck scour prediction equation (Equation 5.2) against the pressure flow deck scour equation (Equation 2.11) developed by Arneson (1997)**

Based on the observation that Equation 5.2 and Equation 2.11, developed by Arneson (1997), both predict similar values, the data sets were combined. On average Equation 5.2 predicts more conservatively (a deeper scour hole) than Equation 2.11 by approximately 13.1 percent. Data from the combined set yielded 186 data points for each

of the independent dimensionless variables previously defined for pressure flow deck scour. Table 5.4 presents 124 data points corresponding to the parameters calculated from Arneson's (1997) data set. The remaining 62 data points of the total 186 data points can be found in Table 5.1.

• Table 5.4 – Summary of calculated pressure flow deck scour data from Arneson (1997)

Bridge Position	y_{pds}/y	y/H_b	$(y_{pds} + H_b)/y$	V_b/V_c
1	-0.02	1.08	0.91	0.46
2	0.01	1.23	0.82	0.58
3	0.02	1.43	0.72	0.71
4	0.03	1.74	0.61	0.94
5	0.04	2.31	0.47	1.03
6	0.15	2.96	0.48	1.07
1	0.01	1.02	0.99	0.89
2	0.05	1.14	0.93	1.20
3	0.18	1.37	0.91	1.33
4	0.31	1.63	0.92	1.43
5	0.32	2.08	0.80	1.45
6	0.42	2.75	0.79	1.56
3	0.25	1.80	0.81	1.70
4	0.42	2.02	0.91	1.37
5	0.45	2.48	0.85	1.71
6	0.50	2.87	0.85	1.73
1	0.00	1.04	0.97	0.55
2	-0.02	1.01	0.97	0.67
3	0.00	1.37	0.74	0.77
4	0.05	1.68	0.65	0.93
5	0.11	2.00	0.61	1.06
6	0.21	2.78	0.57	1.10
1	0.02	1.01	1.01	1.06
2	0.12	1.16	0.98	1.17
3	0.20	1.40	0.92	1.22
4	0.26	1.77	0.82	1.36
5	0.41	2.29	0.85	1.37
6	0.41	3.18	0.72	0.75
2	0.31	1.17	1.17	1.52
3	0.23	1.94	0.74	1.47
4	0.54	2.01	1.04	1.49
1	-0.01	0.98	1.01	0.41
2	0.00	1.25	0.80	0.38
3	-0.01	1.54	0.64	0.53
4	-0.01	1.88	0.53	0.59
5	0.01	2.23	0.46	0.52
6	0.09	2.94	0.43	0.90
1	0.01	0.99	1.01	0.72

• Table 5.4 (continued) – Summary of calculated pressure flow deck scour data from Arneson (1997)

Bridge Position	y_{pds}/y	y/H_b	$(y_{pds} + H_b)/y$	V_b/V_c
2	0.07	1.14	0.95	0.97
3	0.20	1.33	0.95	1.09
4	0.32	1.62	0.94	1.17
5	0.40	2.01	0.90	0.99
6	0.47	2.72	0.84	1.35
1	0.01	1.04	0.97	1.10
2	0.17	1.18	1.02	1.33
3	0.33	1.41	1.04	1.37
4	0.41	2.10	0.88	1.25
5	0.52	2.49	0.92	1.13
6	0.57	3.13	0.89	1.08
1	0.00	1.09	0.92	0.43
2	-0.02	1.34	0.73	0.47
3	-0.02	1.50	0.65	0.40
4	-0.01	1.78	0.55	0.66
5	0.03	2.20	0.49	0.86
6	0.09	2.91	0.43	0.87
2	0.07	1.07	1.00	0.99
3	0.18	1.26	0.97	1.11
4	0.30	1.52	0.95	1.23
5	0.44	1.81	0.99	1.29
6	0.54	2.36	0.97	1.34
2	0.11	1.14	0.98	1.41
3	0.30	1.32	1.06	1.44
4	0.44	1.54	1.08	1.45
5	0.59	1.82	1.14	1.30
1	0.04	0.91	1.14	0.34
2	0.01	1.04	0.97	0.36
3	-0.07	1.19	0.76	0.54
4	-0.07	1.41	0.64	0.60
5	-0.03	1.72	0.55	0.77
6	-0.04	2.27	0.40	0.75
1	0.00	0.96	1.05	0.71
2	-0.01	1.07	0.93	0.89
3	-0.01	1.29	0.77	1.06
4	0.09	1.56	0.74	1.23
5	0.16	2.00	0.66	1.29
6	0.24	2.57	0.63	1.33

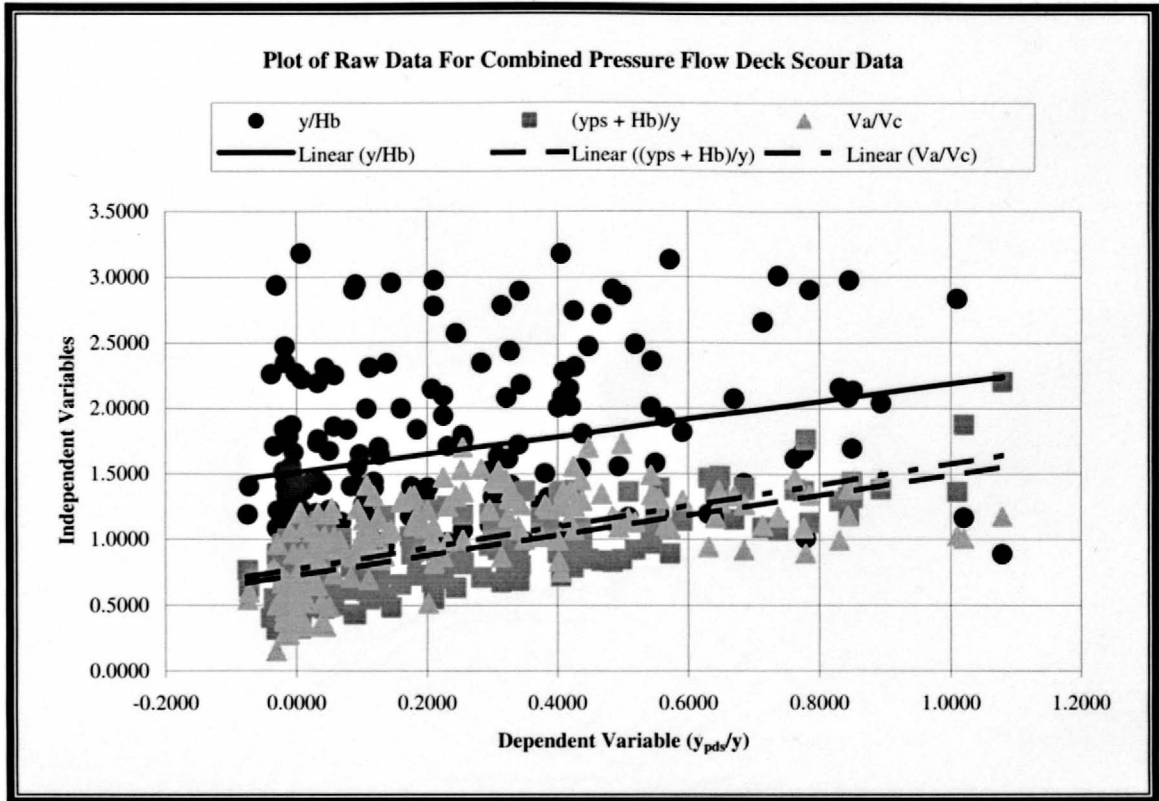
• Table 5.4 (continued) – Summary of calculated pressure flow deck scour data from Arneson (1997)

Bridge Position	y_{pds}/y	y/H_b	$(y_{pds} + H_b)/y$	V_b/V_c
2	0.01	1.06	0.95	1.21
3	0.12	1.40	0.83	1.33
4	0.25	1.71	0.84	1.53
5	0.28	2.35	0.71	1.54
1	0.01	0.91	1.11	0.36
2	-0.01	1.05	0.94	0.37
3	-0.01	1.21	0.81	0.44
4	-0.02	1.41	0.69	0.38
5	-0.01	1.78	0.55	0.68
6	0.00	2.27	0.44	0.47
2	0.03	1.20	0.86	0.98
3	0.03	1.45	0.72	1.20
4	0.13	1.71	0.71	1.16
2	0.05	1.13	0.94	1.24
3	0.18	1.41	0.89	1.31
4	0.23	1.71	0.82	1.25
5	0.33	2.44	0.74	1.31
1	-0.01	1.03	0.96	0.27
3	-0.01	1.49	0.67	0.38
4	0.00	1.67	0.60	0.38
5	-0.02	2.47	0.39	0.37
6	-0.03	2.94	0.31	0.15
1	-0.03	1.09	0.89	0.50
2	-0.02	1.01	0.97	0.72
3	-0.02	1.52	0.64	0.58
4	0.06	1.86	0.59	1.02
5	0.14	2.34	0.56	1.05
1	-0.03	1.08	0.89	0.75
2	-0.03	1.22	0.79	0.96
3	0.12	1.44	0.81	1.03
4	0.18	1.84	0.73	1.19
5	0.43	2.32	0.86	1.25
1	-0.01	1.22	0.81	0.27
2	-0.01	1.38	0.71	0.31
3	-0.01	1.56	0.63	0.40
4	-0.02	1.84	0.52	0.27
5	-0.02	2.35	0.41	0.46
6	0.01	3.18	0.32	0.34

• Table 5.4 (continued) – Summary of calculated pressure flow deck scour data from Arneson (1997)

Bridge	y_{pds}/y	y/H_b	$(y_{pds} + H_b)/y$	V_b/V_c
Position				
1	0.01	1.02	0.99	0.57
2	0.02	1.15	0.88	0.67
3	0.01	1.38	0.74	0.66
4	0.10	1.65	0.70	0.96
5	0.21	2.15	0.67	1.01
6	0.34	2.90	0.69	1.07
2	0.07	1.06	1.02	0.94
3	0.10	1.26	0.89	1.15
4	0.38	1.51	1.05	1.26
5	0.34	2.18	0.80	1.26

Summary tables of the data used to calculate the dimensionless variables in Table 5.4 from Arneson (1997) are presented in the Appendix Tables A3 through A6. Based on the plot for each of the independent variables plotted against the dependent variable shown in Figure 5.8, it was determined that a multivariate linear relationship was valid for describing the data. Figure 5.8 shows that each of the independent variables can be considered a linear function of the dependent variable y_{pds}/y and since each of the slopes of the individual regression lines were approximately equal, a multivariate linear relationship was valid.



• Figure 5.8 – Plot of raw data for combined pressure flow deck scour data

From the statistical analysis presented in Chapter 4 and the regression summary presented in Tables 5.5 and 5.6, the combined pressure flow deck scour prediction equation follows as

$$\frac{y_{pds}}{y} = -1.152 + 0.301 \left(\frac{y}{H_b} \right) + 0.876 \left(\frac{y_{pds} + H_b}{y} \right) + 0.092 \left(\frac{V_b}{V_c} \right)$$

• Equation 5.4

Figure 5.2 presents a graphical definition of the variables used in Equation 5.4. Equation 5.4 was rearranged and resolved for y_{pds}/y to produce the following relationship

$$\frac{y_{pds}}{y} = -9.264 + 2.423 \left(\frac{y}{H_b} \right) + 7.044 \left(\frac{H_b}{y} \right) + .738 \left(\frac{V_b}{V_c} \right)$$

• Equation 5.5

Where,

- y_{pds} = depth of pressure flow deck scour relative to mean bed elevation, L;
- y = depth of flow immediately upstream of the bridge deck, L;
- V_b = average velocity of flow under the bridge, L/T;
- V_c = velocity of flow for incipient motion of bed material, L/T; and
- H_b = distance from bridge low chord to the initial mean bed elevation, L.

During the statistical analysis, the 186 data points were reduced to 183 due to the presence of three outliers. All three outliers were removed because each was beyond two standard deviations from the mean. Table 5.5 presents a multivariate linear regression summary associated with Equation 5.4. Table 5.6 displays an ANOVA table corresponding to Equation 5.4.

• Table 5.5 – Multivariate linear regression summary statistics corresponding to Equation 5.4

Number of Measurements	183					
Dependent Variable	y_{pds}/y					
Independent Variables	Beta	Standard Error of Beta	B	Standard Error of B	t(50)	P-level
Intercept			-1.152	0.025	-46.291	0.000
y/H_b	0.676	0.021	0.301	0.009	32.964	0.000
$(y_{pds} + H_b)/y$	0.954	0.021	0.876	0.019	45.107	0.000
V_b/V_c	0.122	0.020	0.092	0.015	6.199	0.000
R =	0.975					
R ² =	0.951					
Adjusted R ² =	0.950					
F(3,179) =	1153.641					
p <	0.000					
Standard error of estimate	0.060					

• Table 5.6 - ANOVA table associated with Equation 5.4

Source	Degrees of Freedom (df)	Sum of Squares (SS)	Mean Square (MS)	F-Statistic	P-Level
Regression	3	12.652	4.217	1153.641	0.000
Error	179	0.654	0.004		
Total	182	13.306			

Listed in Table 5.5, the adjusted coefficient of determination, R^2 , from the analysis for Equation 5.4 was 0.95, indicating that 95 percent of the variability in the data was explained by the relationship. Therefore, combining both data sets was determined

valid because the coefficient of determination for Equation 5.4 was only slightly lower than the coefficient of determination value for Equation 5.2.

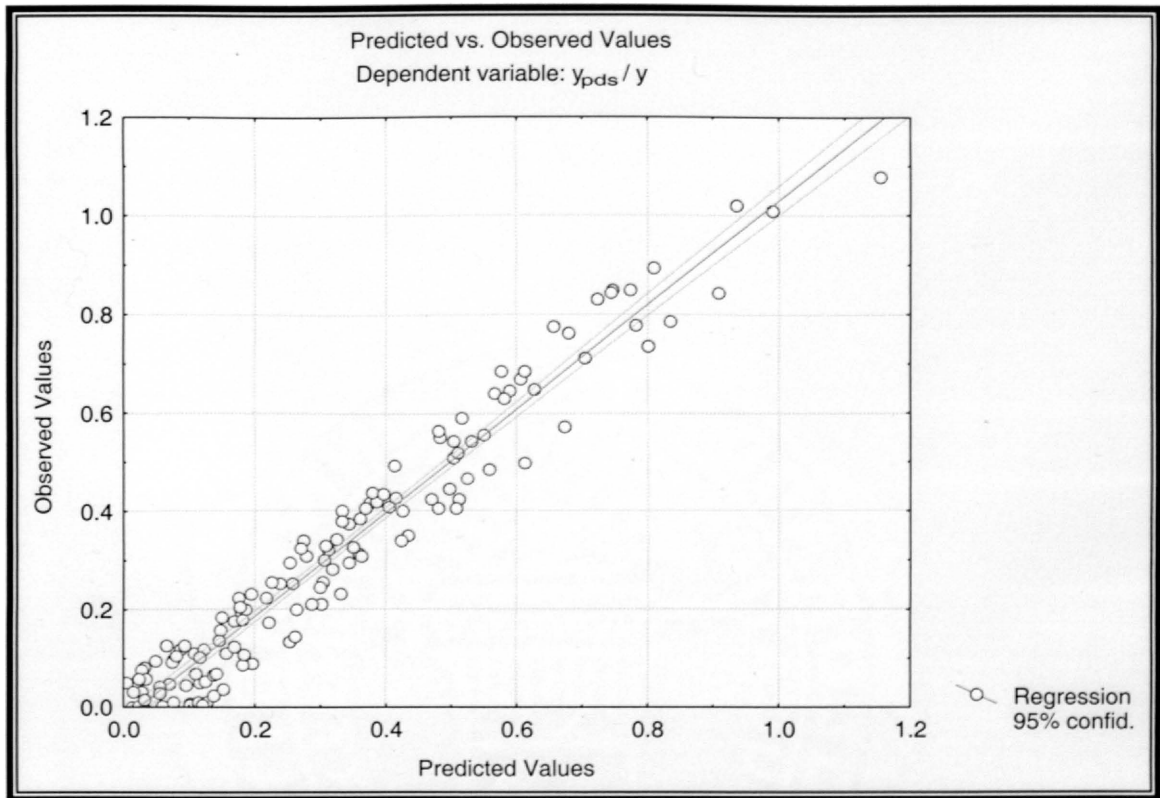
An overall significance test indicated that the critical F value for $k = 3$ and $n = 183$ was 2.66. Since the F-Statistic from Table 5.6 of 1153.64 was greater than 2.66, the three variables explained a significant amount of the variation in the dependent variable y_{pds}/y . Additionally, the P-level of all independent variables and the overall P-level were all less than the selected value of 0.05, therefore the analysis was determined to be statistically significant.

Preliminary statistical significance was computed as three independent variables times 20 (Kleinbaum et al, 1988), yielding a number of 60 for the minimum number of data points for statistical analysis to be valid. For the combined pressure flow deck scour data, there were 183 measurements used for the statistical analysis, therefore the analysis was considered valid.

Partial correlation, Beta, for each of the independent variables indicated that the variable, $(y_{pds} + H_b)/y$, was the most significant with a Beta value of 0.954; the variable, y/H_b , was the next most significant with a Beta value of 0.676; and the variable, V_b/V_c , was the least significant with a Beta value of 0.122. Inclusion of the variable V_b/V_c , while statistically the least significant incorporated the effects of velocity and sediment size used in the experiments due to the use of the median bed material size in computing the critical velocity, V_c .

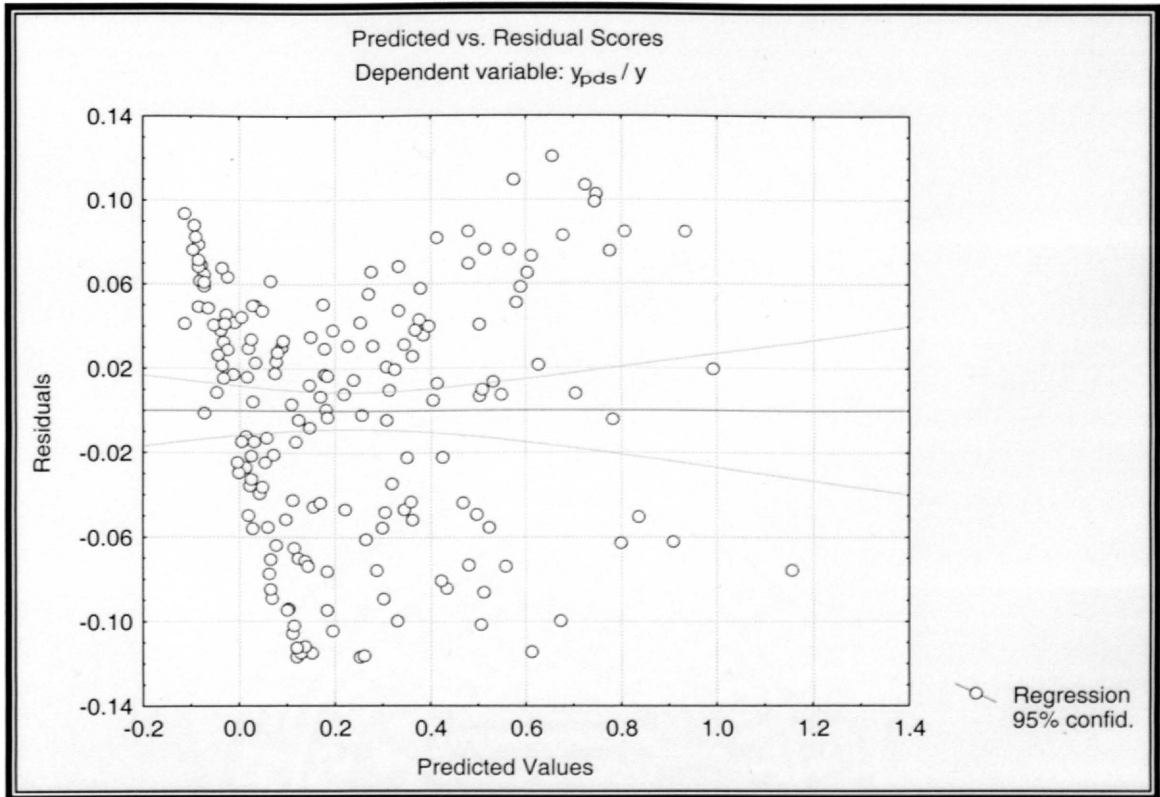
Figure 5.9 graphically displays observed values versus predicted values for the combined pressure flow deck scour data. Figure 5.9 indicates that Equation 5.4 can be

considered a reliable prediction equation, giving points both above and below the line of equal prediction.



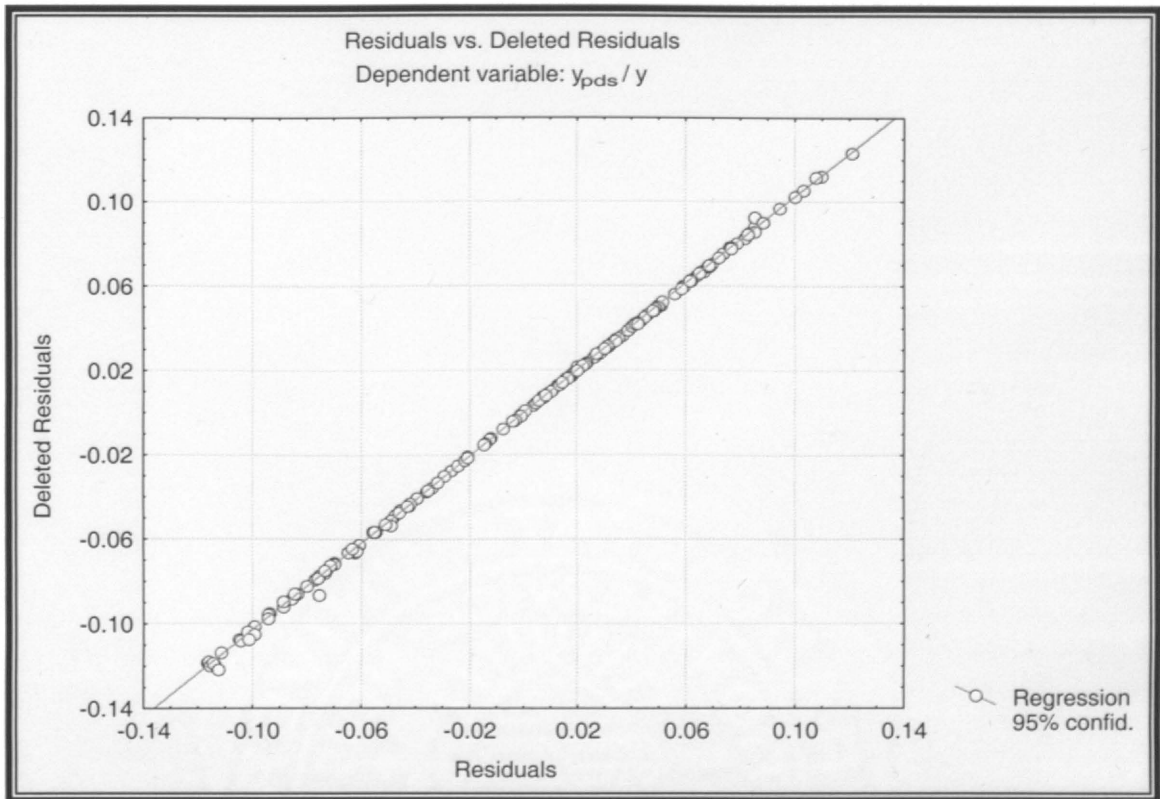
• **Figure 5.9 – Observed versus predicted values for combined pressure flow deck scour data**

Figure 5.10 displays a plot of predicted values versus the residual scores for the dependent variable y_{pds}/y . Data points plotted in Figure 5.10 form a homogeneous distribution of points around the horizontal centerline verifying that the relationship was linear.



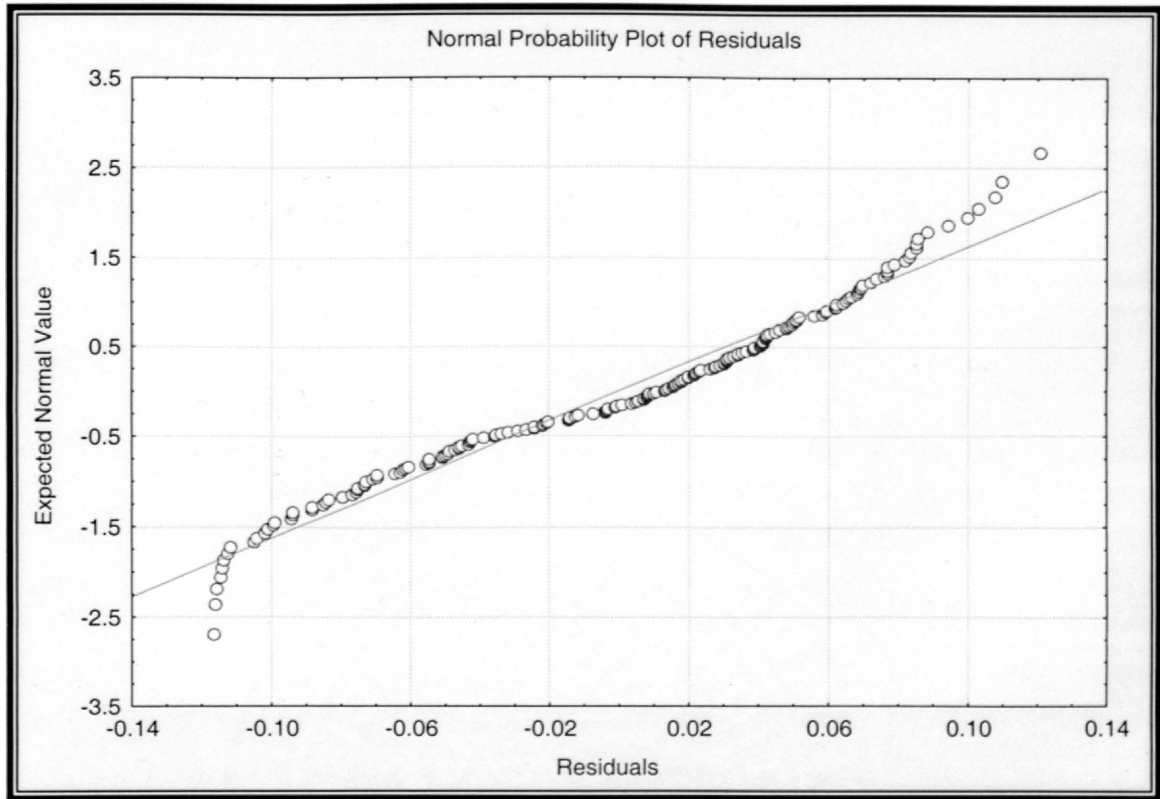
• **Figure 5.10 – Predicted values versus residual scores for combined y_{pds}/y**

Figure 5.11 presents a plot of residuals versus deleted residuals for the dependent variable y_{pds}/y . Figure 5.11 indicates that no additional outliers exist since all plotted points approximate the straight line, indicating that the data points used were valid for development of Equation 5.4.



• **Figure 5.11 – Residuals versus deleted residuals for combined pressure flow deck scour data**

Figure 5.12 shows the normal probability plot of residuals for the combined pressure flow deck scour data. Figure 5.12 indicates that the residuals very closely approximated a normal distribution since the plotted points follow the straight line, assuring that the data could be analyzed using multivariate linear regression.



• **Figure 5.12 – Normal probability plot of residuals for combined pressure flow scour data**

Equation 5.4 had a coefficient of determination, R^2 , of 0.95, indicating that 95 percent of the variability in the data was explained by the relationship. Combining both data sets was determined valid because the coefficient of determination for Equation 5.4 was only slightly lower than the coefficient of determination value for Equation 5.2. Additionally, the data satisfied the overall significance test and the individual tests for checking multivariate linear regression validity. Equation 5.4 is recommended for the prediction of pressure flow deck scour, although Equation 5.4 should be validated with field data prior to use. Additionally, V_b/V_c ratios must be within the range for the development of Equation 5.4 (0.3 – 1.7) and calculation of V_b

should be approximated with an appropriate closed conduit estimate of velocity for turbulent flow using initial bridge opening conditions.

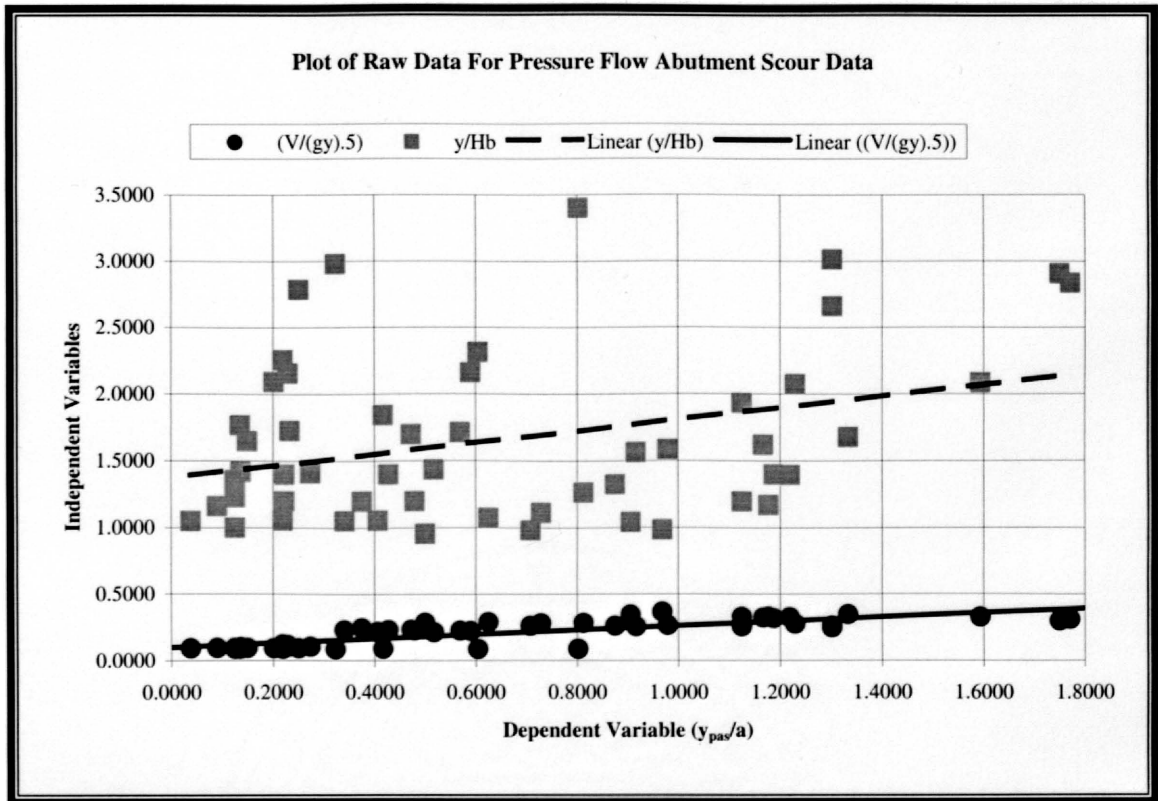
5.3 PRESSURE FLOW ABUTMENT SCOUR EQUATIONS

From the dimensional analysis performed in Section 4.2, it was concluded that a pressure flow abutment scour relationship was a function of the dimensionless independent variables presented in Equation 5.6.

$$\frac{y_{pas}}{a} = f\left(\frac{V_a}{\sqrt{gy}}, \frac{y}{H_b}\right)$$

• Equation 5.6

Based on the plot for each of the independent variables plotted against the dependent variable shown in Figure 5.13, it was determined that a multivariate linear relationship was valid for describing the data. Figure 5.13 shows that each of the independent variables can be considered a linear function of the dependent variable y_{pas}/a and since each of the slopes of the individual regression lines were approximately equal, a multivariate linear relationship was valid.



• Figure 5.13 – Plot of raw data for pressure flow deck scour data

From the statistical analysis presented in Chapter 4 and the regression summary presented in Tables 5.7 and 5.8, the pressure flow abutment scour prediction equation follows as

$$\frac{y_{pas}}{a} = -0.855 + 4.392 \left(\frac{V}{\sqrt{gy}} \right) + 0.361 \left(\frac{y}{H_b} \right)$$

• Equation 5.7

Where,

y_{pas} = depth of pressure flow abutment scour relative to m.b.e., L;

- y = depth of flow immediately upstream of the bridge deck, L;
- V_a = velocity of approach flow upstream of the bridge deck, L/T;
- g = acceleration due to gravity, L/T²;
- H_b = distance from bridge low chord to the initial mean bed elevation, L, and;
- a = abutment protrusion length, L.

During the statistical analysis, the 62 data points were reduced to 53 due to the presence of nine outliers. All nine outliers were removed because each was beyond two standard deviations from the mean. Table 5.7 presents a multivariate linear regression summary associated with Equation 5.7. Table 5.8 displays an ANOVA table corresponding to Equation 5.7.

• Table 5.7 – Multivariate linear regression summary statistics corresponding to Equation 5.7

Number of Measurements	53					
Dependent Variable	y_{pas}/a					
Independent Variables	Beta	Standard Error of Beta	B	Standard Error of B	t(50)	P-level
Intercept			-0.855	0.090	-9.520	0.000
$V_a/(gy)^{0.5}$	0.892	0.050	4.392	0.246	17.870	0.000
y/H_b	0.481	0.050	0.361	0.037	9.638	0.000
R =	0.938					
R ² =	0.879					
Adjusted R ² =	0.874					
F(2,50) =	181.840					
p <	0.000					
Standard error of estimate	0.058					

• Table 5.8 – ANOVA table associated with Equation 5.7

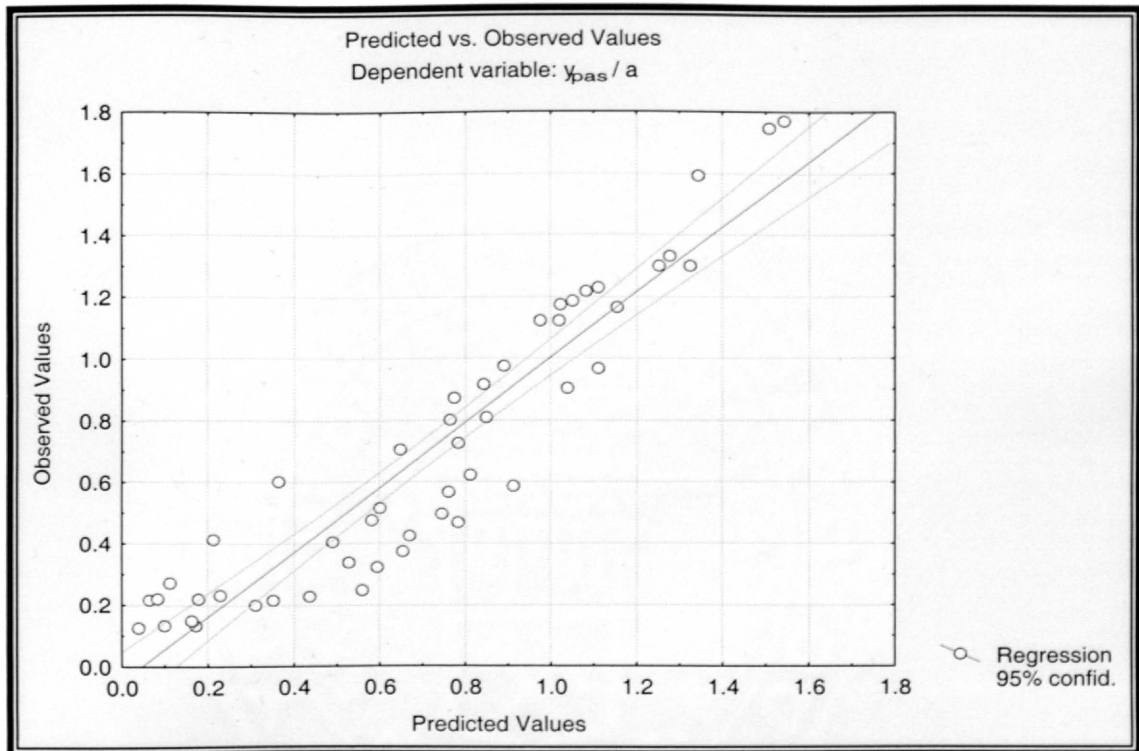
Source	Degrees of Freedom (df)	Sum of Squares (SS)	Mean Square (MS)	F-Statistic	P-Level
Regression	2	10.124	5.062	181.840	0.000
Error	50	1.392	0.028		
Total	52	11.516			

Listed in Table 5.7, the adjusted coefficient of determination, R^2 , from the analysis for Equation 5.7 was 0.87, indicating that 87 percent of the variability in the data was explained by the relationship. An overall significance test indicated that the critical F value for $k = 2$ and $n = 53$ was 3.17. Since the F-Statistic presented in Table 5.8 of 181.84 was greater than 3.17, the two independent variables explained a significant amount of the variation in the dependent variable y_{pas}/a . Additionally, the P-level of both independent variables and the overall P-level were all less than the selected value of 0.05, therefore the analysis was determined to be statistically significant.

Preliminary statistical significance was computed as two independent variables times 20 (Kleinbaum, 1988), yielding a number of 40 for the minimum number of data points for statistical analysis to be valid. For the pressure flow abutment scour data, there were 53 measurements used for the statistical analysis, therefore the analysis was considered valid.

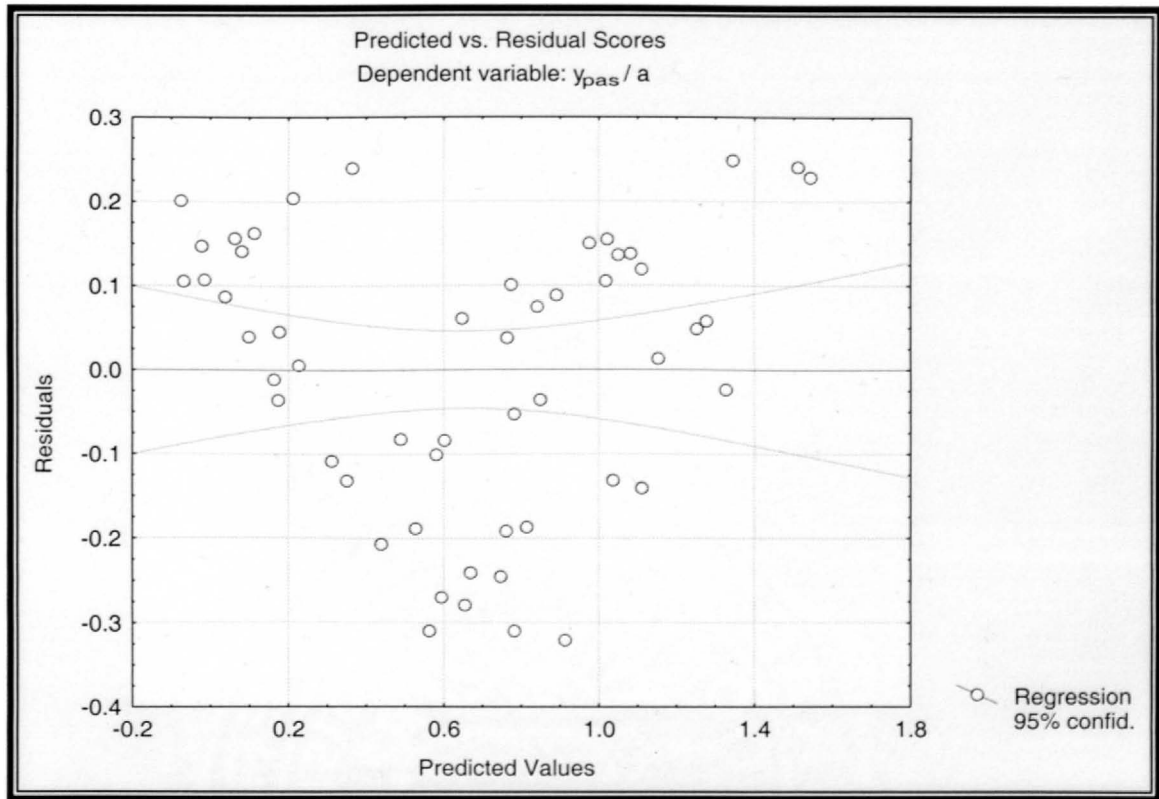
Partial correlation, Beta, for each of the independent variables indicated that the independent variable, $V_a/(gy)^{0.5}$, was the most significant with a Beta value of 0.892 and the independent variable, y/H_b , was the least significant with a Beta value of 0.481. Both Beta values were considered statistically significant.

Figure 5.14 graphically displays observed values versus predicted values for the pressure flow abutment scour data. Figure 5.14 indicates that Equation 5.7 can be considered a reliable prediction equation giving points both above and below the line of equal prediction.



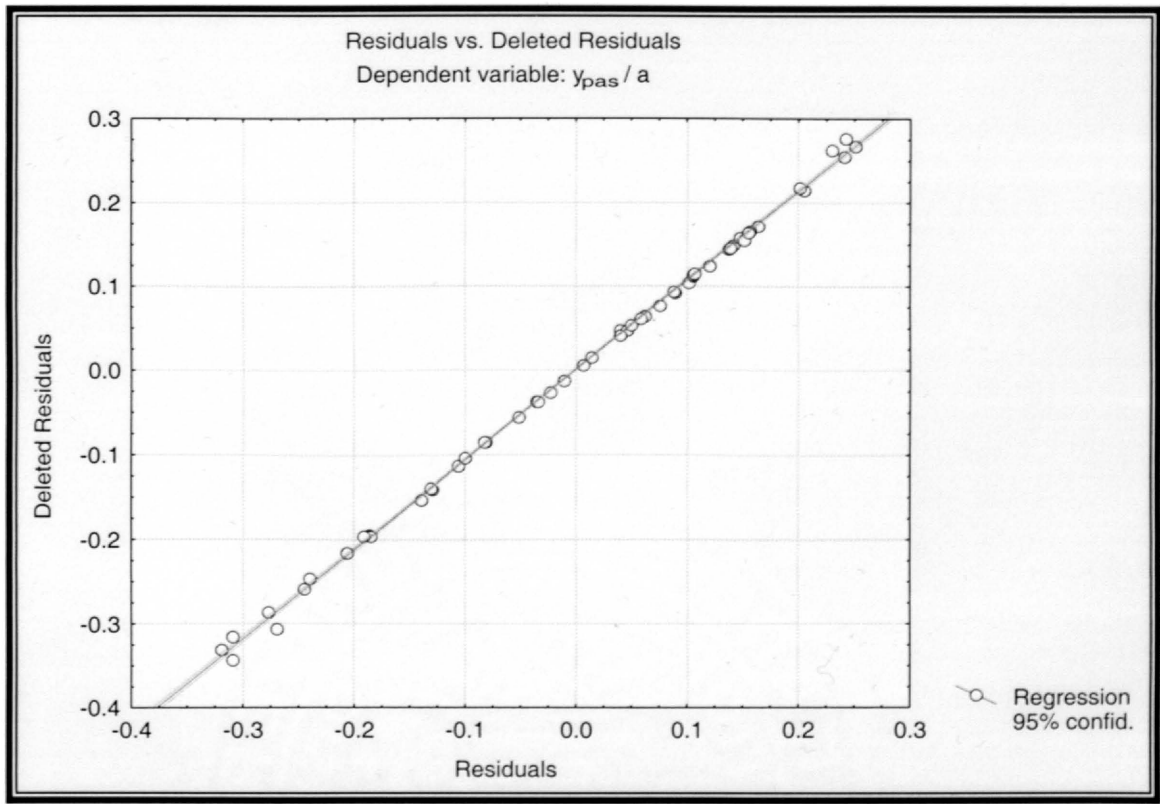
• Figure 5.14 – Observed versus predicted values for pressure flow abutment scour

Figure 5.15 displays a plot of predicted values versus the residual scores for the dependent variable y_{pas}/a . Data points plotted in Figure 5.15 form a homogeneous distribution of points around the horizontal centerline verifying that the relationship was linear.



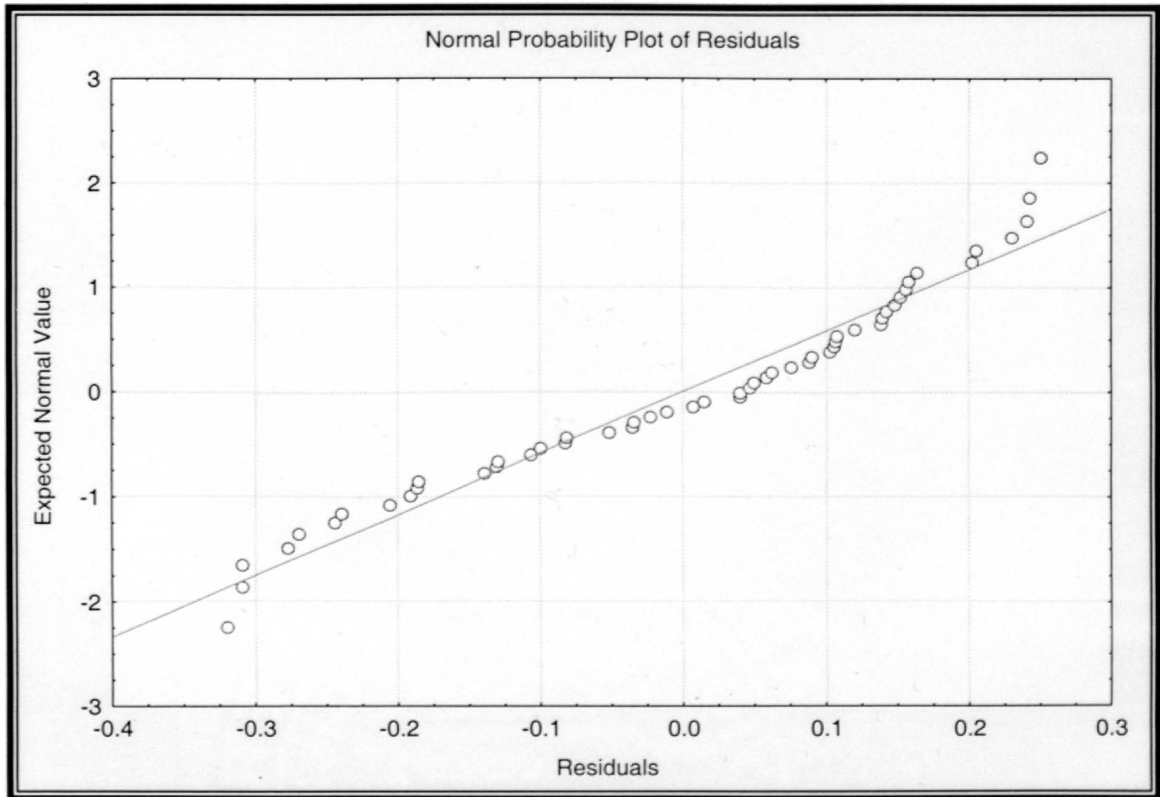
• Figure 5.15 – Predicted values versus residual scores for y_{pas}/a

Figure 5.16 displays a plot of residuals versus deleted residuals for the dependent variable y_{pas}/y . Figure 5.16 indicates that no additional outliers exist since all plotted points approximate the straight line, indicating that the data points used were valid for development of Equation 5.7.



• Figure 5.16 – Residuals versus deleted residuals for y_{pas}/a

Figure 5.17 presents the normal probability plot of residuals for the pressure flow abutment scour data. Figure 5.17 indicates that the residuals very closely approximated a normal distribution since the plotted points follow the straight line, assuring that the data could be analyzed using multivariate linear regression.

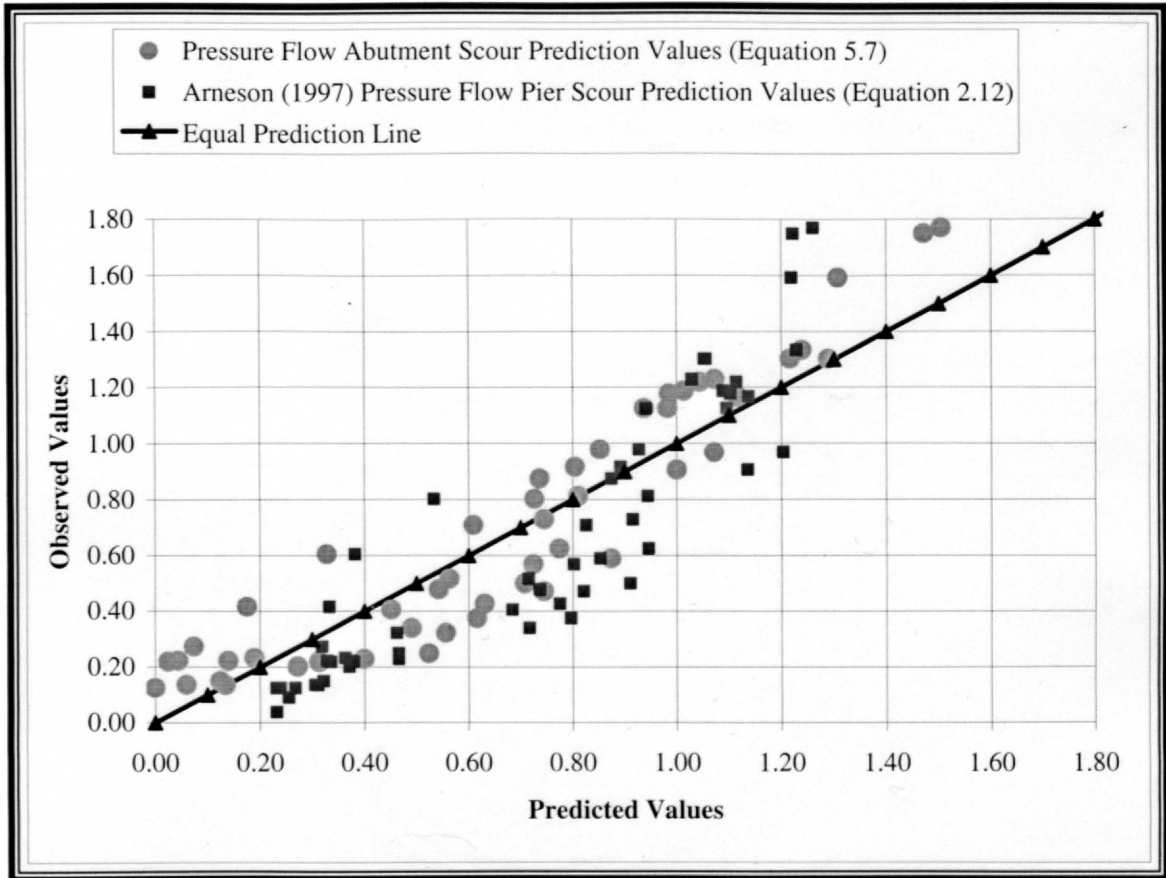


• **Figure 5.17 – Normal probability plot of residuals for pressure flow abutment scour data**

All data collected were developed into independent variables that were used in a multivariate linear regression analysis to develop Equation 5.7. Equation 5.7 had a coefficient of determination, R^2 , of 0.87, indicating that 87 percent of the variability in the data was explained by the relationship. Additionally, the data satisfied the overall significance test and the individual tests for checking multivariate linear regression validity.

Since Equation 5.7 for the prediction of pressure flow abutment scour was developed using techniques similar to Arneson (1997), a comparison with Equation 2.12 for the prediction of pressure flow pier scour from Arneson (1997) was warranted.

Figure 5.18 plots observed versus predicted values for the pressure flow abutment scour prediction equation (Equation 5.7) against the pressure flow pier scour equation (Equation 2.12) developed by Arneson (1997).



• **Figure 5.18 - Observed versus predicted values for the pressure flow abutment scour prediction equation (Equation 5.7) against the pressure flow pier scour equation (Equation 2.12) developed by Arneson (1997)**

Based on the observation in Figure 5.18 that Equation 5.7 and Equation 2.12, developed by Arneson (1997), both predict similar values, the data sets were combined. On average Equation 5.7 predicts less conservatively (a shallower scour hole) than Equation 2.12 by approximately 12.5 percent. Data from the combined set yielded 110

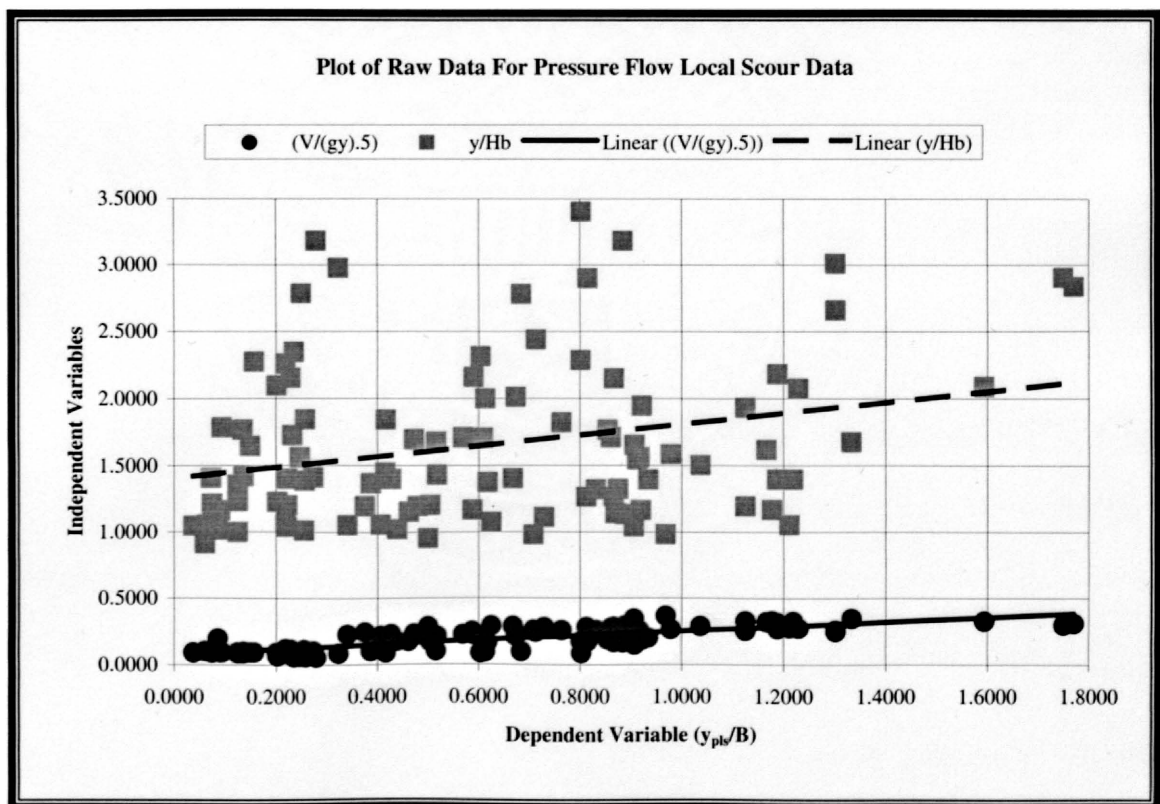
data points for each of the independent dimensionless variables previously defined for pressure flow deck scour. Table 5.9 presents 48 data points corresponding to the parameters calculated from Arneson's (1997) data set. The remaining 62 data points of the total 110 data points can be found in Table 5.1.

• **Table 5.9 – Summary of calculated pressure flow local scour data from Arneson (1997)**

Bridge Position	y_{pls}/B	$(V/(gy)^{0.5})$	y/H_b
1	0.22	0.11	1.04
2	0.26	0.11	1.01
3	0.39	0.10	1.37
4	0.52	0.10	1.68
5	0.61	0.10	2.00
6	0.68	0.10	2.78
1	0.09	0.20	1.01
2	0.92	0.20	1.16
3	0.93	0.20	1.40
4	0.85	0.19	1.77
5	0.80	0.18	2.29
6	0.88	0.17	3.18
2	0.59	0.25	1.17
3	0.92	0.19	1.94
4	0.67	0.21	2.01
2	0.87	0.23	1.14
3	0.83	0.26	1.32
4	0.91	0.24	1.54
5	0.76	0.26	1.82
1	0.06	0.10	0.91
2	0.07	0.10	1.05
3	0.07	0.09	1.21
4	0.07	0.10	1.41
5	0.09	0.09	1.78
6	0.16	0.10	2.27
2	0.50	0.17	1.20
3	0.42	0.19	1.45
4	0.61	0.20	1.71
2	0.89	0.29	1.13
3	0.67	0.29	1.41
4	0.86	0.28	1.71
5	0.71	0.25	2.44

Bridge Position	y_{pls}/B	$(V/(gy)^{0.5})$	y/H_b
1	0.20	0.07	1.22
2	0.26	0.06	1.38
3	0.25	0.06	1.56
4	0.26	0.06	1.84
5	0.24	0.06	2.35
6	0.28	0.06	3.18
1	0.44	0.18	1.02
2	0.46	0.17	1.15
3	0.62	0.17	1.38
4	0.91	0.15	1.65
5	0.87	0.17	2.15
6	0.81	0.18	2.90
2	1.21	0.28	1.06
3	0.87	0.29	1.26
4	1.04	0.29	1.51
5	1.19	0.27	2.18

Summary tables of the data used to form the dimensionless variables in Table 5.9 from Arneson (1997) are presented in the Appendix Tables A3 through A6. Based on the plot for each of the independent variables plotted against the dependent variable shown in Figure 5.19, it was determined that a multivariate linear relationship was valid for describing the data. Figure 5.19 shows that each of the independent variables can be considered a linear function of the dependent variable y_{pls}/B and since each of the slopes of the individual regression lines were approximately equal, a multivariate linear relationship was valid.



• Figure 5.19 – Plot of raw data for combined pressure flow local scour data

From the statistical analysis presented in Chapter 4 and the regression summary presented in Tables 5.10 and 5.11, the pressure flow local scour prediction equation follows as

$$\frac{y_{pls}}{B} = -0.616 + 3.964 \left(\frac{V_a}{\sqrt{gy}} \right) + 0.287 \left(\frac{y}{H_b} \right)$$

• Equation 5.8

Where,

- y_{pls} = depth of pressure flow local scour relative to m.b.e., L;
- y = depth of flow immediately upstream of the bridge deck, L;
- V_a = velocity of approach flow upstream of the bridge deck, L/T;
- g = acceleration due to gravity, L/T²;
- H_b = distance from bridge low chord to the initial mean bed elevation, L, and;
- B = local structure width, L.

During the statistical analysis, the 110 measurements were reduced to 97 due to the presence of 13 outliers. All 13 outliers were removed because each was beyond two standard deviations from the mean. Table 5.10 presents a multivariate linear regression summary associated Equation 5.8. Table 5.11 displays an ANOVA table corresponding to Equation 5.8.

• **Table 5.10 – Multivariate linear regression summary statistics corresponding to Equation 5.8**

Number of Measurements	97					
Dependent Variable	y_{pls}/B					
Independent Variables	Beta	Standard Error of Beta	B	Standard Error of B	t(50)	P-level
Intercept			-0.616	0.069	-8.929	0.000
$V/(gy)^{0.5}$	0.867	0.044	3.964	0.201	19.719	0.000
y/H_b	0.427	0.044	0.287	0.030	9.698	0.000
R =	0.907					
R ² =	0.822					
Adjusted R ² =	0.819					
F(2,94) =	217.485					
p <	0.000					
Standard error of estimate	0.174					

• **Table 5.11 – ANOVA table associated with Equation 5.8**

Source	Degrees of Freedom (df)	Sum of Squares (SS)	Mean Square (MS)	F-Statistic	P-Level
Regression	2	13.117	6.558	217.485	0.000
Error	94	2.835	0.030		
Total	96	15.951			

Listed in Table 5.10, the adjusted coefficient of determination, R^2 , from the analysis for Equation 5.8 was 0.82, indicating that 82 percent of the variability in the data was explained by the relationship. When compared to Equation 5.7, the coefficient of determination decreased from 0.87 to 0.82. When compared to Equation 2.12, the coefficient of determination increased from 0.71 to 0.82. Combining both data sets was

determined valid, because the coefficient of determination for the prediction of pressure flow abutment scour only slightly decreased and the coefficient of determination for the prediction of pressure flow pier scour increased significantly. Combining both data sets was physically valid because the pier and abutment geometry were similar for both data sets.

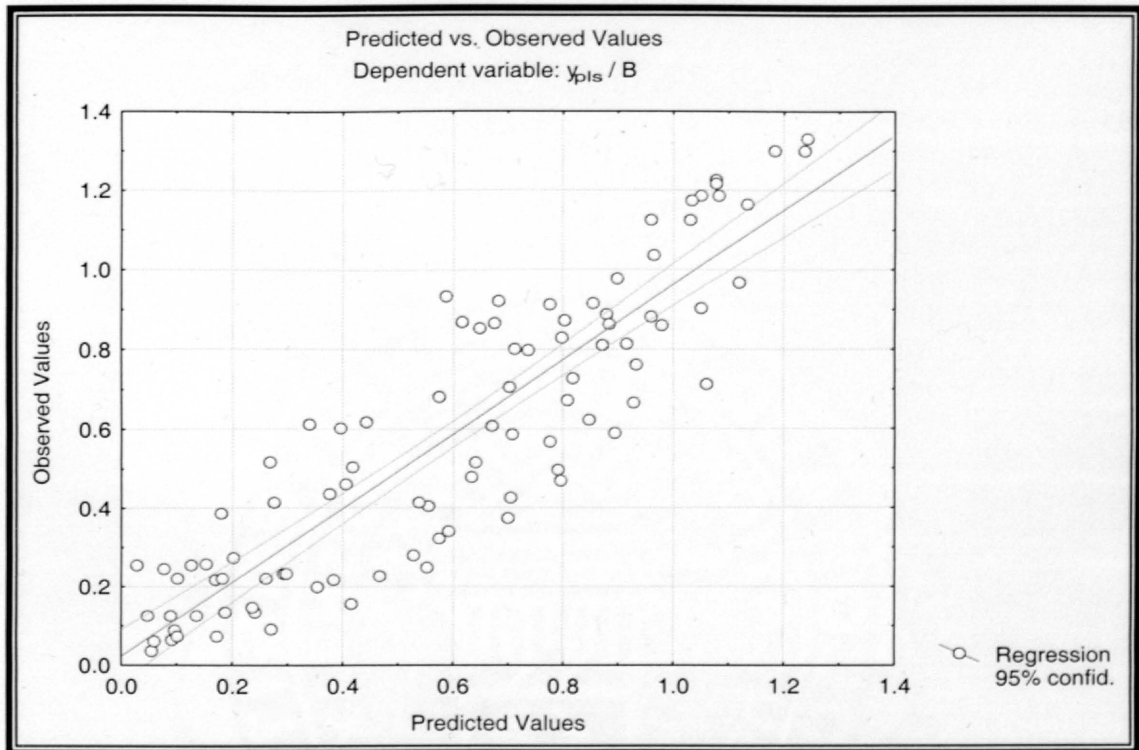
An overall significance test indicated that the critical F value for $k = 2$ and $n = 97$ was 3.09. Since the F-Statistic presented in Table 5.11 of 217.48 was greater than 3.09, the two independent variables explained a significant amount of the variation in the dependent variable y_{pls}/B . Additionally, the P-level of both independent variables and the overall P-level were all less than the selected value of 0.05, therefore the analysis was determined to be statistically significant.

Preliminary statistical significance was computed as two independent variables times 20 (Kleinbaum, 1988), yielding a number of 40 for the minimum number of data points for statistical analysis to be valid. For the pressure flow local scour data, there were 97 measurements used for the statistical analysis, therefore the analysis was considered valid.

Partial correlation, Beta, for each of the independent variables indicated that the independent variable, $V_a/(gy)^{0.5}$, was the most significant with a Beta value of 0.867 and the independent variable, y/H_b , was the least significant with a Beta value of 0.427. Both Beta values were considered statistically significant.

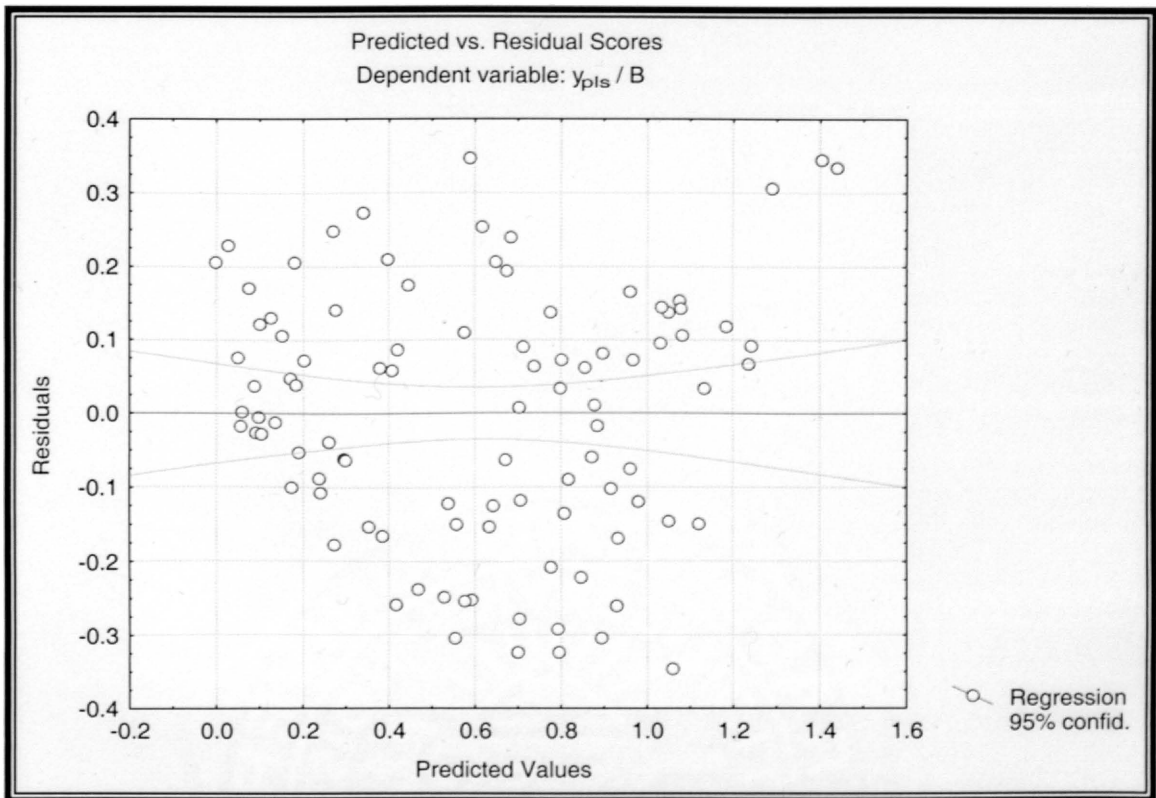
Figure 5.20 graphically displays observed values versus predicted values for the pressure flow local scour data. Figure 5.20 indicates that Equation 5.8 can be considered

a reliable prediction equation giving points both above and below the line of equal prediction.



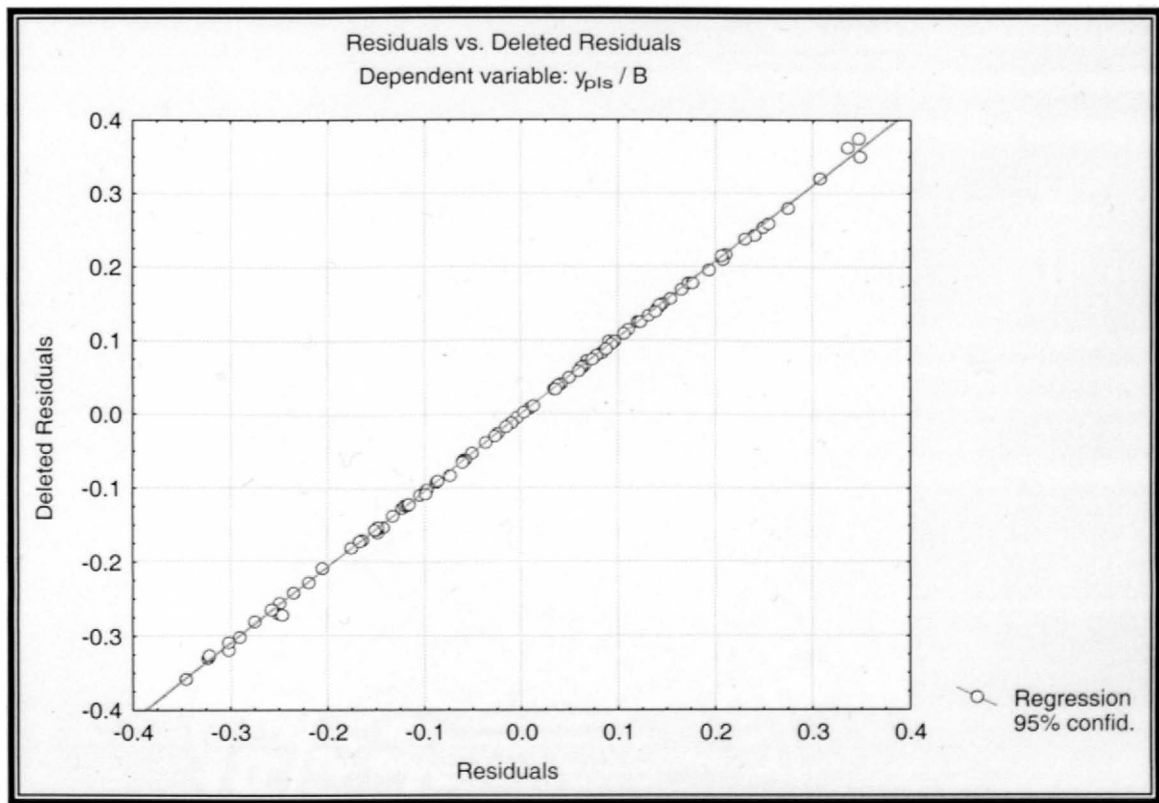
• **Figure 5.20 – Observed versus predicted values for pressure flow local scour**

Figure 5.21 displays a plot of predicted values versus the residual scores for the dependent variable y_{pls}/B . Data points plotted in Figure 5.21 form a homogeneous distribution of points around the horizontal centerline verifying that the relationship was linear.



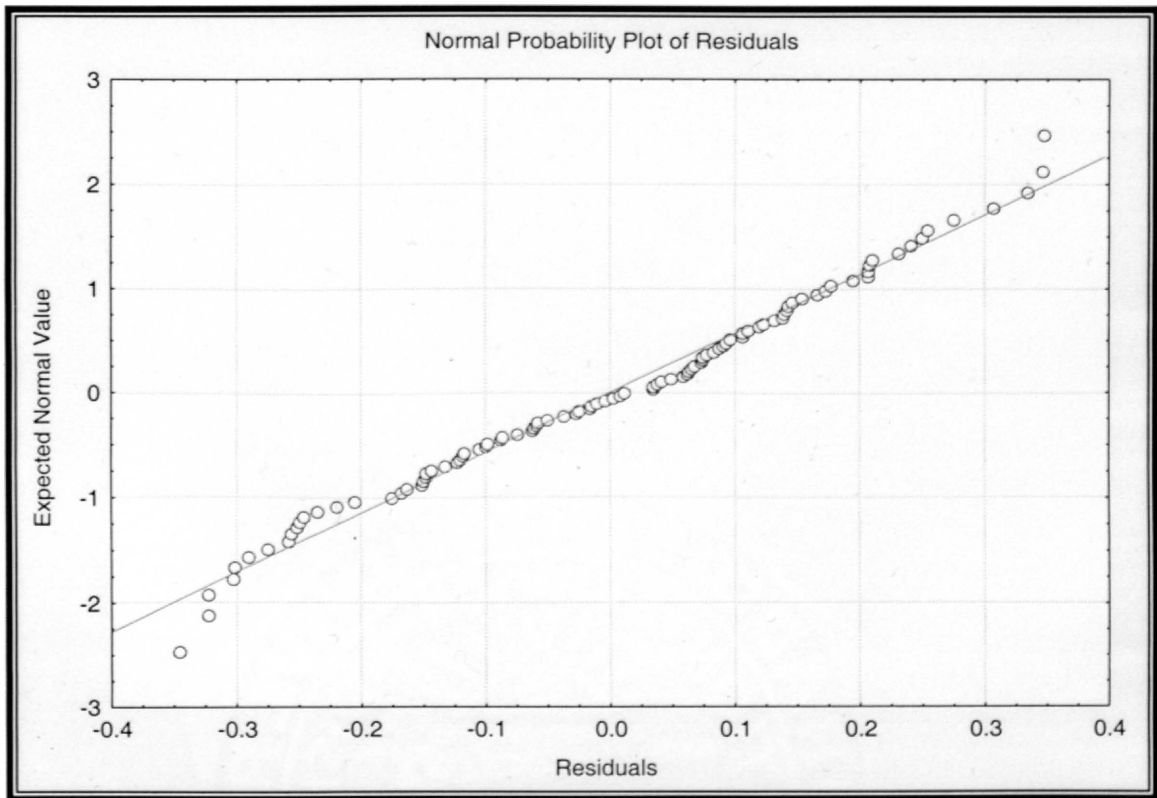
• **Figure 5.21 – Predicted values versus residual scores for y_{pls}/B**

Figure 5.22 displays a plot of residuals versus deleted residuals for the dependent variable y_{pls}/B . Figure 5.22 indicates that no additional outliers exist since all plotted points approximate the straight line, indicating that the data points used were valid for development of Equation 5.8.



• **Figure 5.22 – Residuals versus deleted residuals for y_{pls}/B**

Figure 5.23 presents the normal probability plot of residuals for the pressure flow abutment scour data. Figure 5.23 indicates that the residuals very closely approximated a normal distribution since the plotted points follow the straight line, assuring that the data could be analyzed using multivariate linear regression.



• **Figure 5.23 – Normal probability plot of residuals for pressure flow local scour data**

Equation 5.8 had a coefficient of determination, R^2 , of 0.82, indicating that 82 percent of the variability in the data was explained by the relationship. Combining both data sets was determined valid, because the coefficient of determination for the prediction of pressure flow abutment scour only slightly decreased and the coefficient of determination for the prediction of pressure flow pier scour increased significantly. Additionally, the data satisfied the overall significance test and the individual tests for checking multivariate linear regression validity. Combining both data sets was physically valid because the pier and abutment geometry were similar for both data sets.

5.4 LIMITATIONS

During the development of any predictive relationship performed in a controlled laboratory setting, the boundary conditions or limitations imposed during testing should be considered when attempting to apply the relationship outside of the laboratory. Each of the developed predictive relationships for this study should be applied under the boundary conditions or limitations in which each equation was developed.

For this study, a homogenous sand bed channel with an abutment supported bridge crossing was simulated in the laboratory at an approximate 8:1 scale. During the testing program, pressure flow effects on scour were examined under varying flow conditions with a sediment range from 1.5 mm to 3.3 mm sand. Approach flow conditions were all subcritical (Froude number less than 1.0) and the angle of attack of the approach flow was zero. The average velocity (V_b) under the bridge deck was not greater than 1.7 times the critical velocity (V_c).

Based on the above stated boundary conditions, it is recommended that the practicing hydraulic engineer review the constraints of the physical model as presented in Chapter 3 before applying Equation 5.2, 5.4, 5.7 or 5.8. Additionally, since the developed relationships are empirical, it is recommended that Equations 5.2, 5.4, 5.7, and 5.8 be validated with field data.

6 CONCLUSIONS AND RECOMMENDATIONS

6.1 INTRODUCTION

Based on research presented in this thesis, a better understanding of the processes at work during pressure flow conditions has been presented and a complete set of prediction equations for pressure flow conditions at bridges now exists for the hydraulic engineering community. A series of 62 experiments was conducted to examine the effects of a pressure flow condition on scour at bridges. Subsequent sections present conclusions made from the analysis of the test results and provide recommendations for further research.

6.2 CONCLUSIONS

- A complete set of pressure flow bridge scour prediction equations were developed including pressure flow deck scour, pressure flow abutment scour, pressure flow pier scour, and pressure flow local scour.

- Equation 5.2, for prediction of pressure flow deck scour, developed from 59 data points collected for this study, was presented. Equation 5.2 had a coefficient of determination, R^2 , of 0.96.
- Equation 5.7, for prediction of pressure flow abutment scour, developed from 53 data points collected for this study, was presented. Equation 5.7 had a coefficient of determination, R^2 , of 0.87.
- Equation 5.8, for prediction of pressure flow pier and local scour, developed from 97 data points from the combination of Arneson's (1997) data set and the data collected for this study was presented. Equation 5.8 had a coefficient of determination, R^2 , of 0.82.
- For pressure flow deck scour, the most significant dimensionless parameter was $(y_{pds} + H_b)/y$.
- For pressure flow deck scour, the parameter V_b/V_c , was found to be extremely important for accounting for the velocity and providing a link to the sediment size of the bed material.
- For pressure flow local scour, including abutment and pier scour, the most significant dimensionless parameter was the Froude number, $Fr = V_a/(gy)^{0.5}$.
- Equation 5.2 predicts more conservatively (a deeper scour hole) than Equation 2.11 by approximately 13.1 percent.
- Equation 5.4 is recommended for the prediction of pressure flow deck scour with the following limitations:
 - V_b/V_c ratios must be within the range for the development of Equation 5.4 (0.3 – 1.7).

- Calculation of V_b should be approximated with an appropriate closed conduit estimate of velocity for turbulent flow using initial bridge opening conditions.
- Equation 5.4 improves upon Arneson's (1997) Equation 2.11 with a larger data set (183 data points vs. 116 data points), but needs further validation from field data prior to accepted use.
- Equation 5.7 is recommended for the prediction of pressure flow abutment scour when a bridge is solely supported by abutments.
- Equation 5.7 (pressure flow abutment scour) predicts less conservatively (a shallower scour hole) than Equation 2.12 (pressure flow pier scour) by approximately 12.5 percent.
- Equation 5.7 is the only known pressure flow abutment scour prediction equation and it explains 87 percent of the data variability.
- Equation 5.8 is recommended for the prediction of pressure flow pier scour when a bridge is solely supported by piers or when a combination of piers and abutments (with similar geometry) support a bridge.
- Equation 5.8 improves upon Arneson's (1997) Equation 2.12 with a larger data set (97 data points vs. 45 data points) but needs further validation from field data prior to accepted use.
- All of the developed equations (Equations 5.2, 5.4, 5.7, and 5.8) are limited by the following conditions:
 - Each equation should only be applied for a homogeneous bed material.
 - Each equation should only be applied in sand bed channels.

- Angle of attack of approach flow must be equal to zero unless a correction factor from HEC-18 is applied.
- Each equation must be applied for subcritical flow conditions (Froude numbers less than 1.0).

6.3 RECOMMENDATIONS FOR FURTHER RESEARCH

- Research presented herein was based on data collected in a laboratory flume with an approximate 8:1 scale bridge deck model. Testing under a pressure flow condition in which a larger scale bridge deck model was used would be helpful for verifying the predictive relationships.
- Allowing for more variation in the constriction percentage under the bridge would be useful for obtaining a link between pressure flow deck scour and contraction scour.
- Testing of a non-homogeneous bed material and a cohesive bed material would be much better suited for the transfer of laboratory results to prototype conditions.
- Angle of attack of the approach flow should be varied to verify the correction coefficients often used in HEC-18.
- Provided that the velocity under the bridge deck during pressure flow conditions contributes significantly to the magnitude of pressure flow deck scour, a relationship between the average velocity under the bridge deck and the average velocity upstream of the bridge deck would be very useful. During conditions in which a bridge deck would be submerged, collecting a velocity under the bridge

deck would be impossible, but collecting a velocity upstream of the bridge deck might be possible. For this reason, the above stated relationship between the average velocity under the bridge deck and the average velocity upstream of the bridge deck, would be critical for the true application of the pressure flow deck scour prediction equation developed within this thesis

- Examining each of the three-dimensional velocity components under the bridge deck would prove useful in further verifying the large scale eddy observed by Abed in 1991, causing the increase in hydraulic forces acting on the bed material. Additionally, examining the velocity components could provide insight for developing a pressure flow scour relationship based upon the shear stress acting upon the bed material.
- As Equations 5.2, 5.4, 5.7 and 5.8 for the prediction of pressure flow scour at bridges were developed under laboratory conditions, field data should be collected in order to expand the data set and verify the predictive equations.
- A closer examination of the differences between clear water pressure flow scour and live-bed pressure flow scour is needed to determine which type of equation (clear water or live-bed) should be applied to prototype bridges.

7 REFERENCES

- Abed, L.M., 1991. "Local Scour Around Bridge Piers in Pressure Flow," Ph.D. Dissertation, Department of Civil Engineering, Colorado State University, Fort Collins, CO.
- Abdeldayem, A.W., 1995. "Abutment Scour for Non-Uniform Mixtures," Ph.D. Dissertation, Civil Engineering Department, Colorado State University, Fort Collins, CO.10
- Abdou, M.I., 1993. "Effect of Sediment Gradation and Coarse Material Fraction on Clear-Water Scour Around Bridge Piers," Ph.D. Dissertation, Colorado State University, Fort Collins, CO.
- Ahmad, M., 1962. Discussion of "Scour at Bridge Crossings," by E.M. Laursen, Transactions of the ASCE, Vol. 127, pp. 198-206.
- Arneson, L.A., 1997. "The Effects of Pressure Flow on Local Scour in Bridge Openings," Ph.D. Dissertation, Department of Civil Engineering, Colorado State University, Fort Collins, CO.
- Arneson, L.A., and Abt, S.R., 1999. "Vertical Contraction Scour at Bridges Under Pressure Flow Conditions," Hydraulic Engineering Compendium, ASCE.
- ASCE, 1999. Edited by Richardson, E.V., and Lagasse, P.F. "Stream Stability and Scour at Highway Bridges," Hydraulic Engineering Compendium, ASCE Press.
- Avery, K.R., and Hixson, M.A., 1993. "Case Studies of Bridge Scour in Western New York," Hydraulic Engineering 1993, ASCE, pp 592-597.
- Baker, C.J., 1980. "Theoretical Approach to Prediction of Local Scour Around Bridge Piers," Journal of Hydraulic Research, International Association for Hydraulic Research, Volume 18, No. HY1.
- Baker, C.J., 1981. "New Design Equations for Scour Around Bridge Piers," Journal of the Hydraulics Division, ASCE, Vol. 107, pp. 507-511.
- Blaisdell, F.W., Anderson, C.L., and Hebaus, G.G., 1981. "Ultimate Dimensions of Local Scour," Journal of the Hydraulics Division, ASCE, Vol. 107, pp. 327-337.
- Bradley, J.N., 1978. "Hydraulics of Bridge Waterways," Hydraulic Design Series No. 1, U.S. Department of Transportation, Federal Highway Administration, Washington, D.C., Second Edition Revised 1978.

- Breusers, H.N.C., 1965. "Scour around drilling platforms," Bulletin, Hydraulic Research 1964 and 1965, I.A.H.R., Vol. 19.
- Breusers, H.N.C., Nicollet, G. and Shen, H.W., 1977. "Local Scour Around Cylindrical Piers," Journal of Hydraulic Research, pp. 211-252.
- Butch, G.K., and Lumia, R., 1994. "Effects of Flow Duration on Local Scour at Bridge Piers in New York," Hydraulic Engineering 1994, ASCE, pp 46-50.
- Carstens, M.R., 1966. "Similarity Laws for Localized Scour," Journal of the Hydraulics Division, ASCE, Vol. 9.2, No. HY3, pp. 13-36
- Chang, F.W., and Yevdjovich, V., 1962. "Analytical Study of Local Scour," Report of Civil Engineering Section, Colorado State University, Fort Collins, CO.
- Chang, F.F.M., Jones, J.S., and Davis, S., 1995. "Pressure Flow Scour for Clear Water Conditions," Unpublished handout for FHWA Western Regional Hydraulic Conference, Seattle, WA.
- Chow, V.T., 1959. Open Channel Hydraulics, McGraw-Hill, New York.
- Devore, D.L., 1995. Probability and Statistics for Engineering and the Sciences, Fourth Edition, Duxbury Press.
- Ettema, R., Mostafa, E.A., Melville, B.W., and Yassin, A.A., 1998. "On Local Scour at Skewed Piers," Journal of the Hydraulics Division, ASCE, Vol. 124, pp. 756-760.
- Froehlich, D.C., 1989. "Local Scour at Bridge Abutments," Hydraulic Engineering 1989, ASCE.
- Gao, D.G., Posada, G.L., and Nordin, C.F., 1992. "Pier Scour Equations Used in The Peoples Republic of China," Colorado State University, Department of Civil Engineering, Fort Collins, CO.
- Gessler, J., 1971. "Beginning and Ceasing of Sediment Motion," River Mechanics. (Edited by H.W. Shen), Vol. 1 Ch. 7, Fort Collins, CO.
- Graybill, F.A., and Iyer, H.K., 1994. Regression Analysis: Concepts and Applications, Duxbury Press.
- Hixson, M.A., and Avery, K.R., 1993. "Comparison of Theoretical and Historical Scour," Hydraulic Engineering 1993, ASCE, pp. 1067-1072.
- Hopkins, G.R., Vance, R.W., and Kasraie, B., 1980. "Scour Around Bridge Piers," U.S. Federal Highway Administration, Research Report, No. FHWA-RD-79-103.
- Hjorth, P., 1975. Studies on the Nature of Local Scour, Department of Water Resources Engineering, University of Lund.
- Ishihara, T., 1938 & 1942. "An Experimental Study of Scour Around Bridge Piers," Translated from Journal of the Japan Society of Civil Engineers, Vol. 24, Vol 28.
- Jain, S.C. and Fischer, E.F., 1980. "Scour Around Bridge Piers at High Flow Velocities," Journal of the Hydraulics Division, ASCE, Vol. 106, pp. 1827-1842.
- Jain, S.C., 1981. "Maximum Clear Water Scour Around Circular Piers," Journal of the Hydraulics Division, ASCE, Vol. 107, pp. 611-626.

- Johnson, P.A., 1995. "Comparison of Pier Scour Equations Using Field Data," Journal of the Hydraulics Division, ASCE, Vol. 121, pp. 626-629.
- Jones, J.S., Bertoldi, D.A., and Umbrell, E.R., 1993. "Preliminary Studies of Pressure Flow Scour," Hydraulic Engineering 1993, ASCE.
- Jones, J.S., Bertoldi, D.A., and Umbrell, E.R., 1995-1996. "Interim Procedures for Pressure Flow Scour," ASCE North American Water and Environment Congress Proceedings, Anaheim, CA.
- Karaki, S.S., and Haynie, R.M., 1963. "Mechanics of Local Scour Discussion and Bibliography," Part I and Part II, Civil Engineering Department, Colorado State University, Fort Collins, CO.
- Kleinbaum, D.G, Kupper, L.L, and Muller, K.E., 1988. Applied Regression Analysis and Other Multivariable Methods, PWS-KENT Publishing Company.
- Kwan, T.F., 1988. "A Study of Abutment Scour," Report No. 451, School of Engineering, The University of Auckland, Auckland, New Zealand.
- Lagasse, P.F., Schall, J.D., Johnson, F., Richardson, E.V., and Chang, F., 1995. "Stream Stability at Highway Structures," Hydraulic Engineering Circular 20, FHWA HI-96-032, FHWA, Washington, D.C.
- Lagasse, P.F., Byars, M.S., Zevenbergen, L.W., and Clopper, P.E., 1997. "Bridge Scour and Stream Instability Countermeasures," Hydraulic Engineering Circular 23, FHWA HI-97-030, FHWA, Washington, D.C.
- Laursen, E.M., 1958. "Scour at Bridge Crossings," Bulletin No. 8, Iowa Highway Research Board, Ames, Iowa.
- Laursen, E.M., 1960. "Scour at Bridge Crossing," Journal of the Hydraulics Division, ASCE, Vol. 86, No. HY2, pp. 39-54.
- Laursen, E.M., 1962. "Scour at Bridge Crossings", Transactions of the ASCE, Vol 127, pp. 166-209.
- Laursen, E.M., 1963. "An Analysis of Relief Bridge Scour," Journal of the Hydraulics Division, ASCE, Vol. 86, No. HY 2.
- Liu, H.K., Bradley, J.N., and Plate, E.J., 1957. "Backwater Effects of Piers and Abutments," Civil Engineering Department, Colorado State University, Fort Collins, CO.
- Melville, B.W., and Raudkivi, A.J., 1977. "Flow Characteristics in Local Scour at Bridge Piers," Journal of Hydraulic Research, pp. 373-380.
- Melville, B.W., 1984. "Live Bed Scour at Bridge Piers," Journal of the Hydraulic Division, ASCE, Vol. 110, pp. 1234-1247.
- Melville, B.W., and Sutherland, A.J., 1988. "Design Method for Local Scour at Bridge Piers," Journal of the Hydraulics Division, ASCE, Vol. 114, pp1210-1226.
- Melville, B.W., and Dongol, D.M., 1992. "Bridge Pier Scour with Debris Accumulation," Journal of the Hydraulics Division, ASCE, Vol. 118, No. 9.

- Melville, B.W., 1992. "Local Scour at Bridge Abutments," Journal of the Hydraulics Division, ASCE, Vol. 118, No. 4.
- Melville, B.W., and Coleman, S.E., 2000. Bridge Scour, Water Resources Publications.
- Mostafa, E.A., Yassin, A.A., Ettema, R., and Melville, B.W., 1993. "Local Scour at Skewed Bridge Piers," Hydraulic Engineering 1993, ASCE, pp. 1037-1042.
- Mueller, D.S., 1996. "Local Scour at Bridge Piers in Non-Uniform Sediment Under Dynamic Conditions," Ph.D. Dissertation, Department of Civil Engineering, Colorado State University, Fort Collins, CO.
- Munson, B.R., Young, D.F., and Okiishi, T.H., 1998. Fundamentals of Fluid Mechanics – Third Edition, Von Hoffmann Press.
- Neill, C.R., 1973. "Guide to Bridge Hydraulics," (Editor) Roads and Transportation Association of Canada, University of Toronto Press, Toronto, Canada.
- Noshi, H.M., 1997. "Abutment Scour in Uniform and Stratified Bed," Ph.D. Dissertation, Civil Engineering Department, Colorado State University, Fort Collins, CO.
- Raudkivi, A.J., and Ettema, R., 1977. "Effect of Sediment Gradation on Clear Water Scour," Journal of the Hydraulics Division, ASCE, Vol. 103, pp. 1209-1213.
- Raudkivi, A.J., and Ettema, R., 1983. "Clear Water Scour at Cylindrical Piers," Journal of the Hydraulic Division, ASCE, Vol. 111, pp. 713-731.
- Raddkivi, A.J., 1986. "Functional Trends of Scour at Bridge Piers," Journal of the Hydraulics Division, ASCE, Vol. 112, pp. 1-13.
- Raudkivi, A.J., 1990. Loose Boundary Hydraulics, Pergamon Press.
- Richardson, J.R., and Richardson, E.V., 1994. "Practical Method for Scour Prediction at Bridge Piers," Hydraulic Engineering 1994, ASCE.
- Richardson, E.V., and Davis, S.R., 1995. "Evaluating Scour at Bridges – Third Edition," Hydraulic Engineering Circular No. 18, U.S. Federal Highway Administration, Publication No. FHWA-IP-90-017
- Richardson, E.V., 1999. "History of Bridge Scour Research and Evaluation in the United States," Hydraulic Engineering Compendium, ASCE.
- Schneider, V.R., 1968. "Mechanics of Local Scour," Ph.D. Dissertation, Civil Engineering Department, Colorado State University, Fort Collins, CO.
- Shen, H.W., Schneider, V.R., and Karaki, S.S., 1966. "Mechanics of Local Scour," U.S. Department of Commerce, National Bureau of Standards, Institute for Applied Technology.
- Shen, H.W., Schneider, V.R., and Karaki, S.S., 1969. "Local Scour Around Bridge Piers," Journal of the Hydraulics Division, ASCE, Vol. 89, pp. 1919-1940.
- Shields, A., 1936. "Application of Similarity Principles and Turbulence Research to Bed-Load Movement," California Institute of Technology, Report No. 167, Pasadena, CA.
- Statistica for Windows, 1997. Statsoft, Inc.

Stevens, M.A., Gasser, M.M., and Saad, M.B.A.M., 1991. "Wake Vortex Scour at Bridge Piers," Journal of the Hydraulics Division, ASCE, Vol. 117, pp. 891-904.

Sturm, T.W., and Janjua, N.S., 1993. "Bridge Abutment Scour in a Floodplain," Hydraulic Engineering 1993.

Thomas, A.R., 1962. Discussion of "Local Scour at Bridge Crossings," by Laursen, E.M. Transactions of the ASCE, Vol. 127.

Wiggert, D.C., 1972. "Transient Flow in Free-Surface, Pressurized Systems," Journal of the Hydraulics Division, ASCE, Vol. 98, pp. 11-27.

APPENDIX – SUMMARY DATA TABLES

Table A1 - Summary Data Table for 1.5 mm Sediment Size - Test Numbers 1 to 36

Test Number	Target Q (ft ³ /s)	Measured Q (ft ³ /s)	q _{br} (ft ³ /s)	D ₅₀ (mm)	Bridge Position	Vertical Constriction (%)	Horizontal Constriction (%)	Abutment Protrusion Length, a (ft)	y _{pd} (ft)	y _{pa} (ft)	y (ft)	H _b (ft)	V _a (ft/s)	V _b (ft/s)	V _c (ft/s)	Fr
1	8.00	8.02	1.14	1.50	1	0.00	12.00	0.96	0.17	0.56	1.14	1.37	0.80	1.02	1.95	0.13
2	8.00	8.02	1.14	1.50	2	12.06	12.00	0.96	0.24	0.60	1.17	1.20	0.79	1.00	1.96	0.13
3	8.00	8.02	1.14	1.50	3	24.11	12.00	0.96	0.12	0.26	1.45	1.03	0.71	1.45	2.03	0.10
4	8.00	8.02	1.14	1.50	4	36.17	12.00	0.96	0.12	0.40	1.58	0.86	0.65	1.82	2.06	0.09
5	8.00	8.02	1.14	1.50	5	48.23	12.00	0.96	0.18	0.58	1.60	0.69	0.63	1.94	2.06	0.09
6	8.00	8.02	1.14	1.50	6	60.28	12.00	0.96	0.35	0.77	1.77	0.52	0.67	2.08	2.10	0.09
7	18.00	18.00	2.56	1.50	1	0.00	12.00	0.96	0.31	0.68	1.34	1.37	1.72	1.98	2.00	0.26
8	18.00	18.00	2.56	1.50	2	12.06	12.00	0.96	0.39	0.70	1.33	1.20	1.84	2.44	2.00	0.28
9	18.00	18.00	2.56	1.50	3	24.11	12.00	0.96	0.53	0.84	1.36	1.03	1.73	2.48	2.01	0.26
10	18.00	18.00	2.56	1.50	4	36.17	12.00	0.96	0.75	0.94	1.36	0.86	1.77	2.64	2.01	0.27
11	18.00	18.00	2.56	1.50	5	48.23	12.00	0.96	0.96	1.18	1.43	0.69	1.88	2.70	2.02	0.28
12	18.00	18.00	2.56	1.50	6	60.28	12.00	0.96	1.15	1.25	1.57	0.52	1.77	2.41	2.06	0.25
13	24.00	23.16	3.29	1.50	1	0.00	12.00	0.96	0.58	0.87	1.42	1.37	2.34	2.64	2.02	0.35
14	24.00	23.16	3.29	1.50	2	12.06	12.00	0.96	0.80	1.08	1.43	1.20	2.23	2.66	2.03	0.33
15	24.00	23.16	3.29	1.50	3	24.11	12.00	0.96	0.93	1.14	1.44	1.03	2.17	2.78	2.03	0.32
16	24.00	23.16	3.29	1.50	4	36.17	12.00	0.96	1.06	1.12	1.39	0.86	2.17	2.96	2.02	0.32
17	24.00	23.16	3.29	1.50	5	48.23	12.00	0.96	1.26	1.70	1.41	0.69	2.06	2.93	2.02	0.31
18	24.00	23.16	3.29	1.50	6	60.28	12.00	0.96	1.19	1.68	1.51	0.52	2.09	2.74	2.04	0.30
19	8.00	7.80	1.52	1.50	1	0.00	36.00	2.88	0.16	0.63	1.45	1.37	0.83	1.41	2.03	0.12
20	8.00	7.80	1.52	1.50	2	12.06	36.00	2.88	0.07	0.64	1.44	1.20	0.78	1.92	2.03	0.11
21	8.00	7.80	1.52	1.50	3	24.11	36.00	2.88	0.14	0.64	1.44	1.03	0.82	2.06	2.03	0.12
22	8.00	7.80	1.52	1.50	4	36.17	36.00	2.88	0.50	0.67	1.48	0.86	0.72	2.23	2.04	0.10
23	8.00	7.80	1.52	1.50	5	48.23	36.00	2.88	0.62	0.66	1.49	0.69	0.81	2.33	2.04	0.12
24	8.00	7.80	1.52	1.50	6	60.28	36.00	2.88	0.73	0.75	1.51	0.52	0.85	2.40	2.04	0.12
25	18.00	18.00	3.52	1.50	1	0.00	36.00	2.88	0.61	0.98	1.44	1.37	1.55	2.17	2.03	0.23
26	18.00	18.00	3.52	1.50	2	12.06	36.00	2.88	0.93	1.08	1.43	1.20	1.66	2.60	2.03	0.25
27	18.00	18.00	3.52	1.50	3	24.11	36.00	2.88	0.99	1.23	1.44	1.03	1.58	2.57	2.03	0.23
28	18.00	18.00	3.52	1.50	4	36.17	36.00	2.88	1.24	1.36	1.46	0.86	1.60	2.82	2.03	0.23
29	18.00	18.00	3.52	1.50	5	48.23	36.00	2.88	1.26	1.42	1.48	0.69	1.64	2.83	2.03	0.24
30	18.00	18.00	3.52	1.50	6	60.28	36.00	2.88	1.31	1.61	1.55	0.52	1.50	2.85	2.05	0.21
31	24.00	24.06	4.70	1.50	1	0.00	36.00	2.88	1.31	1.63	1.22	1.37	2.26	2.32	1.97	0.36
32	24.00	n/a	n/a	1.50	2	12.06	36.00	2.88	n/a	n/a	n/a	n/a	n/a	n/a	n/a	n/a
33	24.00	n/a	n/a	1.50	3	24.11	36.00	2.88	n/a	n/a	n/a	n/a	n/a	n/a	n/a	n/a
34	24.00	n/a	n/a	1.50	4	36.17	36.00	2.88	n/a	n/a	n/a	n/a	n/a	n/a	n/a	n/a
35	24.00	n/a	n/a	1.50	5	48.23	36.00	2.88	n/a	n/a	n/a	n/a	n/a	n/a	n/a	n/a
36	24.00	n/a	n/a	1.50	6	60.28	36.00	2.88	n/a	n/a	n/a	n/a	n/a	n/a	n/a	n/a

12X

Table A2 - Summary Data Table for 3.3 mm Sediment Size - Test Numbers 37 to 72

Test Number	Target Q (ft ³ /s)	Measured Q (ft ³ /s)	q _{pr} (ft ³ /s)	D ₅₀ (mm)	Bridge Position	Vertical Constriction (%)	Horizontal Constriction (%)	Abutment Protrusion Length, a (ft)	y _{pda} (ft)	y _{pas} (ft)	y (ft)	H _b (ft)	V _a (ft/s)	V _b (ft/s)	V _c (ft/s)	Fr
37	8.00	8.20	1.16	3.30	1	0.00	12.00	0.96	0.06	0.12	1.37	1.37	0.63	0.88	2.61	0.10
38	8.00	8.20	1.16	3.30	2	12.06	12.00	0.96	0.07	0.12	1.47	1.20	0.61	1.29	2.65	0.09
39	8.00	8.20	1.16	3.30	3	24.11	12.00	0.96	0.06	0.13	1.46	1.03	0.69	1.37	2.64	0.10
40	8.00	8.20	1.16	3.30	4	36.17	12.00	0.96	0.05	0.13	1.52	0.86	0.62	1.73	2.66	0.09
41	8.00	8.20	1.16	3.30	5	48.23	12.00	0.96	0.09	0.21	1.56	0.69	0.63	1.97	2.67	0.09
42	8.00	8.20	1.16	3.30	6	60.28	12.00	0.96	0.33	0.31	1.55	0.52	0.60	2.19	2.67	0.09
43	18.00	18.00	2.56	3.30	1	0.00	12.00	0.96	0.18	0.48	1.31	1.37	1.85	2.27	2.59	0.29
44	18.00	18.00	2.56	3.30	2	12.06	12.00	0.96	0.33	0.60	1.29	1.20	1.87	2.58	2.59	0.29
45	18.00	18.00	2.56	3.30	3	24.11	12.00	0.96	0.49	0.78	1.30	1.03	1.84	2.64	2.59	0.28
46	18.00	18.00	2.56	3.30	4	36.17	12.00	0.96	0.66	0.88	1.34	0.86	1.70	2.84	2.61	0.26
47	18.00	18.00	2.56	3.30	5	48.23	12.00	0.96	0.75	1.08	1.33	0.69	1.69	2.88	2.60	0.26
48	18.00	18.00	2.56	3.30	6	60.28	12.00	0.96	0.99	1.25	1.38	0.52	1.74	2.90	2.62	0.26
49	24.00	23.99	3.41	3.30	1	0.00	12.00	0.96	0.47	0.93	1.35	1.37	2.41	2.60	2.61	0.37
50	24.00	23.99	3.41	3.30	2	12.06	12.00	0.96	0.71	1.13	1.40	1.20	2.23	3.04	2.62	0.33
51	24.00	23.99	3.41	3.30	3	24.11	12.00	0.96	0.92	1.17	1.44	1.03	2.22	3.07	2.64	0.33
52	24.00	23.99	3.41	3.30	4	36.17	12.00	0.96	1.12	1.28	1.44	0.86	2.37	2.88	2.64	0.35
53	24.00	23.99	3.41	3.30	5	48.23	12.00	0.96	1.22	1.53	1.44	0.69	2.24	3.12	2.64	0.33
54	24.00	23.99	3.41	3.30	6	60.28	12.00	0.96	1.49	1.70	1.47	0.52	2.15	2.71	2.65	0.31
55	8.00	7.84	1.53	3.30	1	0.00	36.00	2.88	0.00	0.11	1.43	1.37	0.63	1.13	2.63	0.09
56	8.00	7.84	1.53	3.30	2	12.06	36.00	2.88	0.00	0.26	1.39	1.20	0.64	1.69	2.62	0.10
57	8.00	7.84	1.53	3.30	3	24.11	36.00	2.88	0.00	0.36	1.40	1.03	0.61	1.84	2.62	0.09
58	8.00	7.84	1.53	3.30	4	36.17	36.00	2.88	0.18	0.43	1.42	0.86	0.65	2.23	2.63	0.10
59	8.00	7.84	1.53	3.30	5	48.23	36.00	2.88	0.32	0.58	1.44	0.69	0.63	2.30	2.64	0.09
60	8.00	7.84	1.53	3.30	6	60.28	36.00	2.88	0.46	0.72	1.45	0.52	0.64	2.29	2.64	0.09
61	18.00	18.00	3.52	3.30	1	0.00	36.00	2.88	0.58	1.17	1.45	1.37	1.49	2.19	2.64	0.22
62	18.00	18.00	3.52	3.30	2	12.06	36.00	2.88	0.91	1.38	1.44	1.20	1.55	2.48	2.63	0.23
63	18.00	18.00	3.52	3.30	3	24.11	36.00	2.88	1.01	1.49	1.47	1.03	1.47	2.43	2.65	0.21
64	18.00	18.00	3.52	3.30	4	36.17	36.00	2.88	1.19	1.64	1.47	0.86	1.56	2.71	2.65	0.23
65	18.00	18.00	3.52	3.30	5	48.23	36.00	2.88	1.24	1.70	1.49	0.69	1.55	2.63	2.65	0.22
66	18.00	n/a	n/a	3.30	6	60.28	36.00	2.88	n/a	n/a	n/a	n/a	n/a	n/a	n/a	n/a
67	24.00	24.27	4.74	3.30	1	0.00	36.00	2.88	1.08	1.59	1.39	1.37	2.16	2.35	2.62	0.32
68	24.00	24.27	4.74	3.30	2	12.06	36.00	2.88	1.43	1.70	1.40	1.20	2.28	2.63	2.62	0.34
69	24.00	n/a	n/a	3.30	3	24.11	36.00	2.88	n/a	n/a	n/a	n/a	n/a	n/a	n/a	n/a
70	24.00	n/a	n/a	3.30	4	36.17	36.00	2.88	n/a	n/a	n/a	n/a	n/a	n/a	n/a	n/a
71	24.00	n/a	n/a	3.30	5	48.23	36.00	2.88	n/a	n/a	n/a	n/a	n/a	n/a	n/a	n/a
72	24.00	n/a	n/a	3.30	6	60.28	36.00	2.88	n/a	n/a	n/a	n/a	n/a	n/a	n/a	n/a

Table A3 - Summary Data Table for 0.6 mm Sediment Size - Data Used From Arneson (1997)

Test Number	Target Q (ft ³ /s)	Measured Q (ft ³ /s)	q _{br} (ft ³ /s)	D ₅₀ (mm)	Bridge Position	Vertical Constriction (%)	Horizontal Constriction (%)	Pier Width, b (ft)	y _{pds} (ft)	y _{pps} (ft)	y (ft)	H _b (ft)	V _a (ft/s)	V _b (ft/s)	V _c (ft/s)	Fr
13	8	4.45	0.56	0.60	1	0.00	0.00	0.67	-0.02	n/a	1.43	1.32	0.40	0.68	1.49	0.06
13	8	7.29	0.91	0.60	2	12.06	0.00	0.67	0.01	n/a	1.42	1.15	0.65	0.87	1.49	0.10
13	8	6.38	0.80	0.60	3	24.11	0.00	0.67	0.03	n/a	1.40	0.98	0.62	1.05	1.49	0.09
13	8	7.45	0.93	0.60	4	36.17	0.00	0.67	0.04	n/a	1.41	0.81	0.60	1.39	1.49	0.09
13	8	6.85	0.86	0.60	5	48.23	0.00	0.67	0.06	n/a	1.48	0.64	0.72	1.54	1.50	0.10
13	8	6.51	0.81	0.60	6	60.28	0.00	0.67	0.20	n/a	1.39	0.47	0.67	1.59	1.48	0.10
14	18	15.29	1.91	0.60	1	0.00	0.00	0.67	0.01	n/a	1.44	1.41	1.32	1.33	1.49	0.19
14	18	15.20	1.90	0.60	2	12.06	0.00	0.67	0.07	n/a	1.41	1.24	1.32	1.78	1.49	0.20
14	18	14.39	1.80	0.60	3	24.11	0.00	0.67	0.26	n/a	1.47	1.07	1.26	2.00	1.50	0.18
14	18	13.61	1.70	0.60	4	36.17	0.00	0.67	0.45	n/a	1.47	0.90	1.29	2.14	1.50	0.19
14	18	14.31	1.79	0.60	5	48.23	0.00	0.67	0.49	n/a	1.52	0.73	1.26	2.19	1.51	0.18
14	18	12.82	1.60	0.60	6	60.28	0.00	0.67	0.65	n/a	1.54	0.56	1.23	2.36	1.51	0.17
15	24	20.60	2.58	0.60	3	24.11	0.00	0.67	0.47	n/a	1.85	1.03	1.79	2.65	1.56	0.23
15	24	26.38	3.30	0.60	4	36.17	0.00	0.67	0.73	n/a	1.74	0.86	2.10	2.10	1.54	0.28
15	24	32.07	4.01	0.60	5	48.23	0.00	0.67	0.76	n/a	1.71	0.69	2.04	2.62	1.54	0.27
15	24	24.97	3.12	0.60	6	60.28	0.00	0.67	0.74	n/a	1.49	0.52	1.97	2.60	1.50	0.28
16	8	7.86	1.07	0.60	1	0.00	8.34	0.67	0.01	0.15	1.40	1.35	0.71	0.82	1.49	0.11
16	8	6.44	0.88	0.60	2	12.06	7.33	0.67	-0.03	0.17	1.19	1.18	0.71	0.97	1.45	0.11
16	8	8.21	1.12	0.60	3	24.11	6.33	0.67	0.01	0.26	1.38	1.01	0.68	1.14	1.48	0.10
16	8	7.14	0.97	0.60	4	36.17	5.32	0.67	0.07	0.34	1.41	0.84	0.68	1.39	1.49	0.10
16	8	6.03	0.82	0.60	5	48.23	4.31	0.67	0.14	0.41	1.34	0.67	0.63	1.56	1.48	0.10
16	8	7.79	1.06	0.60	6	60.28	3.32	0.67	0.29	0.46	1.39	0.50	0.66	1.63	1.48	0.10
17	18	14.65	2.00	0.60	1	0.00	8.34	0.67	0.04	0.06	1.47	1.45	1.36	1.59	1.50	0.20
17	18	15.46	2.11	0.60	2	12.06	7.33	0.67	0.19	0.61	1.49	1.28	1.38	1.76	1.50	0.20
17	18	15.69	2.14	0.60	3	24.11	6.33	0.67	0.31	0.62	1.55	1.11	1.43	1.85	1.51	0.20
17	18	15.32	2.09	0.60	4	36.17	5.32	0.67	0.42	0.57	1.66	0.94	1.40	2.08	1.53	0.19
17	18	15.67	2.14	0.60	5	48.23	4.31	0.67	0.72	0.53	1.76	0.77	1.32	2.11	1.54	0.18
17	18	16.07	2.19	0.60	6	60.28	3.32	0.67	0.77	0.59	1.91	0.60	1.31	1.18	1.57	0.17
18	24	23.09	3.15	0.60	2	12.06	7.33	0.67	0.46	0.39	1.47	1.26	1.71	2.28	1.50	0.25
18	24	17.85	2.43	0.60	3	24.11	6.33	0.67	0.48	0.61	2.12	1.09	1.54	2.35	1.59	0.19
18	24	15.30	2.09	0.60	4	36.17	5.32	0.67	1.00	0.45	1.85	0.92	1.65	2.32	1.56	0.21

Table A4 - Summary Data Table for 0.9 mm Sediment Size - Data Used From Arneson (1997)

Test Number	Target Q (ft ³ /s)	Measured Q (ft ³ /s)	q _{br} (ft ³ /s)	D ₅₀ (mm)	Bridge Position	Vertical Constriction (%)	Horizontal Constriction (%)	Pier Width, b (ft)	y _{pds} (ft)	y _{pps} (ft)	y (ft)	H _b (ft)	V _s (ft/s)	V _b (ft/s)	V _c (ft/s)	Fr
1	8	5.80	0.73	0.90	1	0.00	0.00	0.67	-0.02	n/a	1.36	1.39	0.49	0.69	1.69	0.07
1	8	5.57	0.70	0.90	2	12.06	0.00	0.67	0.00	n/a	1.53	1.22	0.52	0.66	1.73	0.07
1	8	7.80	0.98	0.90	3	24.11	0.00	0.67	-0.01	n/a	1.62	1.05	0.49	0.93	1.74	0.07
1	8	7.00	0.88	0.90	4	36.17	0.00	0.67	-0.01	n/a	1.65	0.88	0.52	1.03	1.75	0.07
1	8	6.08	0.76	0.90	5	48.23	0.00	0.67	0.01	n/a	1.58	0.71	0.49	0.90	1.74	0.07
1	8	7.07	0.88	0.90	6	60.28	0.00	0.67	0.14	n/a	1.59	0.54	0.49	1.57	1.74	0.07
2	18	15.17	1.90	0.90	1	0.00	0.00	0.67	0.01	n/a	1.41	1.42	1.34	1.22	1.70	0.20
2	18	14.24	1.78	0.90	2	12.06	0.00	0.67	0.10	n/a	1.42	1.25	1.31	1.66	1.71	0.19
2	18	15.60	1.95	0.90	3	24.11	0.00	0.67	0.28	n/a	1.44	1.08	1.30	1.86	1.71	0.19
2	18	15.89	1.99	0.90	4	36.17	0.00	0.67	0.48	n/a	1.47	0.91	1.37	2.01	1.72	0.20
2	18	15.36	1.92	0.90	5	48.23	0.00	0.67	0.60	n/a	1.49	0.74	1.35	1.71	1.72	0.19
2	18	14.98	1.87	0.90	6	60.28	0.00	0.67	0.72	n/a	1.55	0.57	1.33	2.33	1.73	0.19
3	24	20.23	2.53	0.90	1	0.00	0.00	0.67	0.02	n/a	1.51	1.45	1.67	1.89	1.72	0.24
3	24	17.37	2.17	0.90	2	12.06	0.00	0.67	0.26	n/a	1.51	1.28	1.67	2.29	1.72	0.24
3	24	18.97	2.37	0.90	3	24.11	0.00	0.67	0.52	n/a	1.57	1.11	1.61	2.38	1.73	0.23
3	24	27.08	3.39	0.90	4	36.17	0.00	0.67	0.80	n/a	1.97	0.94	1.80	2.25	1.80	0.23
3	24	28.01	3.50	0.90	5	48.23	0.00	0.67	1.00	n/a	1.92	0.77	1.86	2.03	1.79	0.24
3	24	28.37	3.55	0.90	6	60.28	0.00	0.67	1.08	n/a	1.88	0.60	1.99	1.93	1.79	0.26
4	8	8.06	1.10	0.90	1	0.00	8.34	0.67	0.00	n/a	1.51	1.39	0.65	0.75	1.72	0.09
4	8	6.72	0.92	0.90	2	12.06	7.33	0.67	-0.03	n/a	1.63	1.22	0.51	0.82	1.74	0.07
4	8	6.44	0.88	0.90	3	24.11	6.33	0.67	-0.03	n/a	1.57	1.05	0.51	0.69	1.73	0.07
4	8	9.55	1.30	0.90	4	36.17	5.32	0.67	-0.02	n/a	1.57	0.88	0.53	1.14	1.73	0.07
4	8	6.73	0.92	0.90	5	48.23	4.31	0.67	0.05	n/a	1.56	0.71	0.52	1.49	1.73	0.07
4	8	9.30	1.27	0.90	6	60.28	3.32	0.67	0.14	n/a	1.57	0.54	0.52	1.51	1.73	0.07
5	18	10.50	1.43	0.90	2	12.06	7.33	0.67	0.09	n/a	1.35	1.26	1.29	1.68	1.69	0.20
5	18	11.59	1.58	0.90	3	24.11	6.33	0.67	0.24	n/a	1.37	1.09	1.27	1.88	1.70	0.19
5	18	11.25	1.53	0.90	4	36.17	5.32	0.67	0.41	n/a	1.40	0.92	1.26	2.09	1.70	0.19
5	18	11.90	1.62	0.90	5	48.23	4.31	0.67	0.60	n/a	1.36	0.75	1.30	2.19	1.69	0.20
5	18	12.88	1.76	0.90	6	60.28	3.32	0.67	0.75	n/a	1.37	0.58	1.38	2.27	1.70	0.21
6	24	15.92	2.17	0.90	2	12.06	7.33	0.67	0.16	0.58	1.54	1.35	1.61	2.44	1.73	0.23
6	24	13.74	1.87	0.90	3	24.11	6.33	0.67	0.47	0.55	1.56	1.18	1.85	2.50	1.73	0.26
6	24	17.73	2.42	0.90	4	36.17	5.32	0.67	0.68	0.61	1.56	1.01	1.70	2.52	1.73	0.24
6	24	19.96	2.72	0.90	5	48.23	4.31	0.67	0.90	0.51	1.53	0.84	1.82	2.24	1.73	0.26

Table A5 - Summary Data Table for 1.5 mm Sediment Size - Data Used From Arneson (1997)

Test Number	Target Q (ft ³ /s)	Measured Q (ft ³ /s)	q _{br} (ft ³ /s)	D ₅₀ (mm)	Bridge Position	Vertical Constriction (%)	Horizontal Constriction (%)	Pier Width, b (ft)	y _{pds} (ft)	y _{pps} (ft)	y (ft)	H _b (ft)	V _a (ft/s)	V _b (ft/s)	V _c (ft/s)	Fr
19	8	6.93	0.87	1.50	1	0.00	0.00	0.67	0.05	n/a	1.35	1.49	0.66	0.68	2.00	0.10
19	8	6.67	0.83	1.50	2	12.06	0.00	0.67	0.02	n/a	1.37	1.32	0.62	0.72	2.01	0.09
19	8	6.97	0.87	1.50	3	24.11	0.00	0.67	-0.10	n/a	1.37	1.15	0.63	1.08	2.01	0.10
19	8	6.76	0.85	1.50	4	36.17	0.00	0.67	-0.10	n/a	1.38	0.98	0.63	1.20	2.01	0.09
19	8	6.20	0.78	1.50	5	48.23	0.00	0.67	-0.05	n/a	1.39	0.81	0.64	1.55	2.01	0.10
19	8	7.04	0.88	1.50	6	60.28	0.00	0.67	-0.06	n/a	1.45	0.64	0.64	1.53	2.03	0.09
20	18	15.52	1.94	1.50	1	0.00	0.00	0.67	0.01	n/a	1.35	1.41	1.46	1.43	2.00	0.22
20	18	15.30	1.91	1.50	2	12.06	0.00	0.67	-0.01	n/a	1.33	1.24	1.45	1.78	2.00	0.22
20	18	15.53	1.94	1.50	3	24.11	0.00	0.67	-0.01	n/a	1.38	1.07	1.38	2.13	2.01	0.21
20	18	16.27	2.03	1.50	4	36.17	0.00	0.67	0.13	n/a	1.40	0.90	1.38	2.49	2.02	0.21
20	18	15.99	2.00	1.50	5	48.23	0.00	0.67	0.23	n/a	1.46	0.73	1.36	2.62	2.03	0.20
20	18	15.75	1.97	1.50	6	60.28	0.00	0.67	0.35	n/a	1.44	0.56	1.35	2.69	2.03	0.20
21	24	20.93	2.62	1.50	2	12.06	0.00	0.67	0.01	n/a	1.30	1.23	2.10	2.40	1.99	0.33
21	24	21.49	2.69	1.50	3	24.11	0.00	0.67	0.17	n/a	1.48	1.06	1.90	2.72	2.04	0.28
21	24	21.29	2.66	1.50	4	36.17	0.00	0.67	0.38	n/a	1.52	0.89	1.85	3.13	2.04	0.26
21	24	20.66	2.58	1.50	5	48.23	0.00	0.67	0.48	n/a	1.69	0.72	1.95	3.20	2.08	0.26
22	8	6.63	0.90	1.50	1	0.00	8.34	0.67	0.02	0.04	1.34	1.47	0.68	0.71	2.00	0.10
22	8	7.45	1.02	1.50	2	12.06	7.33	0.67	-0.01	0.04	1.37	1.30	0.68	0.75	2.01	0.10
22	8	5.91	0.81	1.50	3	24.11	6.33	0.67	-0.02	0.05	1.37	1.13	0.62	0.89	2.01	0.09
22	8	6.14	0.84	1.50	4	36.17	5.32	0.67	-0.02	0.05	1.35	0.96	0.64	0.76	2.00	0.10
22	8	7.41	1.01	1.50	5	48.23	4.31	0.67	-0.02	0.06	1.41	0.79	0.64	1.37	2.02	0.09
22	8	6.30	0.86	1.50	6	60.28	3.32	0.67	0.00	0.10	1.41	0.62	0.64	0.95	2.02	0.10
23	18	14.59	1.99	1.50	2	12.06	7.33	0.67	0.04	0.34	1.47	1.22	1.19	2.00	2.03	0.17
23	18	15.59	2.13	1.50	3	24.11	6.33	0.67	0.05	0.28	1.52	1.05	1.30	2.45	2.04	0.19
23	18	17.08	2.33	1.50	4	36.17	5.32	0.67	0.19	0.41	1.52	0.89	1.41	2.37	2.04	0.20
24	24	22.72	3.10	1.50	2	12.06	7.33	0.67	0.08	0.59	1.45	1.28	2.01	2.52	2.03	0.29
24	24	23.50	3.20	1.50	3	24.11	6.33	0.67	0.27	0.45	1.56	1.11	2.04	2.68	2.05	0.29
24	24	23.22	3.17	1.50	4	36.17	5.32	0.67	0.37	0.57	1.61	0.94	2.01	2.58	2.06	0.28
24	24	23.38	3.19	1.50	5	48.23	4.31	0.67	0.62	0.48	1.88	0.77	1.91	2.77	2.12	0.25

Table A6 - Summary Data Table for 3.3 mm Sediment Size - Data Used From Arneson (1997)

Test Number	Target Q (ft ³ /s)	Measured Q (ft ³ /s)	q _{br} (ft ³ /s)	D ₅₀ (mm)	Bridge Position	Vertical Constriction (%)	Horizontal Constriction (%)	Pier Width, b (ft)	y _{pds} (ft)	y _{pds} (ft)	y (ft)	H _b (ft)	V _a (ft/s)	V _b (ft/s)	V _c (ft/s)	Fr
7	8	6.81	0.85	3.30	1	0.00	0.00	0.67	-0.02	n/a	1.39	1.35	0.60	0.71	2.62	0.09
7	8	7.54	0.94	3.30	3	24.11	0.00	0.67	-0.01	n/a	1.50	1.01	0.59	1.01	2.65	0.09
7	8	6.74	0.84	3.30	4	36.17	0.00	0.67	-0.01	n/a	1.40	0.84	0.55	1.01	2.62	0.08
7	8	7.35	0.92	3.30	5	48.23	0.00	0.67	-0.03	n/a	1.41	0.57	0.59	0.98	2.63	0.09
7	8	7.09	0.89	3.30	6	60.28	0.00	0.67	-0.05	n/a	1.47	0.50	0.54	0.40	2.64	0.08
8	18	14.78	1.85	3.30	1	0.00	0.00	0.67	-0.04	n/a	1.44	1.32	1.26	1.32	2.64	0.18
8	18	14.10	1.76	3.30	2	12.06	0.00	0.67	-0.03	n/a	1.16	1.15	1.29	1.82	2.54	0.21
8	18	13.92	1.74	3.30	3	24.11	0.00	0.67	-0.03	n/a	1.49	0.98	1.14	1.54	2.65	0.16
8	18	14.81	1.85	3.30	4	36.17	0.00	0.67	0.09	n/a	1.51	0.81	1.33	2.71	2.66	0.19
8	18	15.35	1.92	3.30	5	48.23	0.00	0.67	0.21	n/a	1.50	0.64	1.23	2.79	2.65	0.18
9	24	24.88	3.11	3.30	1	0.00	0.00	0.67	-0.04	n/a	1.44	1.33	2.28	1.97	2.64	0.34
9	24	20.23	2.53	3.30	2	12.06	0.00	0.67	-0.04	n/a	1.42	1.16	1.82	2.53	2.63	0.27
9	24	20.20	2.53	3.30	3	24.11	0.00	0.67	0.17	n/a	1.43	0.99	1.73	2.70	2.63	0.25
9	24	20.74	2.59	3.30	4	36.17	0.00	0.67	0.28	n/a	1.51	0.82	2.31	3.16	2.66	0.33
9	24	20.58	2.57	3.30	5	48.23	0.00	0.67	0.64	n/a	1.51	0.65	1.83	3.32	2.66	0.26
10	8	7.06	0.96	3.30	1	0.00	8.34	0.67	-0.02	0.14	1.64	1.34	0.48	0.74	2.69	0.07
10	8	6.70	0.91	3.30	2	12.06	7.33	0.67	-0.02	0.17	1.62	1.17	0.45	0.84	2.69	0.06
10	8	7.17	0.98	3.30	3	24.11	6.33	0.67	-0.01	0.16	1.56	1.00	0.44	1.06	2.67	0.06
10	8	6.23	0.95	3.30	4	36.17	5.32	0.67	-0.03	0.17	1.53	0.83	0.42	0.72	2.66	0.06
10	8	7.03	0.96	3.30	5	48.23	4.31	0.67	-0.03	0.16	1.55	0.66	0.43	1.22	2.67	0.06
10	8	6.09	0.83	3.30	6	60.28	3.32	0.67	0.01	0.19	1.56	0.49	0.41	0.90	2.67	0.06
11	18	13.34	1.82	3.30	1	0.00	8.34	0.67	0.02	0.29	1.38	1.35	1.18	1.48	2.62	0.18
11	18	12.06	1.64	3.30	2	12.06	7.33	0.67	0.02	0.31	1.36	1.18	1.15	1.74	2.61	0.17
11	18	11.92	1.63	3.30	3	24.11	6.33	0.67	0.02	0.41	1.39	1.01	1.12	1.72	2.62	0.17
11	18	12.30	1.68	3.30	4	36.17	5.32	0.67	0.13	0.60	1.39	0.84	1.00	2.51	2.62	0.15
11	18	12.45	1.70	3.30	5	48.23	4.31	0.67	0.30	0.58	1.44	0.67	1.16	2.66	2.64	0.17
12	18	12.83	1.75	3.30	6	60.28	3.32	0.67	0.50	0.54	1.45	0.50	1.21	2.84	2.64	0.18
12	24	21.34	2.91	3.30	2	12.06	7.33	0.67	0.09	0.81	1.34	1.27	1.83	2.44	2.60	0.28
12	24	18.79	2.56	3.30	3	24.11	6.33	0.67	0.14	0.58	1.39	1.10	1.92	3.01	2.62	0.29
12	24	18.89	2.58	3.30	4	36.17	5.32	0.67	0.53	0.69	1.40	0.93	1.95	3.32	2.62	0.29
12	24	17.98	2.44	3.30	5	48.23	4.31	0.67	0.57	0.79	1.66	0.76	1.98	3.40	2.70	0.27